Project no. 248992

Project acronym: NEUNEU

Project title: Artificial Wet Neuronal Networks from Compartmentalised Excitable Chemical Media

Small or medium-scale focused research project (STREP)

Deliverable 2.3 - Report or publication on the final version of the simulation model and its experiments

Period covered: from 1.2.2010 to 29.2.2012   Date of preparation: 18.9.2009

Start date of project: 1.2.2010   Duration: 36 months

Project coordinator name: Dr. Peter Dittrich
Project coordinator organisation name: Friedrich Schiller University Jena

Ph.D. Dissertation

Information processing in neuron-imitating chemical systems

Author:

Jan Szymański

Supervisor:

prof. dr hab.

Jerzy Górecki

This dissertation was completed in the framework of International Ph.D. Studies in

Department of Complex Systems and
Chemical Information Processing
Institute of Physical Chemistry
Polish Academy of Sciences
Kasprzaka 44/52
01-224 Warsaw

Warsaw 2012

Acknowledgement

Contents

Chapter 1

Main ideas and notions

1.1   Introduction

The human brain, so close to us physically, has in many respects more rights to be called *terra incognita* by science than the vast wilderness of a tropical rainforest or even the surface of Mars. We can claim with a high degree of certainty that we know which subsystems there are in our brains, and what they are responsible for, but there remain more profound questions. How do the myriads of neurons that make up the brain interact on low levels? What is the exact mechanism by which human brains process information? Until these and similar questions are answered, we cannot hope to build intelligent machines that would be able to "outsmart" us.

The term "information processing", or its synonym "computing" is heard nowadays mainly in the context of computers and information theory. The word "computer" is so ubiquitous that probably not many people wonder at where it came from. In fact, it has its origins in Latin *computare*, "to count, to sum up". The word reflects the initial purpose for which the proto-computers were built: they were to be nothing more than counting machines. Of course, the inventors of first such devices could not predict the degree to which computers would ultimately change the world, but one thing remained

constant: their abilities are limited to counting. The fact that the modern computers are able to count much faster than humans does not mean that they are superior to human brains; so far, we were not able to even approximate the operation of nerve system with computer circuits. They cannot develop new ideas, think independently or in terms of abstract notions; they are built according to predetermined rules and (within a particular task or group of tasks) we can easily predict the reaction of a computer on any input. Thus, despite their practical usefulness, principles of computer operation cannot be of much help to us in understanding the brain.

When we look at the nerve network as a whole, we see that it operates on a completely different principle from a computer: different parts of the network can perform their operations independently at the same time, whereas the processing units of computers can only accept one command at a time. There is, consequently, a need for a different method of approximating the neuronal behaviour, and due to the fact that the functioning of neurons is based on chemistry, it is in this direction that most scientists in the area have been looking. Chemical systems based on so-called oscillating reactions turned out to be one of the most promising, and it has already been shown that while possessing properties similar to neuronal membrane, they were at the same time harnessed to perform some operations known to lie at the heart of computer processors. We can therefore think of them as bridging in a sense the wide gap between silicon circuits and brains. In my thesis, building on what is already known, I'm going to extend the analogies and show that such systems can resemble neurons even more closely.

The first chapter of the thesis is introductory in nature. In section 1.2, I describe the basic principles of computer operation and digital logic employed by the machines. Section 1.3 is concerned with chemistry, more specifically with the general properties and characteristics of the most important oscillating chemical system, the Belousov-Zhabotinsky reaction. The next section briefly introduces the physics of actual information processing in the human nervous system, together with some important models of

the phenomena observed therein. Finally, in section 1.5 the models of signal propagation in neurons and of the Belousov-Zhabotinsky reaction are compared and I show that oscillating reactions are indeed tools with which we can implement some operations that have their counterparts in digital circuits.

1.2   Information processing in computers

1.2.1   The von Neumann architecture

Most of the modern computers operate on the same principles: at their hearts lie the central processing units (CPUs or processors), whose main task is to perform operations sequenced in time. A processor has access to memory, which contains both the data to be worked on and the respective instructions. This architecture can be illustrated as in Figure 1.1 and is named after John von Neumann, an American mathematician and the pioneer of computer science, in honour of his contribution to the majority of concepts which allowed the development of modern computers in his report from 1945 [1].
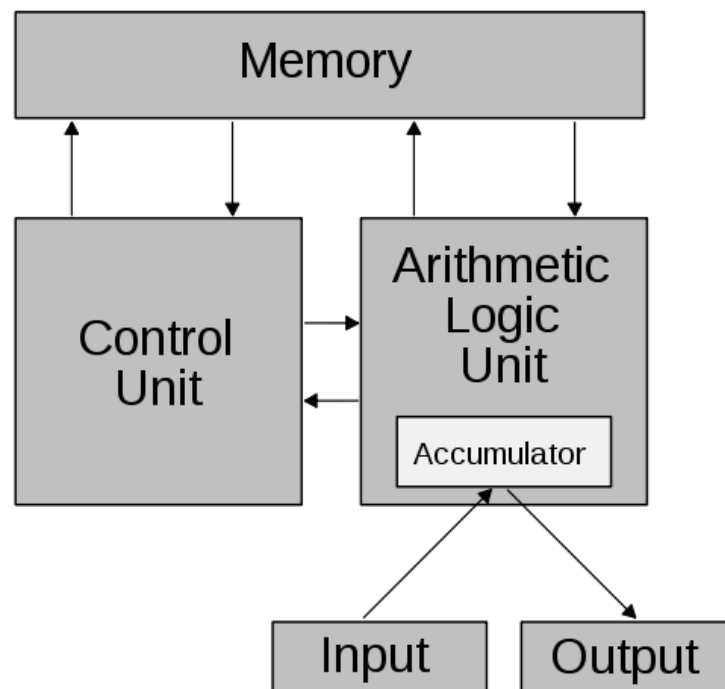
Figure 1.1: The von Neumann architecture. The Arithmetic Logic Unit is the real heart of a CPU, whereas the Control Unit takes care of communication with memory and data flow.

When the report was published, scientists at the Moore School of Electrical Engineering in Pennsylvania had been already working for some time on ENIAC (Electronic

Numerical Integrator and Computer), which went operational at the beginning of 1946. This machine was a so-called fixed-program computer: after finishing any computational task, it needed weeks of laborious work at the hardware level before it could undertake the next one. Not unlike in today's pocket calculators, the very wiring of ENIAC was oriented towards small sets of problems. The von Neumann's report lay ground for the construction of its successor, EDVAC (Electronic Discrete Variable Automatic Computer), which - although weighing almost 8 tons - was at its core much closer to modern PCs. The instructions and data were fed to the machine using a magnetic tape and thus were hardware-independent; such computers were christened stored-program computers. The tape concept, and the von Neumann architecture in general, can be conceived of as being a direct descendant of Alan Turing's ideas from the 1930s. Turing was a brilliant British mathematician among whose foremost contributions to science was a theoretical model of a computing machine [2]. This model, known as the Turing machine, consists of an infinite tape containing data (symbols), a head which can move along the tape and write or read the symbols on it, and a set of instructions describing how exactly the head should move and manipulate the symbols. Despite its simplicity, it is able to emulate any stored-program computer.

1.2.2   Basic logical operations: gates and their power

An average user sitting in front of his or her computer is usually dealing with the graphical user interface (GUI) of an operating system, which takes care of all the hardware functions and acts as a framework for specific programs, or applications, run by the user. We already know that at a lower level computer hardware operates according to principles outlined by von Neumann; still, at its core, the processor is just a collection of electronic elements which control the flow of electrical currents. The power of silicon chips lies in the fact that the high or low values of electric potential can be equated to the logical (Boolean) functions TRUE and FALSE, respectively. These can in turn be treated as

the binary numbers 1 and 0.

A typical microprocessor contains a large number of transistors and diodes, which allow for convenient modifications of electrical signals. Each such modification can be equated to some simple operation on data fed to the CPU in binary form. As was already hinted at, all the complicated tasks which computers are capable of solving can be split up into many operations of this type – it is not the ability to solve sophisticated mathematical problems that makes a processor useful in the modern world, but the speed at which it can deal with the simplest additions, multiplications and the like. Still, even these operations are conducted within the electrical circuits by means of even simpler logic gates. The logic gates [3] are devices which operate on binary numbers 1 and 0, taking one or more input values and returning one distinct output value.

Types of gates

Among the logic gates there exist sets which can be proven to be universal, that is, able to implement any logical function. Two examples of such sets are AND, NOT and OR, NOT, where each of the three gates (AND, OR, NOT) corresponds to particular logical function. The specific values outputted for different inputs are often presented in truth tables, which for the common gates mentioned look as presented. As can be seen, the

Input A	Input B	Output
0	0	0
0	1	0
1	0	0
1	1	1

Table 1.1: Truth table for the AND gate.

AND gate returns TRUE only when both (one AND the other) input values are TRUE, whereas for the OR gate it is sufficient that only one (OR the other) value be TRUE. The NOT gate is equivalent to the logical operation of negation.

Input A	Input B	Output
0	0	0
0	1	1
1	0	1
1	1	1

Table 1.2: Truth table for the OR gate.

Input A	Output
0	1
1	0

Table 1.3: Truth table for the NOT gate.

Capabilities of gates

Even though logical gates, when standing alone, do not seem to be of any use to computing and information processing, they can be coupled in many elaborate ways, giving rise to devices whose usefulness is outside any doubt, for example adders. Adders, as the name implies, are those parts of logical circuits responsible for simple additions of binary number pairs, "simple" here signifying really, really simple - processors, when adding two numbers, look at bits one by one, and, when faced with the input consisting of two 1s, give the result 0 and the remaining 1, which is then carried over to the next step. Let us write down all the possible input combinations for such adder - they appear as in table 1.4. In contrast to the simple AND and OR gates, this particular operation has

Input A	Input B	Sum	Carry
0	0	0	0
0	1	1	0
1	0	1	0
1	1	0	1

Table 1.4: The binary adder.

two input and two output values, one of which influences the input values in the next step of addition. Upon inspection, the carry bit turns out to be the result of applying the AND gate on the A and B, but the sum bit does not seem familiar. There exits,

nevertheless, a particular logic gate corresponding to just that relation, called the EX-CLUSIVE OR (XOR for short), which returns TRUE only if exactly one of two input bits is TRUE. Moreover, it is easily seen that the XOR gate can be constructed using nothing more than the three basic gates already described, as is evident from Figure 1.2. Combining the XOR and AND gates, we are able to design a logical circuit capable of binary addition (Figure 1.3), which in its full form takes three input bits (one of them being the bit carried from previous steps of summation) and outputs two.
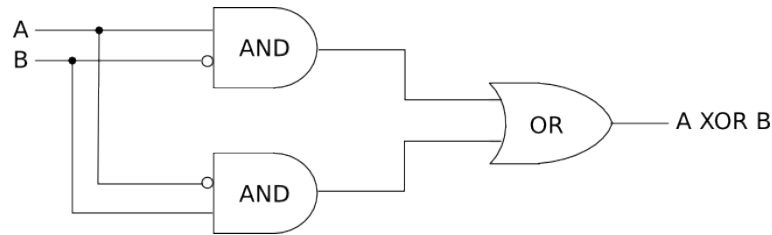
Figure 1.2: The XOR gate as constructed from simpler gates. Empty circles signify NOT gates.
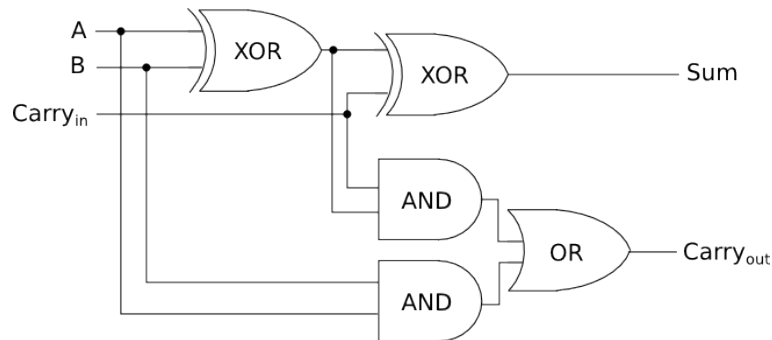
Figure 1.3: The full binary adder.

Implementation of gates in electronic circuits

The theoretical properties of logical gates can be translated to the language of electronic circuits by means of transistors [4], whose principle of operation is based on using the input current to control the flow of another, larger current. A scheme of a transistor is shown in Figure 1.4. When current flows in the wire called "base", V_{in}, the device behaves
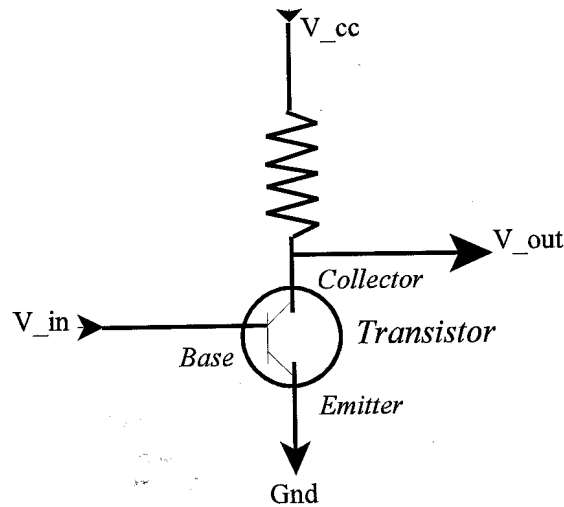
Figure 1.4: A transistor scheme.

conductively and allows the flow of electrons between the wire supplying constant, high voltage (V_{cc}) and ground. There is, however, a voltage drop on the resisting element and thus the output voltage V_{out} is much lower than V_{cc}. In the opposite case, when there is no base current, there is no conductivity in the transistor, no voltage drop and high voltage is registered on the output wire.

It is perhaps obvious that when the presence versus absence of electrical signal is equated to the binary 1 and 0 respectively, the transistor itself acts as a NOT gate. Most modern transistors are, however, used to built such simple gates in groups, comprising the devices with characteristics as described before (NMOS) and their opposites (PMOS), which exhibit low conductivity when the input voltage is high. When the transistors with different properties are adequately arranged, their combined switching properties can implement various logical functions. We can take the NOT gate as an example (Figure 1.5). The two transistors are represented in the middle of the diagram, PMOS above (marked by a circle corresponding to the negation operation) and NMOS below. Therefore, when the input corresponds to binary 0, the current flows in the direction V_{dd}
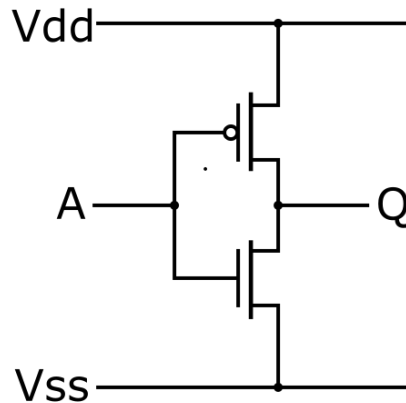
Figure 1.5: A transistor circuit implementing the NOT gate.

(constant high voltage) to Q (output); when to binary 1, in the direction A (input) to V_{ss} (ground).

As for the AND and OR gates, it turns out that from the point of view of circuit design it is easier to start from their negated counterparts, called NAND and NOR (Figure 1.6). The output of these gates is just the negated output of the corresponding "positive" gate for the same input values, for example NAND outputs 0 only if both inputs are 1, while NOR outputs 1 only when both inputs are 0. The current exiting the transistor circuit implementing the negated gates is then fed as an input to the NOT gate.

1.2.3 Unconventional computation

The title of this subsection refers to a "convention" according to which the computing machines of today operate following rules described in section 1.2. According to Moore's law, the computing power at our disposal grows at a constant rate, but it is commonly agreed that we are bound to reach a threshold in the near future. The main candidate for the bottleneck here is the flow of data between CPUs and memory. Some research groups, in hopes of combating this prospect, began work on alternative paradigms of information processing, which are described by an umbrella term "unconventional computation"
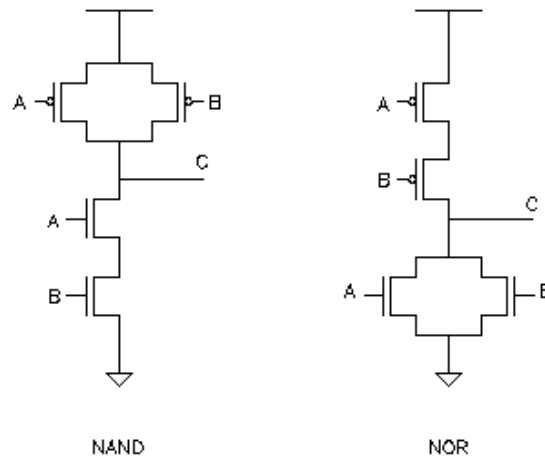
Figure 1.6: Transistor circuits implementing the NAND and NOR gates.

The Holy Grail of all research related to information processing may be assumed to be a machine with abilities comparable to human brain. It is for this reason that many researchers looking for the alternatives to silicon chips are looking towards nature-based methods of information processing [5]. Since nature processes information quite differently from computers, the two models – conventional and unconventional – differ from each other radically. Let us go row by row down the table 1.5, adapted from [6].

Conventional	Unconventional
computation restricted by CPU and memory	computation occurs everywhere
sequential	parallel
error correction by coding	error correction by structure
many simple instructions	a few complex instructions

Table 1.5: Conventional versus unconventional computing.

1. In contrast to computers, information processing in natural systems occurs in the whole available medium at once – if we look at the brain we will notice that it processes a great deal of information in different areas at the same time, whereby different regions are involved in performing a single operation.

2. Parallelism of unconventional computing is directly related to the above point. A chemical or biological medium capable of information processing can be pictured as a collection of countless tiny processors working in parallel.

3. While errors that arise during operation of silicon CPUs must be corrected by a programmer who has to modify the program, the unconventional computing medium is able to auto-correct any discrepancies, because all its elements are in constant contact with each other.

4. Computer programs in their form understandable to humans can take tens upon tens of text pages, but a typical chemical processor needs just a few instructions, albeit complex and carefully selected.

1.3 The oscillating Belousov-Zhabotinsky reaction

1.3.1 The notion of oscillating reaction

The Belousov-Zhabotinsky (BZ) reaction is one member of a wider class of chemical processes commonly labelled "oscillating reactions". In general, chemical reactions are thought of as involving interaction of several substances (substrates) which are transformed into one or more different substances (products). It is expected that, in a closed system, in the course of such transformation the amount of a substrate will steadily decline, while the amount of a product will rise. This is indeed the case with many chemical reactions, but the oscillating reactions do not conform to that pattern, they exhibit instead periodic changes in concentrations of certain chemical species.

The above does not imply that there are any major changes in concentrations of main substrates or products of an oscillating reaction; their amounts change slowly and monotonically, just like in any other chemical process. The difference lies in intermediate products, which are inevitably formed in all reactions. The reactions we are concerned with display rapid and dramatic (several orders of magnitude) changes in concentrations of such products. At first glance, this property seems counter-intuitive. It is worthwhile to recall here the second law of thermodynamics, one of the bases for all physical chemistry:

$$dS_{univ} = dS_s + dS_{surr} \geq 0 \tag{1.1}$$

In simple terms, the equation states that the entropy of the universe cannot decrease in any chemical or physical process. Now, if we were conducting a chemical reaction in a sealed container without energy exchange with the surroundings (which is equivalent to an isolated system), any change of S_{univ} associated with this reaction would be associated only with the processes taking place in the container, hence $dS_s = dS_{univ}$. The appearance of chemical oscillations is associated with local decrease of entropy and such is not possible in isolated system. The situation becomes different when we consider an

open system, i.e. a system which can exchange energy and matter with its surroundings. In this case, provided there exits some process which can increase the entropy of surroundings, local negative changes in entropy become possible [7].

1.3.2 A bit of history

It is useful at this point to present a brief historical overview of research activity related to oscillating reactions in general and to the BZ reaction in particular.

Initial theoretical studies

Already in 1910, Alfred J. Lotka, American biophysicist trying to devise mathematical models for various ecological interactions, considered a set of imaginative chemical reactions leading to oscillatory changes in concentrations of the substances involved [8]. His system consisted of two substances, S_1 and S_2, P stood for some unidentified product, and S_0 for constant source of one of the reagents.

$$S_0 \rightarrow S_1 \tag{1.2}$$

$$S_1 + S_2 \rightarrow 2S_2 \tag{1.3}$$

$$S_2 \rightarrow P \tag{1.4}$$

After solving this set of equations analytically, he obtained solutions corresponding to damped oscillations in concentrations of both reagents (Figure 1.7). One point of note here is the second reaction of the model, in which, as is evident from basic chemical kinetics, the substance 2 influences its own rate of production. This is an example of autocatalysis, and, as we shall see later, such property is crucial to the oscillatory chemical dynamics.

Ten years later, Lotka expanded on his model [9]. He decided to add a second autocatalytic step, so that both components of the system were now produced autocatalytically
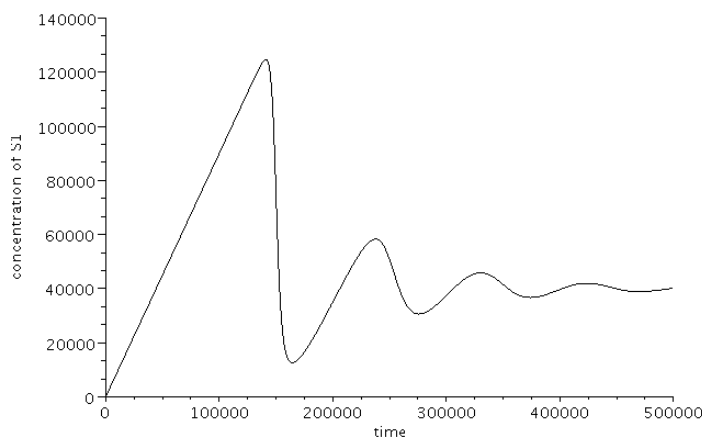
Figure 1.7: Damped oscillations in the concentration of substance S_1 in the Lotka model.

at some point in the process. The refined model looked as follows:

$$S_0 + S_1 \rightarrow 2S_1 \tag{1.5}$$

$$S_1 + S_2 \rightarrow 2S_2 \tag{1.6}$$

$$S_2 \rightarrow P \tag{1.7}$$

This modification allowed him to get undamped oscillations (Figure 1.8), the result which he was after to begin with, as evidenced in his paper. This finding had important biological implications - already in 1920 Lotka himself found his models useful in describing relations between the number of herbivorous animals and the amount of vegetation available [10]. Research in this direction was also pursued by Vito Volterra, who extended the biological parallels [11]. Nowadays the whole model, commonly known as Lotka-Volterra model, is often presented in biology courses as the simplest model of predator-prey interactions, which exhibit clearly oscillatory dynamics (Figure 1.9).

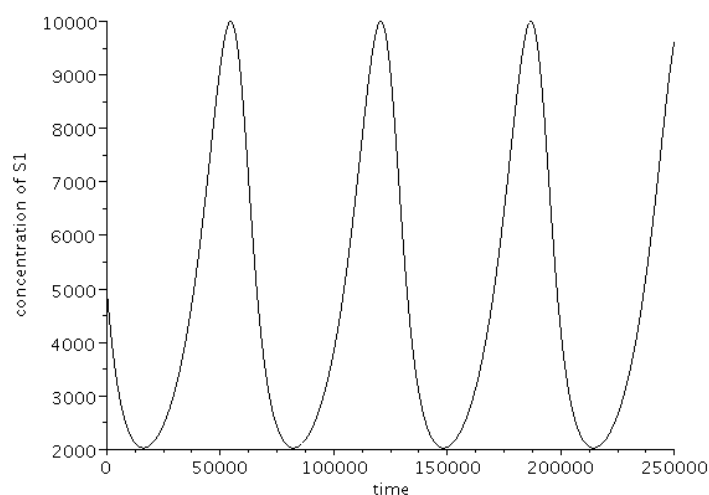Figure 1.8: Oscillations in the modified Lotka model.

The first oscillating reaction

When Alfred Lotka published his results in 1920, he probably did not expect any real homogenous chemical oscillations to be found any time soon. However, as soon as the next year, William C. Bray from Berkeley reported precisely such oscillations in a reaction which does not look very interesting at a first glance, namely catalytic decomposition of hydrogen peroxide to water and oxygen [13]. Bray's aim was to test catalytic potential of iodate ion (IO_3^-) in this process and he monitored the evolution of oxygen at 60 °C. For some values of acidity of the solution, he observed periodic changes in the amount of gas evolved. In order to study the phenomenon more closely, he cooled the system to the room temperature and followed the changes in the concentration of iodine, the final product of the reaction between iodate and peroxide. The oscillatory behaviour soon became apparent (Figure 1.10), and Bray immediately commented on its similarity to solutions of Lotka-Volterra model.

Bray's results, later augmented by collaboration with his student, Liebhafsky [14] (whose contribution was large enough to earn him a place in history alongside his men-
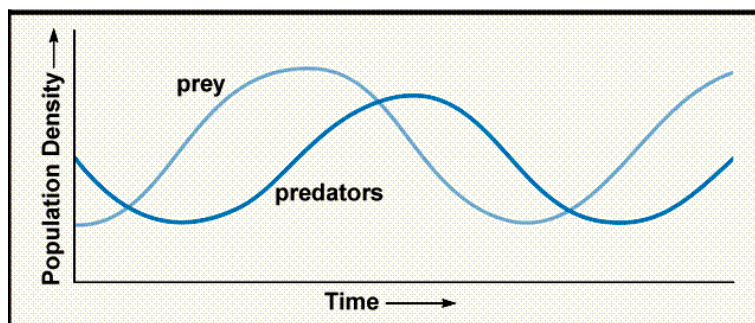
Figure 1.9: Predator-prey interaction [12].
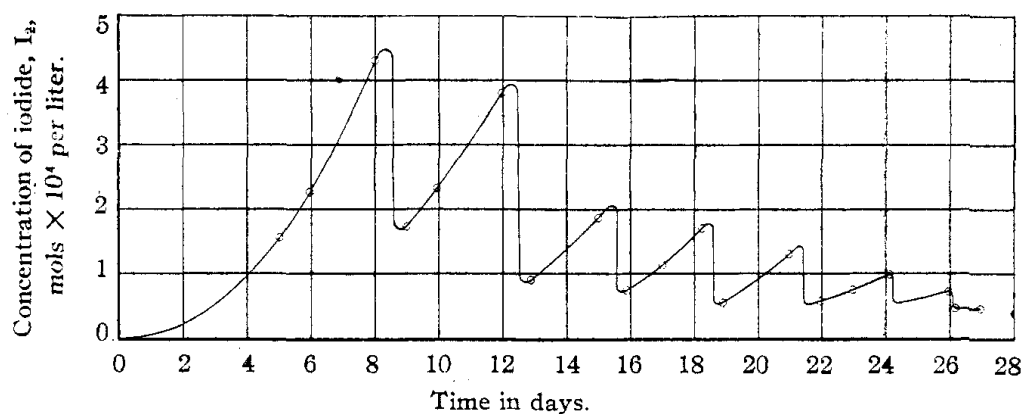
Figure 1.10: Changes in concentration of I_2 during oscillatory decomposition of H_2O_2. Initial concentrations: H_2O_2 0.0327 M, HIO_3 0.0090 M [13].

tor - the reaction is today referred to as the Bray-Liebhafsky reaction) were met with scepticism of the scientific community; the oscillations were commonly attributed to dust particles [15] or physical processes related to formation of oxygen bubbles [16]. It was not until 1976 that a commonly accepted basic mechanism was published [17]. By then, the oscillating chemical reactions were established as a scientific fact, the result of a real breakthrough sparked by the discovery of Belousov-Zhabotinsky reaction, to which we shall now turn.

Boris Belousov and Anatol Zhabotinsky

Boris Pavlovich Belousov was a biochemist heading the Biophysics Laoratory of the Soviet Ministry of Health [18]. At the beginning of 1950s his main area of interest was metabolism, specifically Krebs cycle. This important set of processes plays a role in the final parts of mitochondrial oxidation of various organic substances, such as proteins, fats and carbohydrates, to carbon dioxide. The problem Belousov was working on was a simple inorganic analogue of the cycle. He used citric acid, the core substance of the whole biological sequence, bromate, which served as an oxidant, and cerium ions (Ce^{3+}), emulating active centres of various enzymes involved in the Krebs cycle.

After he mixed all the ingredients together in an acidic medium, he soon observed that the colourless solution turned yellow, then became colourless again, and the switching of colours lasted about 1 hour. Belousov immediately attributed the colour changes to changes in oxidation state of cerium ions: Ce^{3+} is colourless, but Ce^{4+} is dark yellow. The mysterious process thus appeared to involve periodic oxidation and reduction of cerium ions. At the same time, the carbon dioxide was produced as expected via the oxidation of citric acid by bromate.

These results were not well received; the paper written by Belousov was repeatedly rejected at several journals and was published only in 1958, in obscure proceedings of a conference related to radiotherapy [19]. The original recipe, whose origin became unknown by then, was presented to doctoral student Anatol Zhabotinsky by his advisor Simon Schnoll in 1961. Zhabotinsky replaced citric acid, which apparently caused some unwanted precipitation processes, with simpler analogue, malonic (propanedioic) acid. He then began detailed investigation and provided some first detailed analyses of influence of various factors such as temperature and initial concentrations [20]. The Western scientists first became aware of the potential significance of this reaction when the first article in English appeared [21], which was more than fifteen years after Belousov's discovery. Nevertheless, next 5 years saw a tremendous progress in understanding the mech-

anism of the process, due mainly to the work of Richard Noyes' group at the University of Oregon in Eugene.

1.3.3 Mechanism

As was outlined in the preceding section, the basic substrates of the Belousov-Zhabotinsky reaction (henceforth referred to simply as the BZ reaction) are: bromate (typically sodium salt, $NaBrO_3$), malonic (propanedioic) acid and cerium (III) ions (cerium sulphate, $Ce_2(SO_4)_3$). Sulphuric acid is then added to provide necessary acidity. Normally the onset of oscillations is preceded by so-called induction period, during which there are no dramatic changes in the concentrations of the reagents, and addition of a small amount of bromide salt, NaBr or KBr, markedly shortens this period. In fact, bromide ions play a crucial role in the whole mechanism of the reaction.

What follows is the description of the BZ reaction mechanism as outlined in a truly ground-breaking article of Field, Körös and Noyes [22]. Their model, constructed on the grounds of huge amounts of experimental data, became known as the FKN model and served as a basis for all future work on mechanisms of oscillating reactions.

As we already know, in order for chemical oscillations to appear there must exist some net, irreversible chemical process in the system responsible for the steady increase in the entropy of the universe. In the BZ system, it is the slow oxidation of malonic acid by bromate:

$$2NaBrO_3 + 3CH_2(COOH)_2 + 2H^+ \rightarrow 2BrCH(COOH)_2 + 4H_2O + 3CO_2 \qquad (1.8)$$
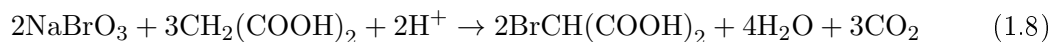
Because of this reaction, oscillations cannot proceed for an infinite period of time. Just like energy dissipation eventually damps the oscillations of a pendulum, the unavoidable drive to the equilibrium eventually brings all chemical periodic behaviour (without external supply of reagents) to a stop.

Let us now turn to the oscillations themselves. The plots in Figure 1.11 show the oscillatory changes in the concentrations of cerium (III) and bromide ions, the induction period is also evident. The reactions constituting the BZ mechanism were conveniently
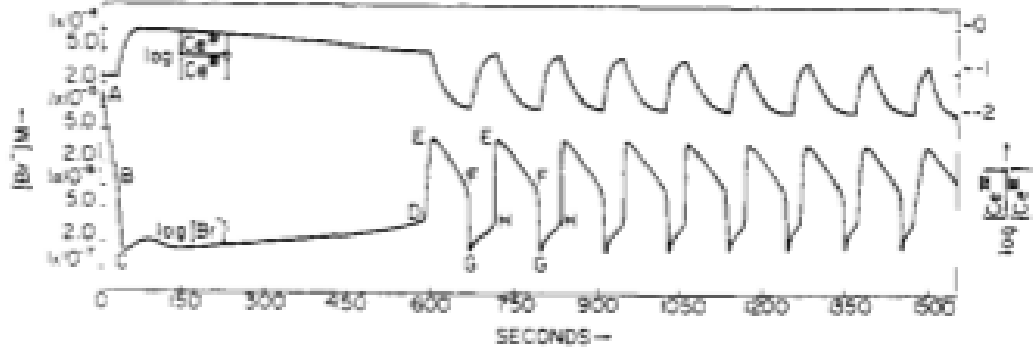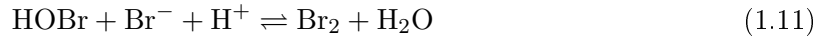

Figure 1.11: Oscillations in the BZ reaction. Initial concentrations: [malonic acid] = 0.032 M, [BrO_3^-] = 0.063 M, [Br^-] = 1.5 × 10^{-5} M, [Ce^{3+}] = 0.001 M, [H_2SO_4] = 0.8 M [22].

divided in the FKN model into three groups, which we shall call A, B, and C, following the original notation. After mixing all the reagents together, reactions from the A subset take place:

$$BrO_3^- + Br^- + 2H^+ \rightleftharpoons HBrO_2 + HOBr \tag{1.9}$$

$$HBrO_2 + Br^- + H^+ \rightleftharpoons 2HOBr \tag{1.10}$$

$$HOBr + Br^- + H^+ \rightleftharpoons Br_2 + H_2O \tag{1.11}$$
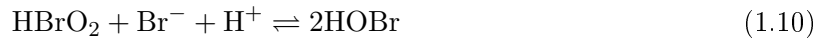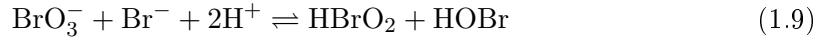
Molecular bromine formed in this sequence then brominates malonic acid:

$$Br_2 + CH_2(COOH)_2 \rightarrow BrCH(COOH)_2 + Br^- + H^+ \tag{1.12}$$

In total, the reactions of the subset A are responsible for the decrease in the bromide ion concentration, as well as the appearance of bromomalonic acid and bromous acid $HBrO_2$.

We can sum them up to give the following process:

$$2Br^- + BrO_3^- + 3CH_2(COOH)_2 + 3H^+ \rightarrow 3BrCH(COOH)_2 + 3H_2O \qquad (1.13)$$
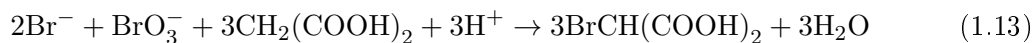
As the concentration of bromide drops, the reactions of the aforementioned group slow down and become less and less important. At the same time, the concentration of an intermediate product $HBrO_2$ rises until at some point bromous acid wins the competition for bromate ions. This leads to an autocatalytic cascade:

$$BrO_3^- + HBrO_2 + H^+ \rightleftharpoons 2BrO_2\bullet + H_2O \qquad (1.14)$$

$$BrO_2\bullet + Ce^{3+} + H^+ \rightleftharpoons HBrO_2 + Ce^{4+} \qquad (1.15)$$

A close look at the two equations above reveals that each $HBrO_2$ molecule created in the first reaction produces two such molecules in the second step; this is pure autocatalysis.
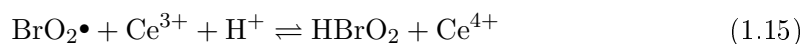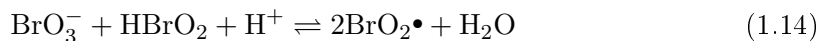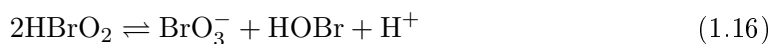
As the concentrations of bromous acid and oxidized metal cations grow, another processes gain importance. First of all, $HBrO_2$ undergoes decomposition:

$$2HBrO_2 \rightleftharpoons BrO_3^- + HOBr + H^+ \qquad (1.16)$$

Simultaneously, bromide ions start being regenerated by a group of reactions which essentially bring the system back to its initial state, reducing the cerium ions back to the Ce^{3+} form.

$$Ce^{4+} + mCH_2(COOH)_2 + nBrCH(COOH)_2 \rightarrow fBr^- + Ce^{3+} + \text{other products} \qquad (1.17)$$
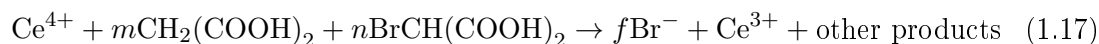
This part of the reaction, featuring some unspecified stoichiometric factors m, n and f, has caused the most controversy among chemists working on the BZ reaction. It is usually agreed upon that it involves various kinds of organic radicals originating in

malonic acid and its derivatives, such as •CH(COOH)$_2$, •CBr(COOH)$_2$, •COOH and others; these radicals interact with each other and with other reactants present in the system, producing a wide variety of organic molecules. The specific details are irrelevant for further discussion, but it is worth pointing out that a whole branch of research on the BZ reaction is devoted to elucidating the entire mechanism in as much detail as possible. After the importance of organic radicals was established [23], a detailed model, composed of 80 reactions and 26 chemical species, was proposed [24]. As recently as 2002, collaborating German, Hungarian and American groups provided a massive update of many rate constants and elementary processes [25]. Nevertheless, it is agreed upon that bromide ions play the role of the main inhibitor of the autocatalytic loop and thus of the oscillations themselves.

1.3.4 Extending the applications of the reaction: ferroin and ruthenium catalysts

The color changes of the BZ reaction conducted according to the original recipe, between colorless and light-yellow, were hard to follow visually and not very appealing. To overcome this shortcoming and strengthen the contrast, Zhabotinsky added ferroin, complex of iron (II) cation with three 1,10-phenanthroline ligands (Figure 1.12). This complex is red in its basic form and blue in oxidized (III) form, which provides for a stark contrast. This allowed much more detailed observations of various interesting phenomena arising
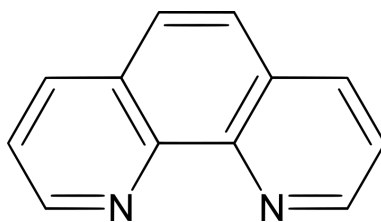

Figure 1.12: 1,10-phenanthroline molecule.

in the reaction. Zaikin and Zhabotinsky [26] were the first to observe what is known to-

day as "chemical waves": they studied thin, unstirred layers of BZ solution and obtained waves of reagent concentrations, similar in appearance to the waves caused by throwing stones into water. When autocatalytic reaction starts at some point, usually triggered by touching the surface with a silver wire (which causes a local decrease in the concentration of the inhibitory bromide ions due to the formation of AgBr) the blue oxidized form of ferroin (known as ferriin) is free to diffuse around and leaves behind a zone in which the concentration of bromide ions is high and red ferroin predominates (Figure 1.13). The reaction is of course periodic, so blue zone keeps appearing in the same place, sending a sequence of concentric reaction fronts. The breakage of such front causes curling of free ends and formation of a spiral [27]. These structures, periodic both in time and space, are
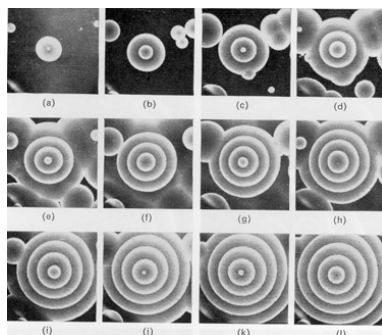
Figure 1.13: Chemical waves in the ferroin-catalyzed BZ reaction. Bright areas correspond to the oxidized (blue) form of the catalytic complex [26].

to this day one of the most important examples of self-organization in chemical systems, and investigation of their properties belong to thriving branches of research concerned with oscillating reactions. The spiral and target shapes are actually even more general, appearing most importantly in many biological systems [28, 29]. Because of their being the result of interplay between complicated chemistry of BZ systems and diffusion, they are very often referred to as reaction-diffusion structures.

The question of replacing the metal catalyst to get more interesting effects does is not exhausted with ferroin. Another branch of research [30] focuses on catalyst which is a complex of ruthenium (II) cation with three 2,2'-bipyridyl ligands (Figure 1.14).

This catalyst was originally used to produce photoluminescent chemical waves in the BZ

Figure 1.14: 2,2'-bipyridyl ligand.

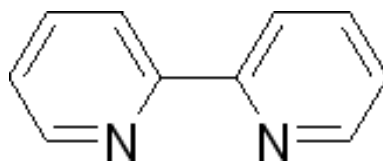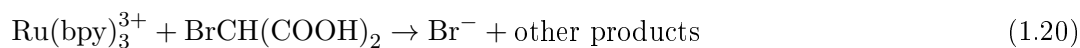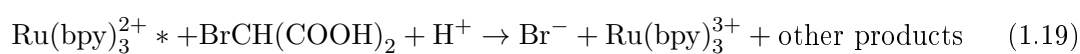reaction, because of its strong fluorescence when illuminated with UV light [31]. Some ten years later, it was found that the complex makes the BZ reaction photosensitive, i.e. its presence causes the dynamic behaviour of the reaction to change on application of visible light [32]. The most profound effect was the decrease in oscillation period in illuminated areas, leading eventually to a complete inhibition of oscillatory behaviour and explained by influence of an excited form of the catalytic complex [33].

$$Ru(bpy)_3^{2+} \rightleftharpoons Ru(bpy)_3^{2+}* \qquad (1.18)$$

$$Ru(bpy)_3^{2+}* + BrCH(COOH)_2 + H^+ \rightarrow Br^- + Ru(bpy)_3^{3+} + \text{other products} \qquad (1.19)$$

$$Ru(bpy)_3^{3+} + BrCH(COOH)_2 \rightarrow Br^- + \text{other products} \qquad (1.20)$$

1.3.5 Numerical models

Oregonator

FKN mechanism, as well as more complicated mechanisms just described, was subject to verification by numerical solution of differential equations resulting from it, but the need for simple model, which would make it possible to relate the results to Lotka models more closely and to conduct mathematical analyses, was apparent already in the 1970s. In 1974, Field and Noyes published the now-famous work on a simplified model of the BZ reaction. As was mentioned, they were based in Oregon, so their model came to be known as Oregonator [34]. The basic idea was to reduce the whole mechanism to several

key steps:

$$A + Y \rightarrow X + P \tag{1.21}$$

$$X + Y \rightarrow 2P \tag{1.22}$$

$$A + X \rightarrow 2X + 2Z \tag{1.23}$$

$$2X \rightarrow P + A \tag{1.24}$$

$$B + Z \rightarrow fY \tag{1.25}$$
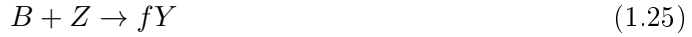
This scheme looks confusing until we consider how the symbols relate to the BZ reagents: $A = \mathrm{BrO}_3^-$, $B = \mathrm{CHBr(COOH)}_2$, $X = \mathrm{HBrO}_2$, $Y = \mathrm{Br}^-$, $Z = \mathrm{Me}_{Ox}$, $P = \mathrm{HOBr}$ (as P never appears on the left-hand side, it can be treated as a "sink" variable; Me_{Ox} refers to the oxidized form of metal catalyst). The consecutive processes become then equivalent to the respective reactions in the FKN mechanism. Using the basic laws of chemical kinetics it is possible to write down ordinary differential equations describing the time evolution of three dynamic variables: X, Y and Z (A and B are assumed to be constant), which symbols we take for convenience to denote concentrations of the respective reagents.

$$\frac{dX}{dt} = k_1 AY - k_2 XY + k_3 AX - 2k_4 X^2 \tag{1.26}$$

$$\frac{dY}{dt} = -k_1 AY - k_2 XY + fk_5 BZ \tag{1.27}$$

$$\frac{dZ}{dt} = 2k_3 AX - k_5 BZ \tag{1.28}$$

An important follow-up work was published in 1980 by Tyson and Fife [35]. The authors greatly simplified the mathematical analysis of the model by introducing dimensionless variables u, w and v, dimensionless time τ and parameters dependent on rate constants and the values of A and B. They were defined as follows: $u = \frac{2k_4}{k_3 A} X$, $w = \frac{k_2}{k_3 A} Y$, $v = \frac{k_4 k_5 B}{(k_3 A)^2} Z$, $\tau = k_5 Bt$, $\epsilon = \frac{k_5 B}{k_3 A}$, $\epsilon' = \frac{2k_4 k_5 B}{k_2 k_3 A}$, $q = \frac{2k_1 k_4}{k_2 k_3}$. This operation

permitted them to reduce the number of parameters from eight (rate constants plus two constant concentrations and f) to four (ϵ, ϵ', q and the parameter relating t with τ), and the resultant equations were

$$\epsilon\frac{du}{d\tau} = qw - uw + u - u^2 \tag{1.29}$$

$$\epsilon'\frac{dw}{d\tau} = -qw - uw + 2fv \tag{1.30}$$

$$\frac{dv}{d\tau} = u - v \tag{1.31}$$

Tyson and Fife further noticed that for typical, realistic values of parameters the variable w changes very fast if compared with u, and thus can be at any given instant linked to the values of u and v according to the expression $w = \frac{2fv}{q+u}$. Upon substitution of this expression to the equations 1.29, they become

$$\epsilon\frac{du}{d\tau} = u - u^2 - 2fv\frac{u - q}{u + q} \tag{1.32}$$

$$\frac{dv}{d\tau} = u - v \tag{1.33}$$

Finally, one important modification which allowed studying the effect of illumination on ruthenium-catalysed systems was made by Krug et al. [36]. They introduced an additional parameter ϕ, whose value was taken as proportional to the light intensity used. The simplest model was

$$\epsilon\frac{du}{d\tau} = u - u^2 - (2fz + \phi)\frac{u - q}{u + q} \tag{1.34}$$

$$\frac{dv}{d\tau} = u - v \tag{1.35}$$

This model has been commonly used as a standard model of light-sensitive BZ reaction and it is the model employed for that purpose in the present thesis.

Models of the ferroin-catalyzed BZ reaction

The Oregonator model was in its essence based on the cerium-catalysed version of the BZ reaction. There are, however, some differences in the shape and period of oscillations if compared with the ferroin-catalysed system [37], which is to be expected if one considers the difference in redox potentials between Ce^{3+}/Ce^{4+} and $Fe(phen)_3^{2+}/Fe(phen)_3^{3+}$ redox couples (*phen* is a standard shorthand for the 1,10-phenanthroline ligand) [38] and the presence of ligands themselves, which can take part in the already complicated chemical processes characterizing the BZ reaction [39, 40]. From a qualitative point of view, the most important differences include the degree to which the catalyst is oxidized (in case of the cerium catalyst this degree depends on concentrations of other reagents and can vary from 5 to 8 percent, but ferroin catalyst is oxidized completely) and the shape of oscillations - in ferroin-catalysed version, reduction of oxidized form back to the starting state takes much more time than in the case of cerium. Moreover, it was determined that, when working with ferroin as the catalyst, it is only necessary to mix bromomalonic acid, bromate and sulphuric acid in order for the oscillations to start.

First important model of the ferroin-catalyzed BZ reaction is credited to Russians Rovinsky and none other than Zhabotinsky [41]. Let us look at the set of chemical reactions constituting the starting point for its basic version.

$$X + A \rightleftharpoons 2U \tag{1.36}$$

$$U \rightleftharpoons X + Z \tag{1.37}$$

$$2X \rightarrow A + P \tag{1.38}$$

$$X + Y \rightarrow P \tag{1.39}$$

$$A + Y \rightarrow X + P \tag{1.40}$$

$$Z + B \rightleftharpoons R \tag{1.41}$$

$$R \rightarrow fY \tag{1.42}$$

Most of the reactions have their counterparts in the Oregonator model, marked difference is noticed in introduction of two additional variables, U = $HBrO_2^+$ and R = $\bullet CBr(COOH)_2$, which split the reactions 3 and 5 of Field and Noyes' model into component processes. The remaining symbols are assumed to have the same meaning as in the Oregonator, with an important exception of A, which marks $HBrO_3$.

There are some novel elements in the form of differential equations describing time evolution of the system's chemical composition. The acidity is taken into account by introducing the Hammett acidity function h_0 [42, 43, 44], which is a good indicator of actual proton concentration in solutions of sulphuric acid. The appearance of h_0 indicates that the rate of a given reaction depends on the system acidity. An obvious fact, though not taken into account within the Oregonator, is that the rates of reactions producing the oxidized form of ferroin (i.e. ferriin) should depend, among others, on the concentration of the reduced form. This concentration was not treated as a variable by Rovinsky and Zhabotinsky; instead, they used difference $C - Z$, where C stands for the total catalyst concentration $[Fe(phen)_3^{2+}] + [Fe(phen)_3^{3+}]$. Finally, the relation $[HBrO_3] = h_0[BrO_3^-]/(0.2 + h_0)$ was assumed to hold (reflecting the equilibrium $BrO_3^- + H^+ \rightleftharpoons HBrO_3$).

$$\frac{dX}{dt} = k_2 U(C - Z) - k_{-2}XZ - k_1 h_0 AX + k_{-1}U^2 - 2k_3 h_0 X^2 - k_4 h_0 XY + k_5 h_0 AY$$

$$(1.43)$$

$$\frac{dY}{dt} = fk_7 R - k_5 h_0 AY - k_4 h_0 XY \tag{1.44}$$

$$\frac{dZ}{dt} = k_2 U(C - Z) - k_{-2}XZ - k_6 BZ + k_{-6}h_0 R(C - Z) \tag{1.45}$$

$$\frac{dU}{dt} = -k_2 U(C - Z) + k_{-2}XZ + 2k_1 h_0 AX - 2k_{-1}U^2 \tag{1.46}$$

$$\frac{dR}{dt} = k_6 BZ - k_{-6}h_0 R(C - Z) - k_7 R \tag{1.47}$$

Taking into account the fact that the variables U and R change very fast, this equation
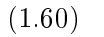
set can be made dimensionless and simplified in a similar manner to the Oregonator; without going into detail, we give the final two-variable scaled model, which allows for direct comparisons with the Field and Noyes' model:

$$\epsilon \frac{du}{d\tau} = u - u^2 - 2f\alpha \frac{v}{1-v}\frac{u-q}{u+q} \tag{1.48}$$

$$\frac{dv}{d\tau} = u - \alpha \frac{v}{1-v} \tag{1.49}$$

In contrast to the Oregonator, the inhibiting influence of the v variable is modified in relation to the acidity of the system, because the control parameter α is inversely proportional to the square of h_0. Therefore, the higher the acid concentration, the weaker the inhibition by v. Additionally, the growth of both variables is controlled by the expression $1 - v$ appearing in the denominator and preventing the corresponding simulated concentration of $Fe(phen)_3^{3+}$ from ever exceeding the total catalyst concentration. In fact, it turned out that the Rovinsky-Zhabotinsky (RZ) model, although based eventually on the FKN reaction scheme developed on the basis of data for cerium-catalysed systems, described the experimental results regarding ferroin-catalysed reaction more accurately than the Oregonator ever did for cerium.

A modified model was introduced by Zhabotinsky working with the Epstein group at Brandeis University as a tool for accurate modelling of systems wherein catalyst remains oxidized for a major part of the reaction cycle [45].

$$X + A \rightleftharpoons 2U \tag{1.50}$$

$$U \rightleftharpoons X + Z \tag{1.51}$$

$$2X \rightarrow A + P \tag{1.52}$$

$$X + Y \rightarrow P \tag{1.53}$$

$$A + Y \rightarrow X + P \tag{1.54}$$

$$Z + B \rightleftharpoons R_1 \tag{1.55}$$

$$R_1 \rightarrow Y + R_2 \tag{1.56}$$

$$B \rightarrow Y \tag{1.57}$$

$$2R_2 \rightarrow products \tag{1.58}$$

$$R_1 + R_2 \rightarrow products \tag{1.59}$$

$$\tag{1.60}$$

In accordance with what was said earlier about the complicated nature of the organic part of the mechanism, two radicals were introduced: $\bullet CBr(COOH)_2$ (R_1), known already from the RZ model, and $\bullet COH(COOH)_2$ (R_2). These modifications allowed the authors to successfully simulate shapes and periods of oscillations for both the cerium- and ferroin-catalysed systems.

Reaction-diffusion equations

The aforementioned models reproduce more or less accurately the chemical oscillations in stirred solutions. It is not possible, however, for those models to similarly describe the various phenomena occurring in thin unstirred layers of BZ solution. The models which

we would like to exploit to this end should incorporate diffusion somehow.

Fortunately, the process of diffusion is well described mathematically and in most cases it is enough to add the respective terms to the differential equations, the equations themselves becoming of course partial in the process. The example below is the reduced Oregonator model capable of reproducing reaction-diffusion phenomena.

$$\epsilon \frac{\partial u}{\partial \tau} = u - u^2 - 2fv\frac{u-q}{u+q} + D_u\nabla_u^2 \tag{1.61}$$

$$\frac{\partial v}{\partial \tau} = u - v + D_v\nabla_v^2 \tag{1.62}$$

D_u and D_v are the diffusion coefficients (in reality they are often set to simply 1 to facilitate mathematical analysis), whereas ∇^2 is the nabla operator, which is responsible for the dependence of reagent concentrations on the spatial coordinates:

$$\nabla^2 = \sum_{i=1}^{D} \frac{\partial^2}{\partial x_i^2} \tag{1.63}$$

where x_is $(i = 1,...D)$ form an orthogonal coordinate system in D dimensions. Because the layer of solution is very thin, it can be treated as two dimensional and hence $D = 2$.

1.4 The human nervous system

The human nervous system is the most sophisticated of any living organism, mainly due to the brain, whose degree of development is unparalleled in the animal kingdom - the human brain is around three times larger than brains of other mammals with similar size [46]. It functions as the "command center" of the whole neuronal network and together with the spinal cord makes up the central nervous system. All the other nerve cells belong to the peripheral nerve system, which is responsible for direct control of the muscles and receiving the signals from receptors.

1.4.1 Action potential

The basics building blocks of the nervous systems are nerve cells, called neurons. Their distinctive morphological outlook is the result of their function (Figure 1.15), which is essentially to transmit electrical impulses from and to other neurons, muscles and receptors. The dendrites are responsible for receiving the impulses, which then propagate along the axon (insulated from the surrounding due to the presence of the myelin sheath produced by Schwann cells) towards the terminals, where their arrival triggers the release of neurotransmitter molecules. These molecules migrate through synapses (narrow junction separating the neighbouring neurons) and trigger the electrical pulses in the subsequent dendrites. When the exciting impulse is too weak, it will quickly die out and no impulse will arise in the receiving neuron; dendrites will be excited, however, by any stimulus whose strength is above some specific threshold; this property is known as excitability.

From the physicochemical point of view, the electrical signal reflects the differences in membrane potential of a neuron [47]. When the neuron is in the resting state, the concentration of sodium cations outside the cell is greater than the concentration of potassium and chloride ions inside, and, as a result, the membrane is polarised negatively
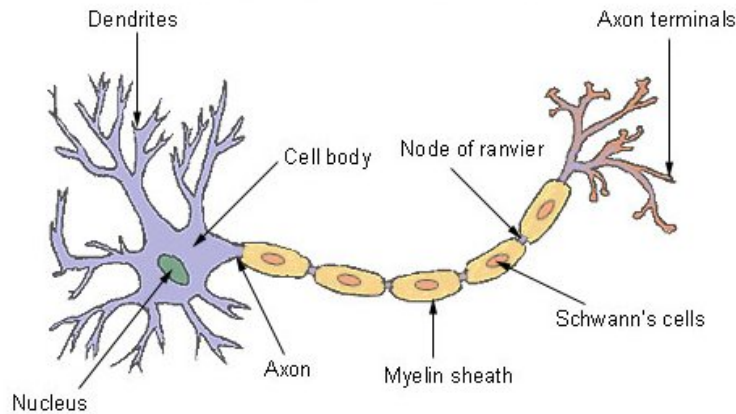
Figure 1.15: Structure of a typical neuron.

to around -70 mV. When the cell is sufficiently excited, the sodium channels start to open and the Na$^+$ ions enter rapidly. This causes depolarization and the membrane potential rises to around +30 mV - this process is known as firing. As the excitation fades, the sodium channels close and the potassium channels open, allowing the K$^+$ ions to leave the cell. Before the potassium channels are closed, there is a brief period of time when the membrane is hyperpolarized, i.e. its potential is below the value corresponding to the resting state - neurons cannot be excited again during this period, commonly called refractory period. Enzymes, called sodium-potassium pumps, then actively transport both types of cations across the membrane, restoring the resting conditions.

1.4.2   Theoretical models

The first attempt at modelling neurons dates from 1907, when the very mechanism of generation of neuronal impulses was unknown. The model (see review in [48]) treats the neuron membrane as a simple capacitor and considers the changes in voltage as the current flows through:

$$\frac{dV_m}{dt} = \frac{I(t)}{C_m} \tag{1.64}$$

C_m stands for the membrane capacitance. One of the model parameters is the threshold voltage V_{th}. When the current flow causes the voltage to rise above this value, the excitation spike is generated and the voltage is reset to the resting value. One important shortcoming of this particular model was the fact that this reset did not occur for the voltages below V_{th}, and so the firing could be caused by the accumulation of such redundant voltage values. The shortcoming could be eliminated by adding a term $-\frac{V_m(t)}{R_m C_m}$, with R_m marking the membrane resistance. This addition might represent, for example, slow leaking of ions from the cell.

In 1952, Alan L. Hodgkin and Andrew Huxley introduced a model of neuronal excitation which is still, together with its derivatives, in wide use today and became known as the Hodgkin-Huxley (HH) model [49]. The cell membrane is represented with a capacitor and the ion channels by resistance elements, so that the input current enters a simple circuit as outlined in Figure 1.16 [50]. The symbols Na and K correspond to sodium and potassium channels, while the R represents the leakage channel, through which some unspecified ions leave the cell. It is then possible to write an expression for the changes
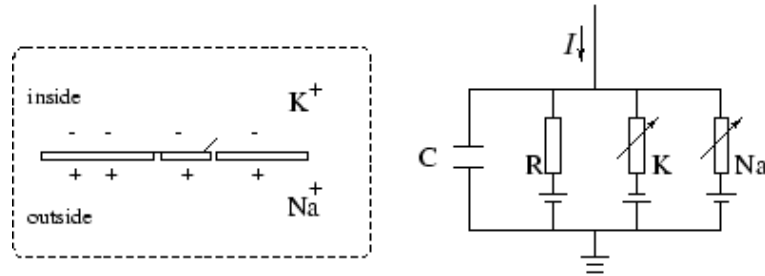

Figure 1.16: Schematic representation of the Hodgkin-Huxley model.

of voltage in time, similar to the one presented in the preceding paragraph.

$$\frac{dV_m}{dt} = \frac{1}{C_m}(I(t) - \sum_k I_k(t)) \tag{1.65}$$

The symbol I_k stands for a current which flows through a channel, and the sum ensures

that all three channels are considered. Hodgkin and Huxley represented the sum as

$$\sum_k I_k = g_{\text{Na}} m^3 h(V_m - E_{\text{Na}}) + g_{\text{K}} n^4 (V_m - E_{\text{K}}) + g_{leak}(V_m - E_{leak}) \quad (1.66)$$

where g are the respective conductances, and E the so-called reversal potentials; both the potentials and conductances were determined empirically. m, n and h are called gating variables and their time evolution is described by differential equations incorporating the values of membrane voltage, which coupled with the equation 1.65 form a system of four equations lying at the core of the model. The output of an example run is presented in Figure 1.17. A constant stimulus, which is translated in the model as a constant current, gives rise to a train of excitation spikes separated by refractory periods during which the membrane is hyperpolarized.
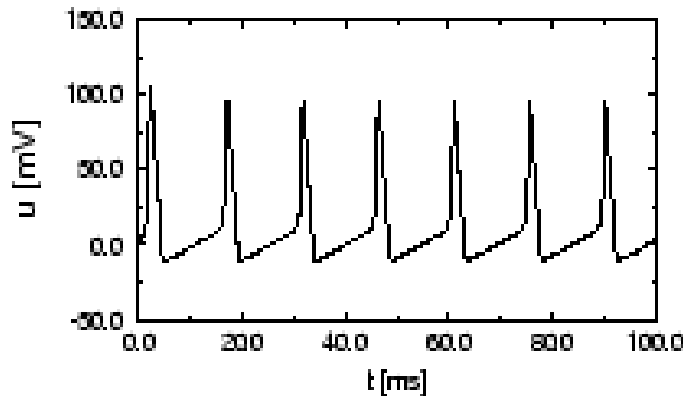

Figure 1.17: Train of spikes produced by a constant input $I(t)$ in the Hodgkin-Huxley model.

The HH model proved to be the most influential model of the action potential and its authors were honoured with the Nobel Prize in Medicine in 1963. Nevertheless, its complexity prevented it from being easily analysable mathematically as a model of the excitation phenomenon itself. This was changed at the beginning of the 1960s, when FitzHugh conceived [51, 52] and Nagumo built [53] a circuit described by mere two

differential equations corresponding to two time-dependent variables: membrane voltage v and the recovery variable w, which provided for slow diffusion of ions from the cell. In its essence, the model was based on the van der Pol oscillator [54], a model for nonlinearly damped oscillator:

$$\frac{d^2x}{dt^2} - \epsilon(1 - x^2)\frac{dx}{dt} + x = 0 \tag{1.67}$$

If we introduce a second variable of the form

$$y = x - \frac{x^3}{3} - \frac{1}{\epsilon}\frac{dx}{dt} \tag{1.68}$$

we get the system of two ordinary differential equations:

$$\frac{dx}{dt} = \epsilon(x - \frac{x^3}{3} - y) \tag{1.69}$$

$$\frac{dy}{dt} = \frac{x}{\epsilon} \tag{1.70}$$

Finally, after eliminating ϵ from the first equation and introducing two additional variables a and b, as well as the input current I, we arrive at the common form of FitzHugh-Nagumo equations:

$$\frac{dv}{dt} = v - \frac{v^3}{3} - w + I \tag{1.71}$$

$$\epsilon\frac{dw}{dt} = v - a - bw \tag{1.72}$$

The model indeed simplified the mathematical analysis of the various excitation-related phenomena; furthermore, as will be presented in detail in the next section, it proved to be of importance in the analysis of oscillating chemical reactions.

1.5 Chemical computation: modelling neurons with the BZ reaction

As remarked in subsection 1.3.4, chemical waves, or pulses, arise when a thin layer of unstirred solution of the BZ reaction is locally excited, for example with a silver wire. The use of the word "excitation" in this context is no coincidence: in many respects it exhibits the same properties as the excitation in neurons. For example, the exciting factor must be above a specific threshold in order to start the autocatalytic reaction sequence. Furthermore, as diffusion causes the chemical oxidation front to move outwards from the centre of excitation, the system around that point enters a refractory period, during which no further waves can appear. When the first theoretical models of oscillating reactions, such as the Oregonator, were published, their formal similarity to the FitzHugh-Nagumo model of neuronal excitation became obvious.

1.5.1 Analogies between the FitzHugh-Nagumo and the two-variable Oregonator models

Let us now compare the two models directly, with the notation changed slightly to make the similarities evident:

$$\frac{du}{dt} = u - \frac{u^3}{3} - v + I \tag{1.73}$$

$$\epsilon \frac{dv}{dt} = u - a - bv \tag{1.74}$$

$$\epsilon \frac{du}{d\tau} = u - u^2 - 2fv\frac{u-q}{u+q} \tag{1.75}$$

$$\frac{dv}{d\tau} = u - v \tag{1.76}$$

The most important analogy between the models lies in the behaviour of their two variables: they can be conveniently described as either activatory (u) or inhibitory (v); upon examining the equations, it becomes clear that the variable u speeds up and v slows down the production of both components. In fact, the FitzHugh-Nagumo model has been used quite widely in applications related to excitable chemical media, including reaction-diffusion systems. We are justified, therefore, to place the phenomena occurring in BZ solutions next to the electric impulses running along neurons. As for the details of actual implementation in experiments, there are two approaches: one utilizing carefully controlled external conditions and another mirroring nature more closely and featuring self-organizing, compartmentalized medium. I shall describe both of them in turn.

1.5.2 Neuron implementation using spatially restricted excitable medium

Background

The idea of restricting the area in which the BZ reaction takes place and utilising it to imitate neuronal activity can be dated to initial works of Kenneth Showalter and his co-workers at the West Virginia University, concerned with propagation of chemical waves through narrow capillary tubes [55]. The experimental procedures described were used to construct the first logic gates employing the BZ reaction [56], such as the OR and AND gates depicted in Figure 1.18. The chemical wave exiting the capillary in Figure 1.18(a) is able to excite the medium situated between capillaries (leading in the absence of waves in the other capillary to behaviour characterising the OR gate – output 1 when inputs are 1 and 0) but when the concentration of NaBrO$_3$ is smaller, the same input condition leads to output 0 (Figure 1.18(b)), the AND gate.

The young line of research has really taken off after the Showalter group followed with another paper [57] in which he demonstrated that logic gates could be also constructed with tailor-made excitable areas created by printing the ferroin catalyst on a membrane. This time the gates were capable of more complicated signal manipulations. Figure 1.19
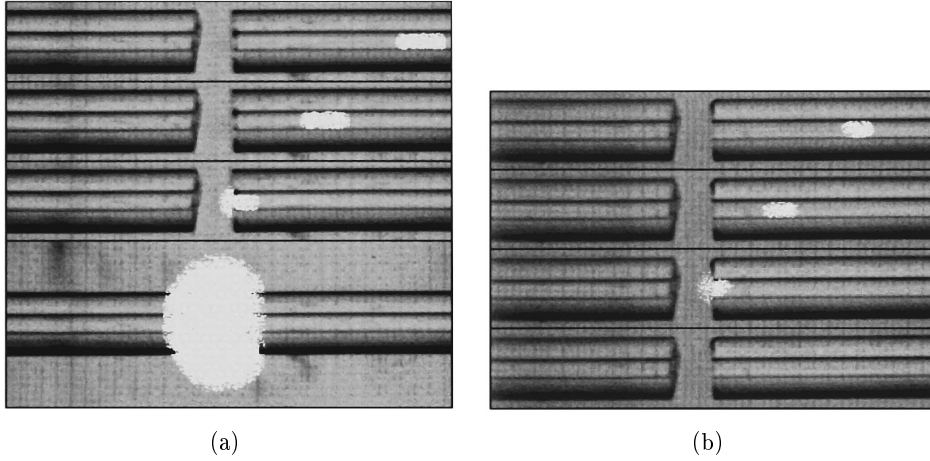
Figure 1.18: The chemical OR and AND gates built with capillary tubes [56]. The state of medium at the junction between tubes defines the output.

presents examples of two complex gates. The gate (Figure 1.19(a)) has four input values,
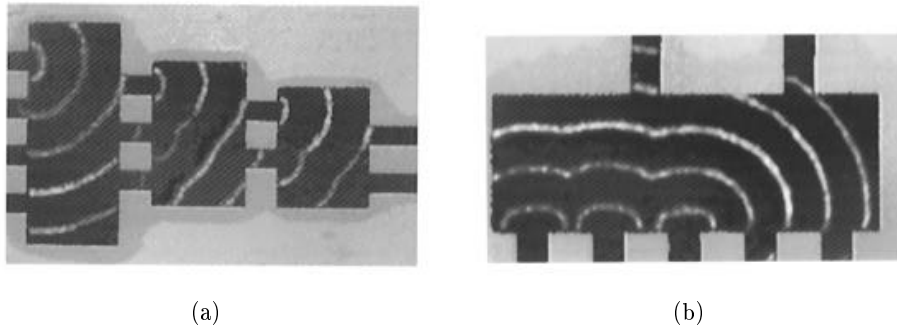

Figure 1.19: The complex gates built with printed patterns of ferroin catalyst [57].

one of which is always 1, and the remaining three represent the proper input of the gate. When the chemical pulses appear in the two output channels simultaneously, the system is assumed to be returning 1, when they are not synchronized − 0. In this case, the latter is observed only for input composed of nothing but zeroes, therefore it is an OR gate. On the other hand, Figure 1.19(b) shows a network implementing three gates at the same time: OR gate on each pair of inputs (the leftmost value is always 1, as before) and AND gate on the output values of the two OR gates.

Finally, it is necessary to mention the paper of Agladze et al. [58], in which the authors demonstrated the feasibility of constructing a first chemical diode, that is a device allowing the signals to pass in only one direction and widely used (in its electronic form) in computer circuits. The diode (Figure 1.20) was composed of two pieces of mesoporous glass soaked in ferroin and covered in the rest of the BZ reagents; chemical waves coming from the right were too weak to excite the planar area on the left, but the propagation of oxidation front was not hindered in the opposite direction. The numerical
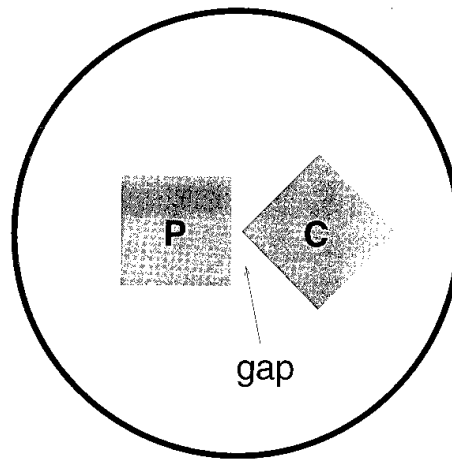
Figure 1.20: The chemical signal diode [58].

investigation [59] within the framework of the Rovinsky-Zhabotinsky model revealed that this behaviour is consistent with the diffusion of $HBrO_2$ molecules (corresponding to activator u in the model) between the two plates, while the z variable (oxidized catalyst) is restricted to them.

Light-controlled computing devices

The first actual examples of using illumination-discriminated excitability to perform some computational tasks were published in 2003 and drew on an important work of Japanese researchers from the laboratory of Kenichi Yoshikawa in Kyoto, who demonstrated numerically, using the FitzHugh-Nagumo model, the variety of tasks which the medium is

able to implement [60], including logical operations, coincidence detection, diode operation, time-difference sensing and memory. Most of the results were later successfully demonstrated experimentally, starting with the memory cell. This device [61], shown in Figure 1.21, was employ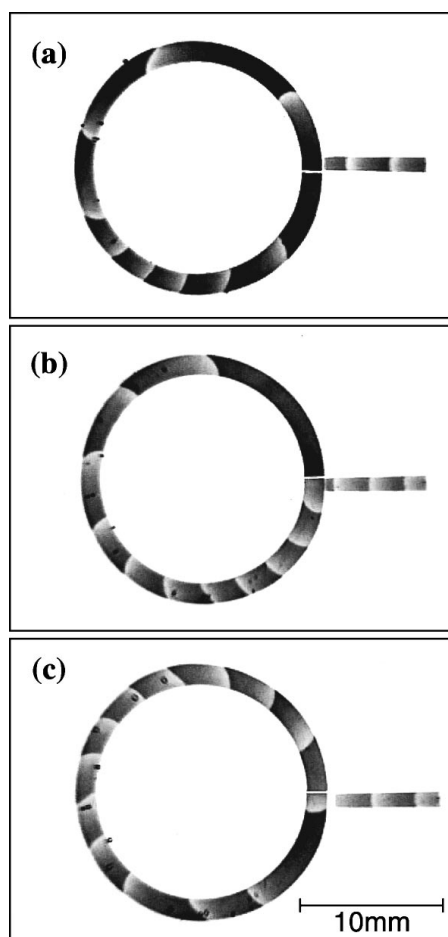ing the ferroin-catalysed BZ reaction, but more intricate arrangement of channels was characteristic of light-controlled systems, which were soon to

Figure 1.21: Memory cell built with the BZ reaction [61]. The incoming pulses can be made to rotate clockwise or counter-clockwise, as well as erased, depending on the placement on the input channel, because they are not able to propagate through the gap perpendicular to their direction of motion. On the other hand, pulses already in the cell can move straight through the gap.

rangement of channels was characteristic of light-controlled systems, which were soon to follow.

Ruthenium-catalysed BZ reaction was used in various later experiments demonstrating the practical feasibility of the Yoshikawa group's results, such as the ones related to coincidence detection, i.e. signalling the collision of two excitation pulses. One type of such detector is presented in Figure 1.22; due to the presence of a narrow illuminated (therefore non-excitable) gap between the two channels the bottom channels can be excited only when subject to relatively strong stimulus, such as the collision of two waves directly above the gap – this is, in fact, equivalent to the AND gate. The authors further
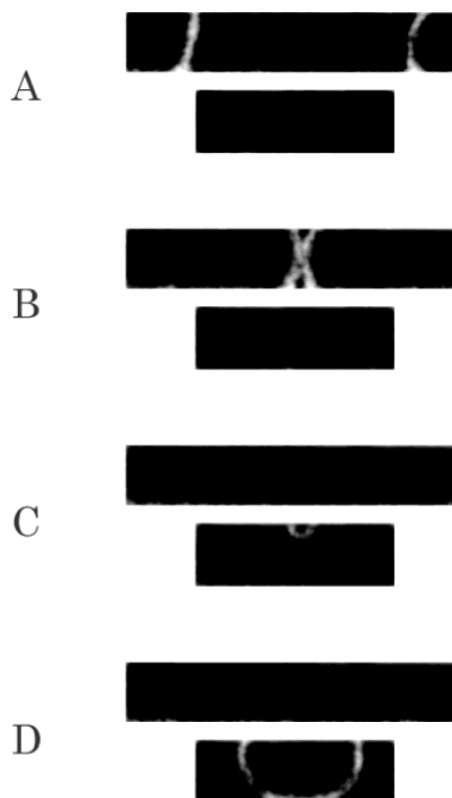
Figure 1.22: Coincidence detector outputting an excitation on collision of two incoming pulses [62].

demonstrated that, combined with diodes and memory cells, such device can be used to count chemical pulses [62]. In a related work [63], besides slightly different type of collision detector, the authors have built chemical devices sensing time-difference between arriving pulses and recreated the idea of chemical diode, this time without cutting glass

pieces, producing the desired arrangement of excitable areas with light. Common to all these works was the use of membranes, which were soaked in the solution of the BZ reagents, placed under silicon oil layer and illuminated in a desired fashion from below.

An important complementary result was the discovery that systems performing chemical computation could be generalized and made one-dimensional. This was thanks to the introduction of additional level of light intensity, corresponding to third, intermediate excitability level. The local weakening of excitation, necessary for the construction of diodes and controlling gaps (as seen above) could be achieved without tampering with shape of the channels, as was proven already in 2000 by implementing a diode with the aid of ferroin printed on a membrane in layers characterized by different thickness and separated by inexcitable gap [64]. Figure 1.23 shows the same effect achieved in a photosensitive system [65].
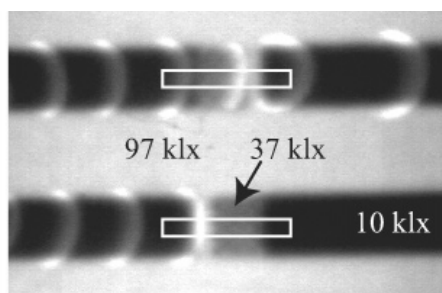
Figure 1.23: One-dimensional chemical diode [65].

1.5.3 Biomimetic BZ systems

The aforementioned systems served the initial aims of researchers looking for analogies between neurons and chemical systems well. There even appeared a report on what could be called direct neuron imitation with channels created by illumination [66]. In a manner similar to real neurons, the system received its input from several channels ("dendrites") and outputted the result to one, wider channel ("axon" - Figure 1.24). In this way, various information processing operations could be performed in a setting
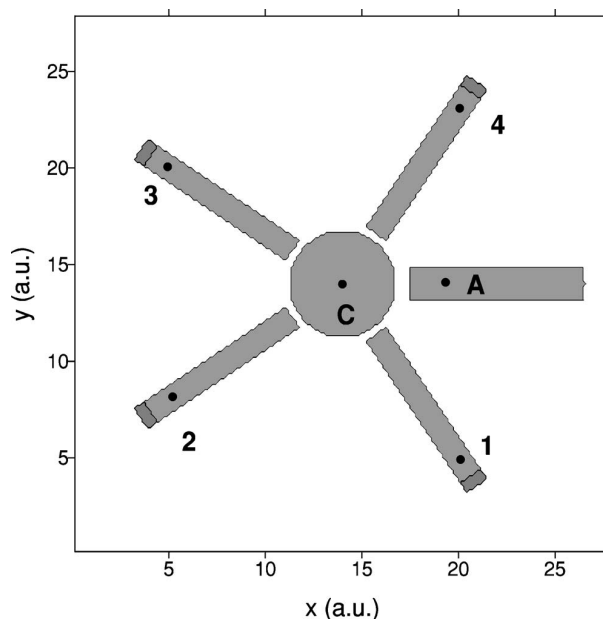
Figure 1.24: Neuron-like arrangement of excitable channels implementing simple logical operations [66].

simpler than arrays of logic gates strung together. The whole structure was, however, introduced externally – the medium had to be forced by experimentalists and there was no structural self-organization whatsoever. The approach pursued in this thesis involves creating systems based on the BZ reaction which would be structurally organized by their very nature.

An important example of what exactly is meant here is provided by the ground-breaking work of nonlinear dynamics group at Brandeis University. Using a water-in-oil microemulsion composed of aqueous solution of BZ reagents, hydrocarbon oil (most commonly octane) and surfactant sodium bis(2-ethyl-hexyl)sulphosuccinate (AOT) [67] they were able to obtain patterns impossible to observe in ordinary BZ medium, such as oscillatory clusters, standing waves, Turing structures (structures stationary in time and space [68], considered important from the point of view of morphogenesis) [69], segmented waves [70] and spirals [71]. Figure 1.25 shows the elementary building block of these systems, a nanometre-sized micelle formed with the surfactant molecules.
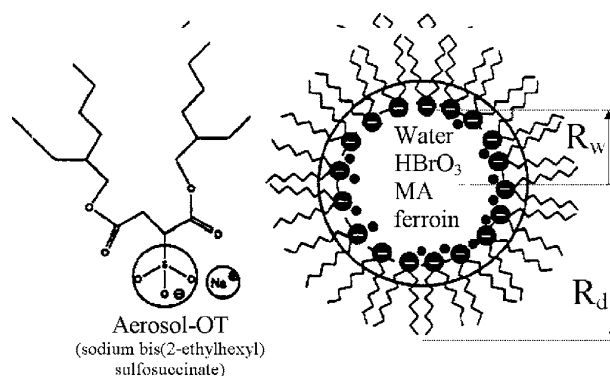
Figure 1.25: Structure of a BZ-AOT micelle [72].

Among the later achievements of the Epstein group was the introduction of microfluidic systems into systematic study of the BZ reaction. Such systems, based on manipulation of flow of droplets having volumes in the nanolitre range or below, were proven to be able to perform information processing operations even on their own [73, 74] and were considered as possible really powerful computational devices after coupling with oscillating reactions [75], but their construction naturally involves high degree of external influence. The direction taken by researchers at Brandeis was slightly different: they studied synchronization of oscillations in aqueous droplets of micrometer size separated by oil and placed in a microfluidic channel [76]. Depending on solution composition,
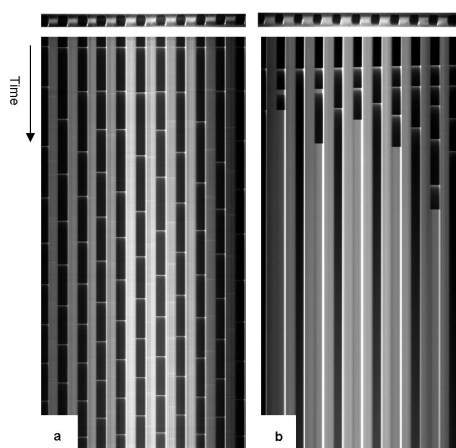
Figure 1.26: Anti-phase oscillations (a) and Turing structures (b) in BZ microdroplets [76].

the initially in-phase oscillations transformed into either stationary Turing structures or anti-phase oscillations (Figure 1.26). Similar effects were also observed in 2D arrays of droplets such as the one pictured in Figure 1.27 [77]. Moreover, more complex patterns of synchronization could arise when the number of droplets was limited [78].
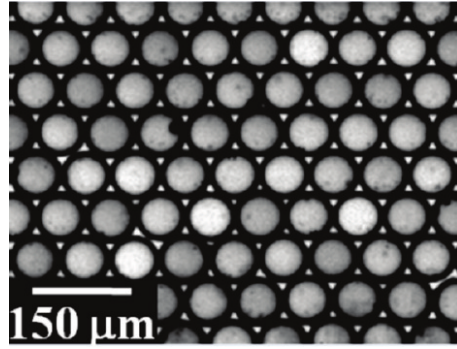

Figure 1.27: A 2D array of BZ microdroplets [77].

Chapter 2

Perspectives: the objectives of the thesis

As it was mentioned in the previous chapter, the majority of reported examples demonstrating chemical information processing operations involved restricting the region in which the chemical pulses could propagate, either by using capillary tubes or with the aid of photosensitivity. The real neurons, besides being spatially restricted by their nature, exhibit different arrangements and geometries, which manifests itself for example in various shapes and diameters of dendrites and has a direct influence on their excitability properties [79]. It was therefore of interest to investigate the behaviour of chemical waves in channels whose properties change along their length, for example in glass capillary tubes of conical shape, getting more narrow towards one of the ends [80].

One disadvantage of such systems was the fact that the glass surface interfered with the chemical processes occurring inside the capillary. In order to separate the genuine effects of the geometry and the physicochemical influence of the capillary material itself, an idea was put forward to create capillary-shaped illumination patterns and use them with the photosensitive, ruthenium-catalyzed BZ reaction taking place in a thin reagent-soaked membrane [81]. In the first part of my thesis (chapter 4), building on these results,

I would like to investigate the behaviour of this system on a longer time-scale, which is impossible in the membrane environment, chiefly because only a very small amount of reactive solution is present and the reagents get depleted quickly. On the other hand, when the BZ catalyst is immobilized on some sort of support, the volume of solution containing all the other reagents can be arbitrarily large. Indeed, reactors with the ruthenium complex on a gel layer have proven useful in studies on effects of forcing on chemical wave segments [82, 83], as well as on control of such segments by coevolutionary algorithms [84], because both applications require rather stable reaction conditions for extended periods of time. The addition of a flow reactor, in which the solution above the gel layer is constantly replenished, can extend the system lifetime even further, and this is the direction I would like to pursue in this work.

The second part of my thesis, with the results described in chapter 5 is directed towards modifying the biomimetic BZ systems so that they are able to sustain chemical waves necessary for the implementation of information processing operations. The droplets described by Toiya et al. [76] were useful as tools for the discovery of important collective effects, but their importance for biologically inspired unconventional computing was minimal, because there was no easy way to equate the observed phenomena with information processing operations. The principal reason for this was the absence of clearly defined directionality in systems of such microreactors, whereas any form of BZ-based computation must possess some kind of such property, which is best expressed in trains of travelling chemical pulses. In order to be able to observe such pulses, one needs droplets of markedly larger diameters, but also a direct communication between the different droplets.

The inspiration for progress in this field has been drawn from results concerning aqueous droplets surrounded by lipid monolayers which are able to form bilayers when forced into contact (Figure 2.1). Such systems have been studied mainly due to their promising biological relevance [86]. Although Funakoshi et al. [85] were the first to
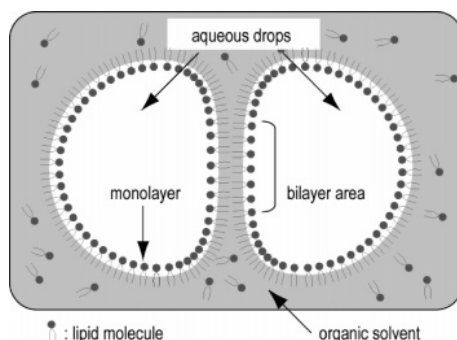
Figure 2.1: Two aqueous volumes surrounded by lipid monolayers can form a bilayer when in close contact [85].

create bilayers in the aforementioned way, the droplets were still enclosed in microfluidic channels. Next year, a group from Oxford reported creation of stable networks of aqueous droplets (Figure 2.2), with bilayers formed in the areas where the droplets touched each other, which was verified by incorporating channel proteins into membranes and recording the through current [87]. An important fact demonstrated by the same group was that
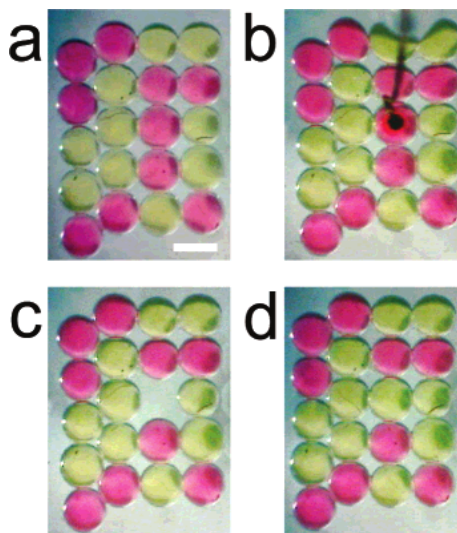
Figure 2.2: Dyed droplets contacting through lipid bilayers arranged in a stable network [87]. The scale bar is 700 μm.

the droplets in a network can communicate with each other in a directionally well-defined manner when modified channel proteins, allowing the current transmission in only one

direction, are incorporated into the membranes [88]. Taking all these results into account, it is a remarkably well-motivated task to investigate the possibilities of inter-droplet communication by introducing a system with well-described computational analogies, such as the BZ reaction, into the lipid-enclosed droplets.

The main objective of the present thesis is to demonstrate that both systems described above open new perspectives in reasearch concerning unconventional information processing, as well as providing hints on the simplest elements needed to perform such processing.

Chapter 3

The methods

In this chapter, I describe the experimental as well as the numerical techniques which were used in my thesis.

3.1 The light-sensitive ruthenium-catalysed system in a gel matrix

3.1.1 Experimental setup

Stock solutions of sodium bromate (1.5 M, Fluka), malonic acid (1.0 M, Alfa Aesar), sulphuric acid (3.0 M, Chempur) and potassium bromide (1.0 M, ABCR) were prepared using deionized water (Millipore, ELIX 5). The water glass solution was prepared by mixing equal volumes of water and commercially available sodium silicate solution (Roth). The gel with the immobilized ruthenium catalyst was fabricated according to the general procedure described in [89]: 1.829 ml of water glass, 0.082 ml of water, 0.468 ml of $[Ru(bpy)_3]Cl_2$ (Aldrich) 8.5 mM stock solution and 0.371 of 3M H_2SO_4 were mixed in a beaker and poured into a Petri dish whose diameter was equal to 58 mm. After solidification (taking several minutes) the gel was kept under 1M sulphuric acid for half an hour and finally rinsed with water.

The main part of the setup (Fig. 3.1) was the flow reactor fed with two separate syringes, one containing bromate and bromide solutions, the second one - malonic and sulphuric acid. The two solutions were mixed with the aid of a dedicated magnetic stirrer and pumped into the Petri dish containing the gel layer and 10 ml of BZ solution (0.45 M NaBrO$_3$, 0.35 M H$_2$SO$_4$, 0.35 M malonic acid, 0.06 M KBr), with another pump pumping the solution out of the dish at the same rate (0.24 ml/min), so that the reagent concentrations above the gel were kept constant. The image of the capillary was projected
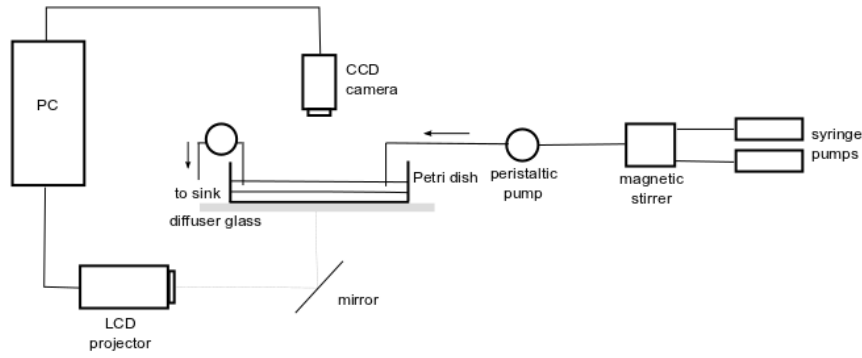
Figure 3.1: The experimental setup for long-time observations of chemical waves in a gel layer.

onto the reactive layer from below using a LCD projector connected to a PC and the medium was recorded by a CCD camera equipped with a blue filter.

3.1.2   Numerical methods: *in silico* experiments

The basis for the numerical simulations of the system was the two-dimensional Oregonator model modified to incorporate medium photosensitivity (1.34-35) and diffusion:

$$\frac{du}{d\tau} = \frac{1}{\epsilon}[u - u^2 - (fz + \phi)\frac{u-q}{u+q}] + D_u\nabla^2 u \qquad (3.1)$$

$$\frac{dz}{d\tau} = u - z \qquad (3.2)$$

The variables u and z represent the concentrations of activator HBrO$_2$ and oxidized ruthenium catalyst, respectively, D_u denotes the diffusion coefficient of the activator (taken as 1 for simplicity), while ϕ corresponds to the illumination intensity. The absence of the diffusion term for z is related to the fact that the catalyst is immobilized in the gel layer. The values of the simulation parameters were as follows: $\epsilon = 0.02272, f = 1.4, q = 0.002$.

In order to represent the reaction conditions accurately, the simulations were performed on a 2D grid with space-dependent illumination intensity (hence $\phi = \phi(x, y)$) assigned to all the grid points. I assumed that $\phi(x, y)$ could have one of the two ϕ values, corresponding to illuminated (ϕ_{out}) or dark (ϕ_{in}) areas of the gel layer, whose arrangement is illustrated in Figure 3.2. The chemical pulses were initiated on the left-hand side
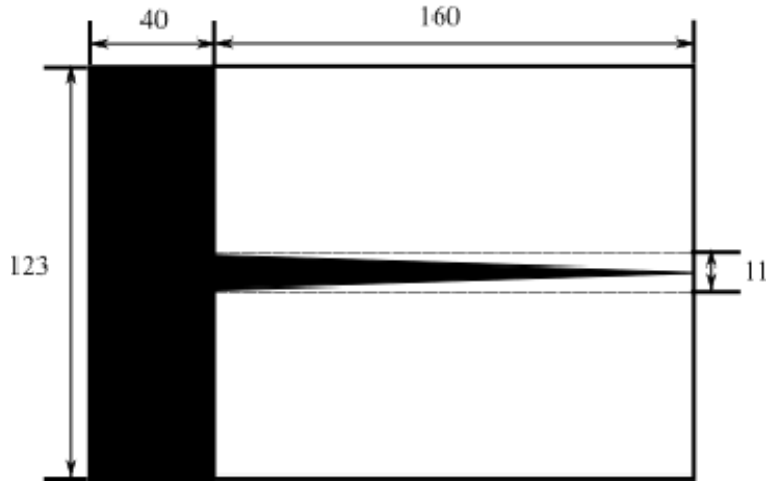

Figure 3.2: Geometrical arrangement of the optical capillary considered in the simulations. The value of ϕ in the dark areas is set to ϕ_{in} , in the illuminated ones - to ϕ_{out} . The numbers, denoting grid points, represent sizes of the different areas.

of the dark area by setting the value of u to 1.0 at a stripe which was 2 grid points wide and 11 points long, then they were allowed to propagate into the capillary (Figure 3.3). The Oregonator equations were integrated numerically using explicit Euler method for the diffusion part and the fourth order Runge-Kutta method for chemical kinetics, with temporal and spatial steps equal to 0.00025 and 0.125, respectively. I studied the time
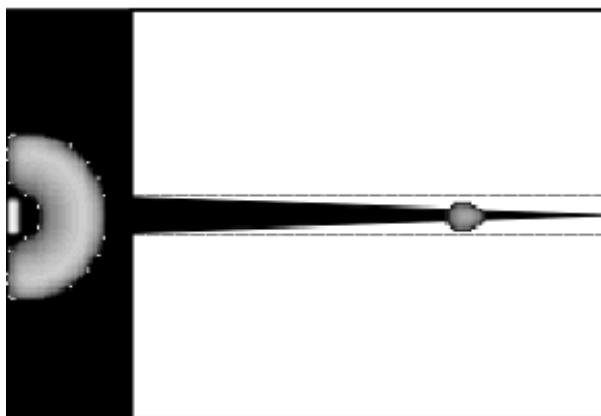
(a)
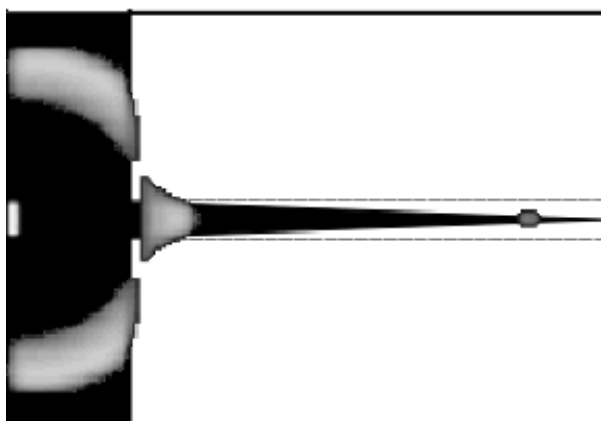
(b)

Figure 3.3: Snapshots of different stages of the system evolution. Gray pixels represent travelling excitation pulses, i.e. areas in which concentration of u is equal to at least 0.3.

evolution of the position of wave fragment closest to the capillary tip, i.e. the maximum penetration depth, which was saved every 160 steps.

It was assumed that a profile of u represents a pulse if the maximum value of this variable was equal to at least 0.3. The position of the rightmost point at which the u value satisfied this condition was then plotted as a function of time.

3.2 The BZ reaction in lipid-enclosed droplets

Stock solutions of sodium bromate (1.5 M, Fluka), malonic acid (1.0 M, Alfa Aesar), sulphuric acid (3.0 M, Chempur) and potassium bromide (1.0 M, ABCR) were prepared using deionized water (Millipore, ELIX 5). The 0.025 M stock solutions of ferroin and bathoferroin disulphonate catalytic complexes were prepared by mixing iron (II) sulphate (Roth), in molar proportion 1:3, with 1,10-phenanthroline (Roth) and disodium salt of bathophenanthrolinedisulphonic acid (Alfa Aesar), respectively. The aqueous BZ phase was prepared by mixing the aforementioned solutions in a small beaker in the order: sulphuric acid, bromate, malonic acid, bromide and adding the catalyst after disappearance of brownish colour which was due to bromine production. The oil phase was prepared by dissolving a predetermined amount of lipid mixture asolectin (Sigma) in decane (Sigma), with the most commonly used mass concentration being 5 mg/ml.

To prepare the working medium, a small volume (between 1.5 and 3 ml) of the oil phase was placed in a reaction vessel, which could be either a Petri dish or a PMMA container with trenches drilled in the bottom (Figure 3.4). Droplets of the aqueous phase were then immersed in the oil with the help of a micropipette and settled at the bottom of the vessel due to the density difference. In some experiments, a larger amount of the BZ solution was mixed with the lipid solution in volume proportion 1:3 and stirred, which gave rise to droplet formation. For the experiments during which the individual droplets had to be studied independently of one another, a reactor shown in Figure 3.5 was used; it consisted of several small glass tubes embedded into a PMMA support. The vessel was placed on a glass plate, illuminated from below with a slide projector and recorded with a DV camera (Sony DCR-HC88), with the output saved directly to a PC via WinDV application. The resulting movie clips were transformed into frame sequences with the aid of encoding software TMPGEnc and then further investigated using image analysis program ImageJ.
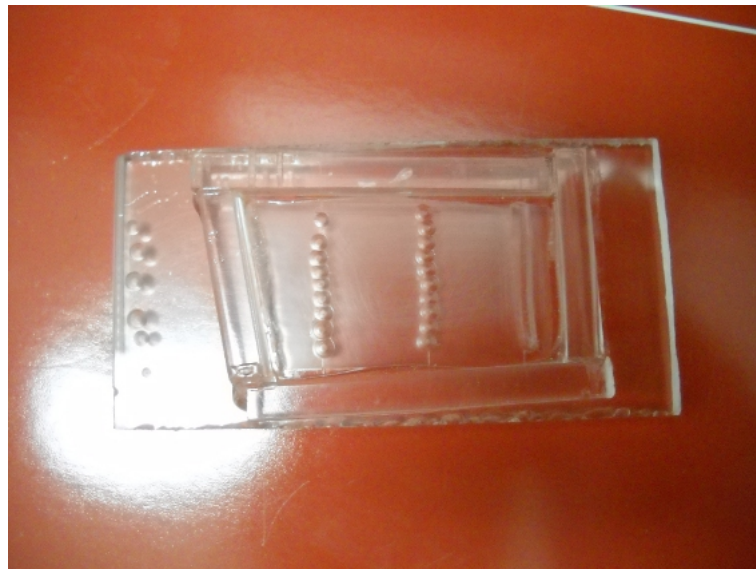
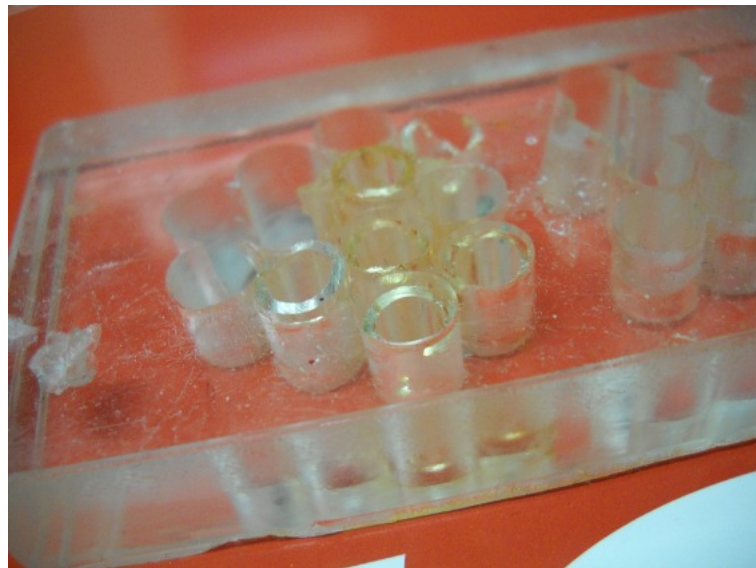Figure 3.4: PMMA reactor with the trench used for droplet experiments visible on the right.

Figure 3.5: Glass tubes used for independent measurements of oscillation period in droplets.

Chapter 4

The time evolution of chemical pulses propagating inside an optical capillary

4.1 Results

4.1.1 Experimental results

Figure 4.1 shows a top view of the reaction system consisting of the gel layer with the capillary pattern projected from below. The BZ reaction is initiated in a standard way with the aid of a silver wire and the pulses are restricted to the non-illuminated region.

Introduction of the flow reactor allowed, as expected, for the observations of the system behaviour on a long (over 60 minutes) time scale. What is more important, the observed behaviour was remarkably stable throughout a typical experiment. Usually, after an initial period of time required for stabilization, a pattern set in whereby every second pulse, rather than disappearing under the influence of light near the capillary tip, died out significantly earlier (Figure 4.2).
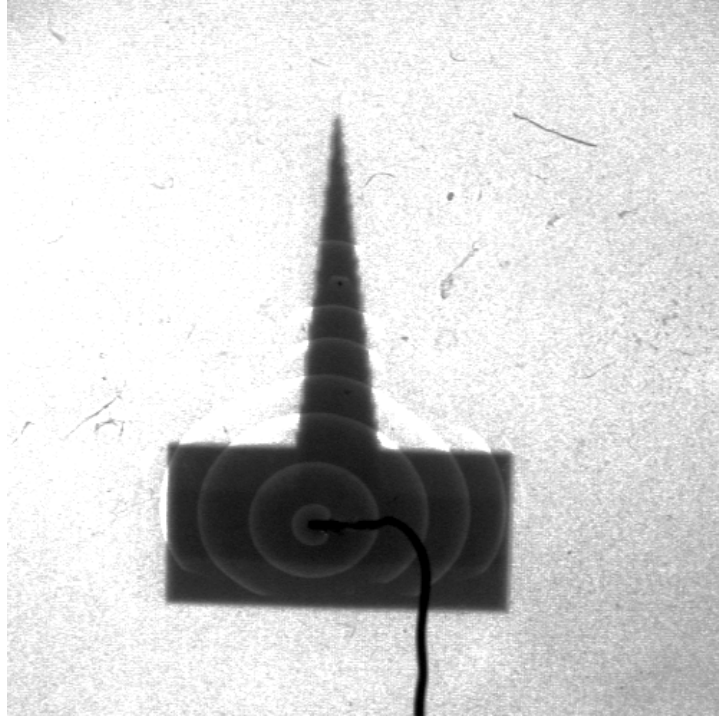
Figure 4.1: A snapshot showing the optical capillary experiment in progress. The triangular channel is 3 centimetres long and the length of its base is ca. 5 millimetres.

Due to local fluctuations in the thickness of the gel layer, the initial pulse frequencies at the point where the silver wire excited the system differed slightly between individual experiments. For larger frequencies, more complicated effects could be observed, for example similar to those presented in Figure 4.3. Here, for quite a long period of time, only one in three pulses was able to reach the capillary tip, the second disappeared approximately 5 millimetres before that, and the third - further 5 millimetres earlier.

4.1.2   Numerical results

Throughout all the simulations the parameter describing the illumination level inside the capillary (ϕ_{in}) was kept constant at 0.01, while that corresponding to the illuminated area (ϕ_{out}) was varied between the runs of the model. Such conditions corresponded to an experimental situation in which the optical capillary is not illuminated and the
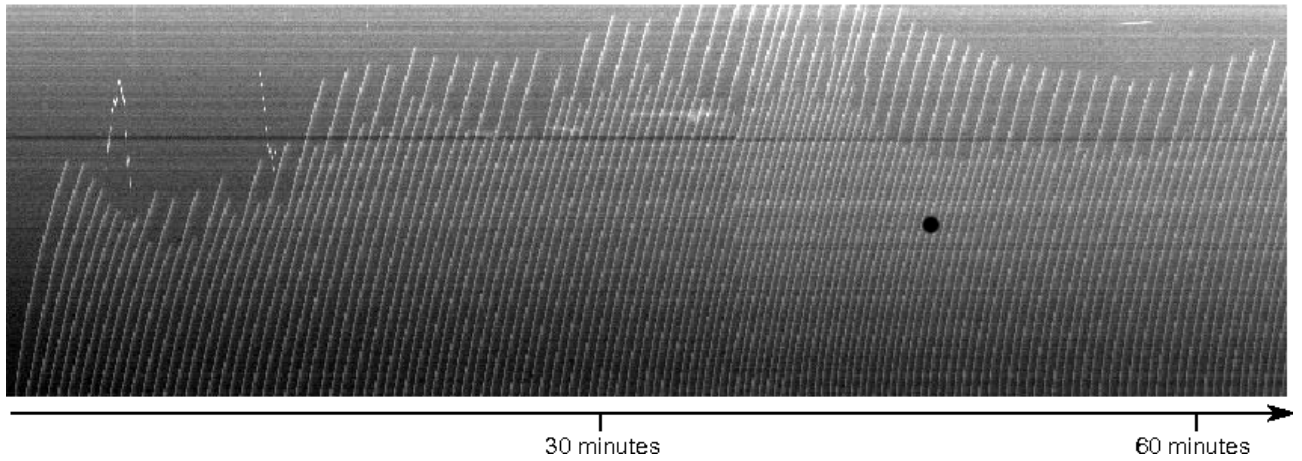
Figure 4.2: Space-time plot for a flow experiment, created by aligning concentration profiles taken along the symmetry axis of the channel. The vertical axis covers the length of the capillary, 3 centimetres, tip is at the top.
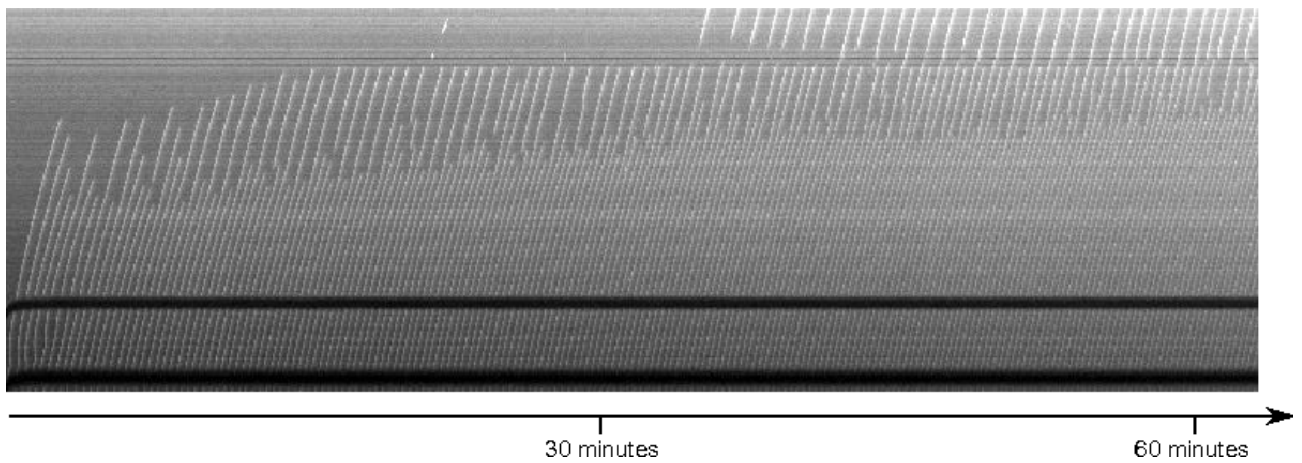

Figure 4.3: Space-time plot for a system with higher frequency of incoming pulses. The vertical axis covers the length of the capillary, 3 centimetres, tip is at the top.

illumination level outside it is treated as a free parameter. Depending on ϕ_{out}, two different regimes were observed with respect to the behaviour of the system - period-2 regime with every second pulse terminating a bit further away from the capillary tip than the rest, and period-1 regime with all the pulses dying out at the same point. Both types of behaviour are demonstrated in Figure 4.4. While searching for the critical value for which the transition between them takes place, we determined it to be equal to approximately 0.103 (figure 4.5).
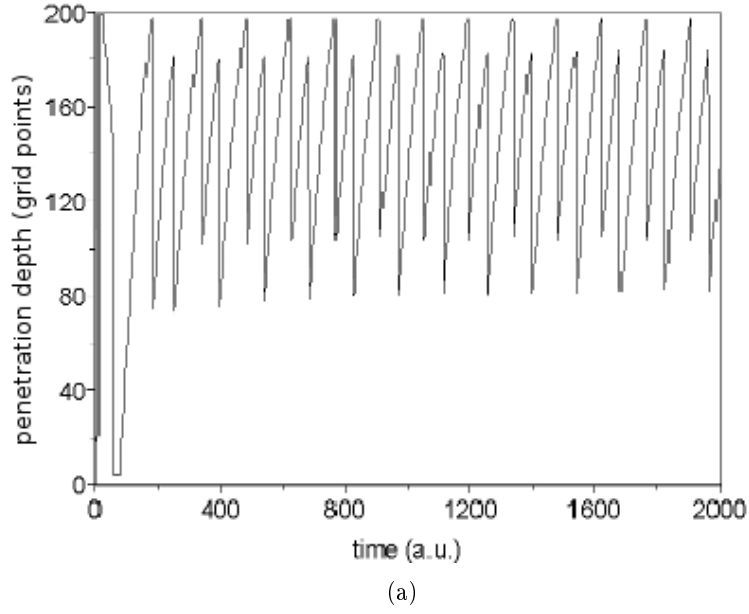
(a)

(b)
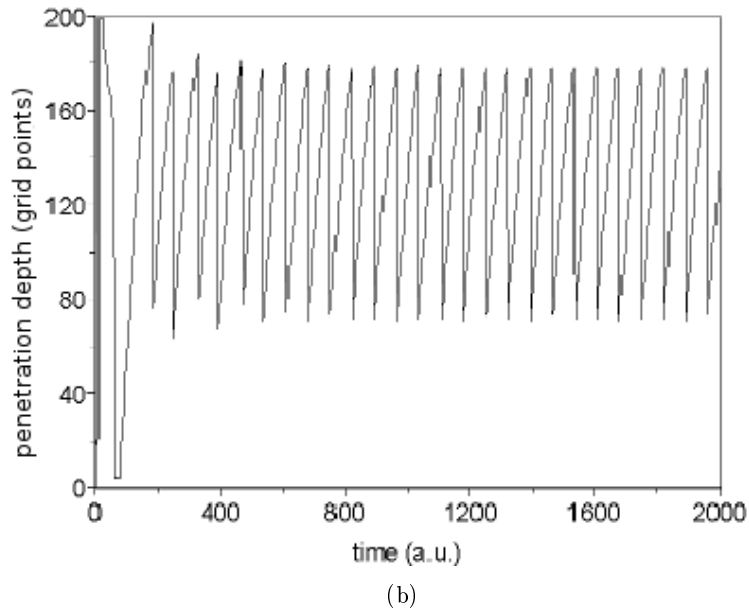
Figure 4.4: Position of an excitation pulse closest to the capillary tip as a function of time for ϕ_{out} equal to 0.1 (a) and to 0.11 (b). Number of time steps: 320,000.
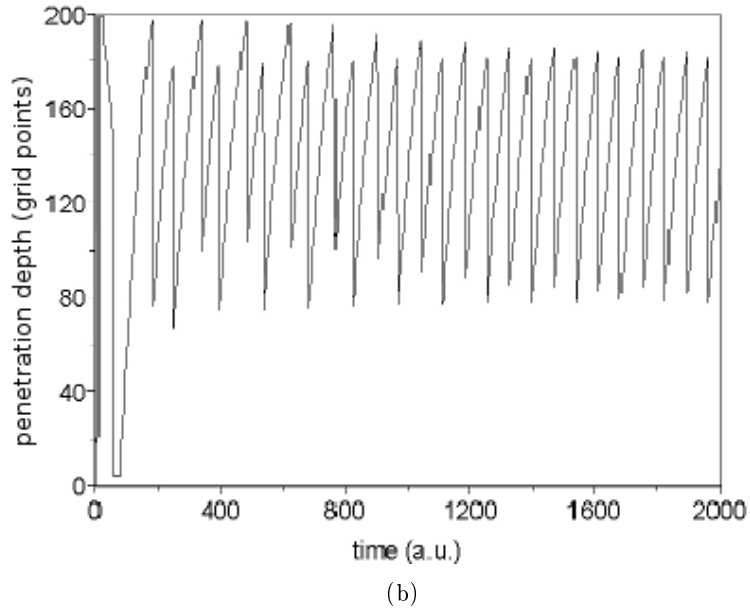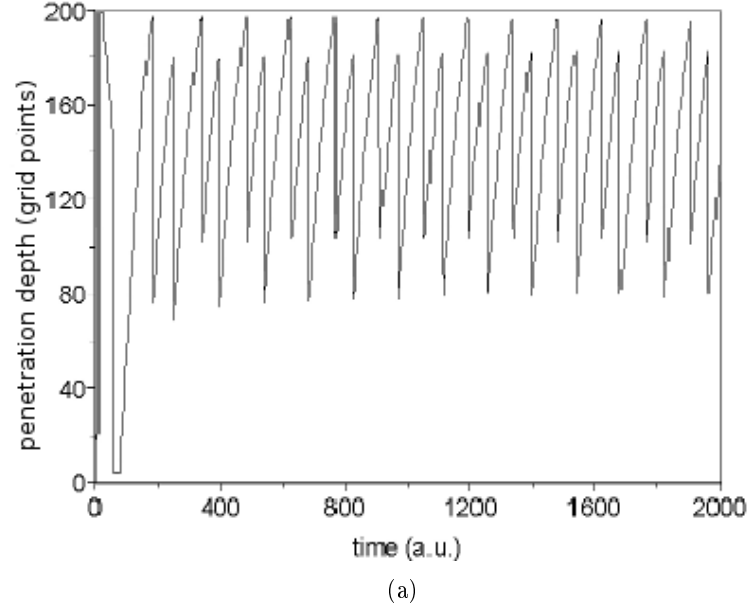
(a)

(b)

Figure 4.5: Position of an excitation pulse closest to the capillary tip as a function of time for ϕ_{out} equal to 0.102 (a) and to 0.104 (b). Number of time steps: 320,000.

In the subsequent simulations, I considered the situation in which the value of ϕ_{out} was gradually changed during the single *in silico* experiment, from the values characteristic for the period-1 regime to those conditioning the period-2 behaviour and vice versa. The value of ϕ_{out} was kept constant for a fixed number of time steps, then linearly decreased or increased towards a desired final value and remained constant for some more time steps.

An important observation was that while for increasing ϕ_{out} the expected transition occurred around the predicted value of 0.103 (as deduced from the type of the function describing the increase - Figure 4.6), the decrease in the parameter led to a different scenario. In this case, it is expected that the character of system evolution switches from the period-1 to the period-2 behaviour around the critical value of $\phi_{out} = 0.103$, but, as it turns out, the transition takes place only after the control parameter reaches its final value, regardless of the amount of time that the system is allowed to adapt to changing conditions (Figure 4.7) In order to confirm this effect, further simulations with even larger number of time steps devoted to linear decrease in ϕ_{out} were conducted; the final value of the control parameter was placed deeper into the region corresponding to the period-1 regime as well. The results are shown in Figure 4.8 and they demonstrate that the stable state corresponding to period-2 is harder to attain, this being possible only when ϕ_{out} has stabilized. For example, from Figure 4.8(b) it is evident that the transition occurs for $t > 4375$, although ϕ_{out} is below the critical value of 0.103 already for $t > 2875$.

Finally, the hysteresis-like nature of switching between the two modes was confirmed in simulations featuring sawtooth profiles of the parameter ϕ_{out}, in which the period-2 profile practically did not appear at all (Figure 4.9).
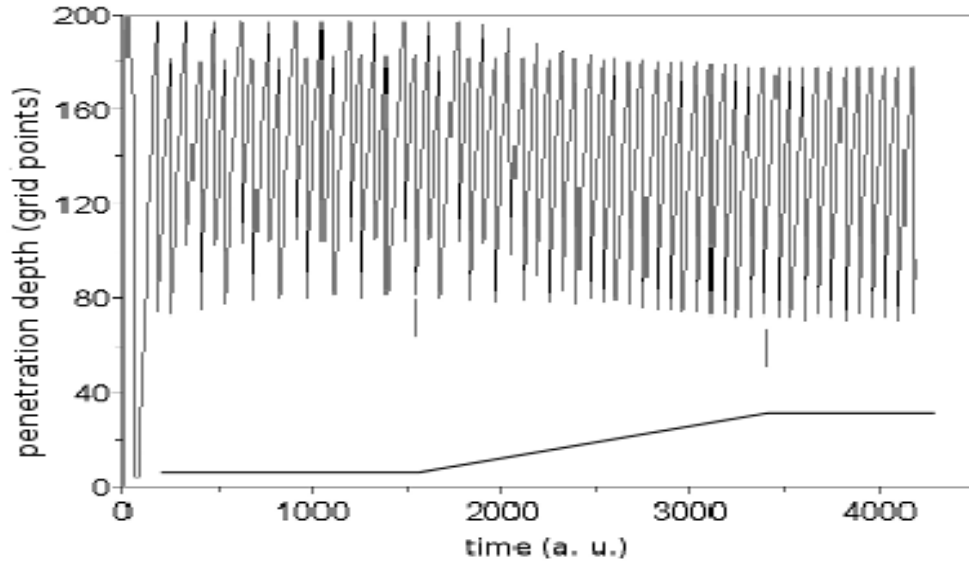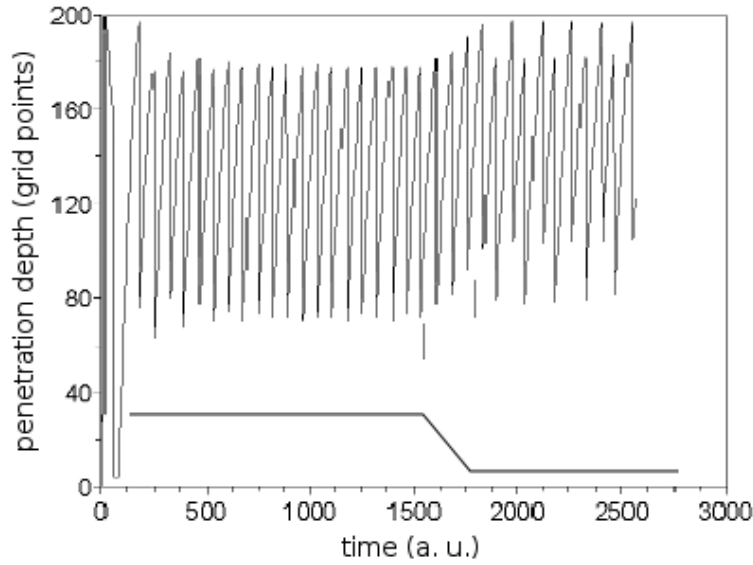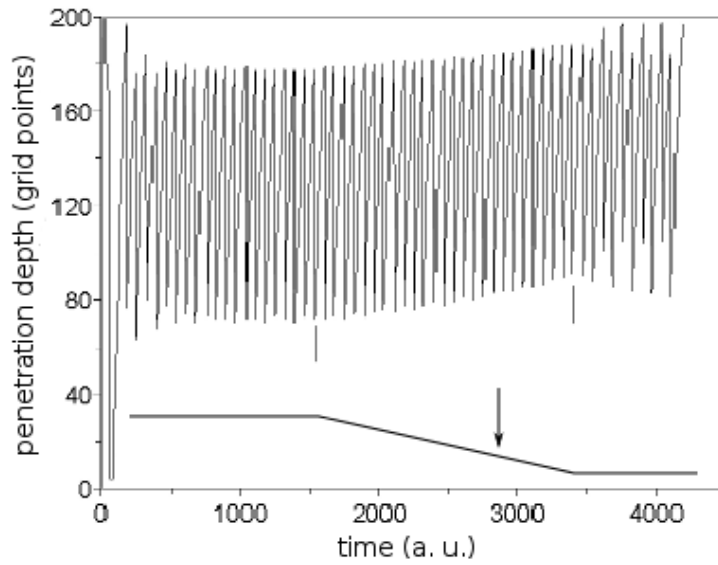
(a)
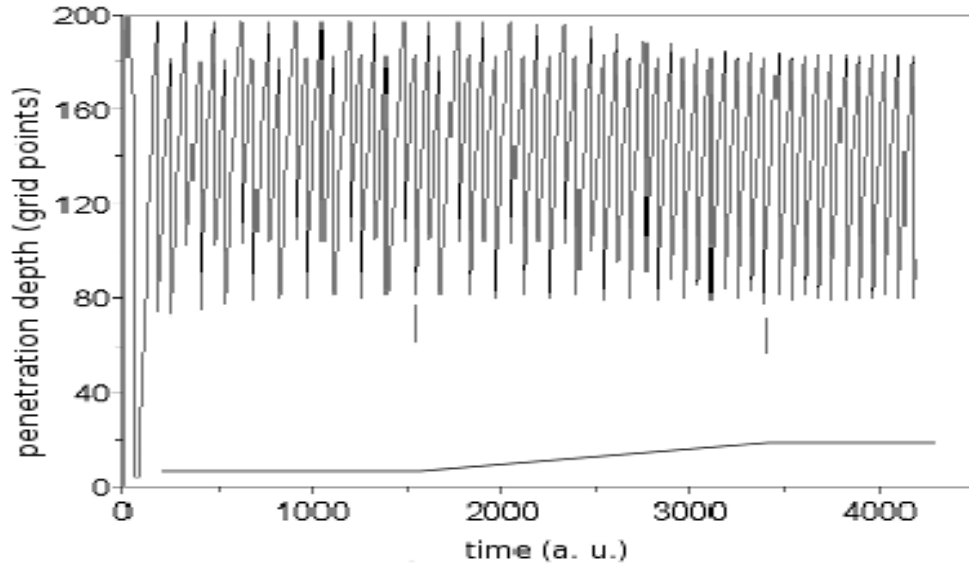
(b)

Figure 4.6: Position of an excitation pulse closest to the capillary tip as a function of time. ϕ_{out} was kept at 0.1 for 250,000 time steps, then increased linearly over 300,000 steps according to the function $\phi_{out}(t) = 0.1 + A\frac{t-t_0}{T}$, where $t_0 = 1562.5$, $T = 1875$, A was equal to 0.01 (a) or 0.00425 (b), so that the final values of ϕ_{out} were 0.11 and 0.10425, respectively. The parameter was kept at the final value for further 120,000 steps. The transition points are marked with lines. The values of the parameter as a function of time are given below the plots.
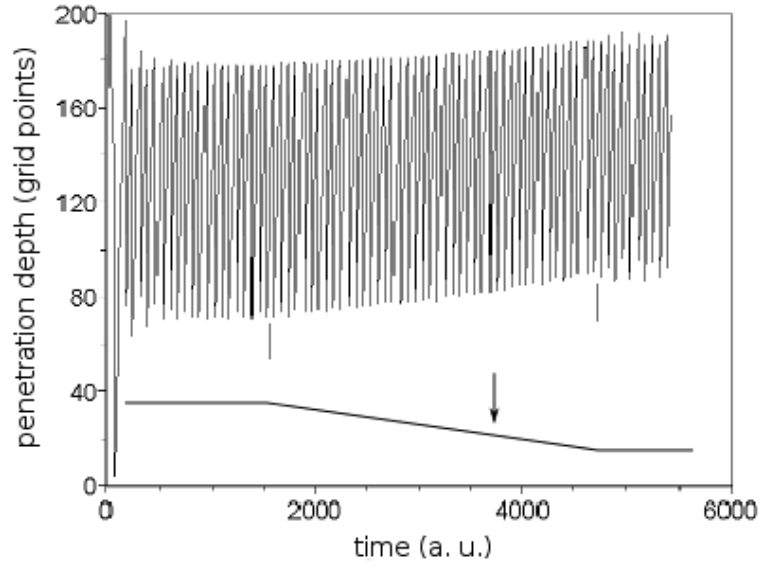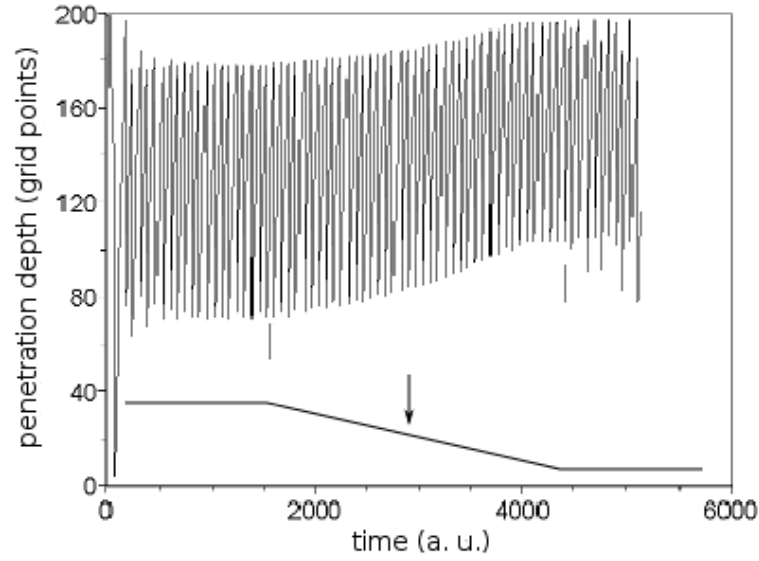
(a)

(b)

Figure 4.7: Position of an excitation pulse closest to the capillary tip as a function of time. ϕ_{out} was decreased linearly from 0.11 over 40,000 (a) and 300,000 time steps (b) according to the function $\phi_{out}(t) = 0.11 - A\frac{t-t_0}{T}$, where $t_0 = 1562.5$, $T = 250$ (a) or 1875 (b), $A = 0.01$, so that the final value of ϕ_{out} was equal to 0.1. The numbers of time steps used for stabilization and relaxation were the same as before. The transition points are marked with lines. The values of the parameter as a function of time are given below the plots; the arrow indicates the expected time for the switch to the period-2 regime.

(a)

(b)

Figure 4.8: Position of an excitation pulse closest to the capillary tip as a function of time. ϕ_{out} was decreased linearly from 0.11 over 500,000 (a) and 450,000 steps (b) according to the function $\phi_{out}(t) = 0.11 - A\frac{t-t_0}{T}$, where $t_0 = 1562.5$, $T = 3125$ (a) or 2812.5 (b), A = 0.01 (a) or 0.015 (b), so that the final value of ϕ_{out} was equal to 0.1 (a) or 0.0895 (b). The numbers of time steps used for stabilization and relaxation were the same as before. The transition points are marked with lines. The values of the parameter as a function of time are given below the plots; the arrows indicate the expected times for the switch to period-2 regime.
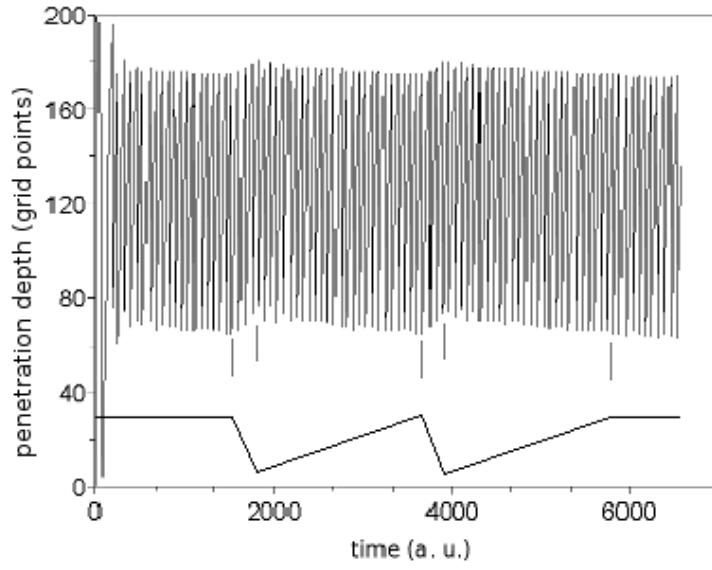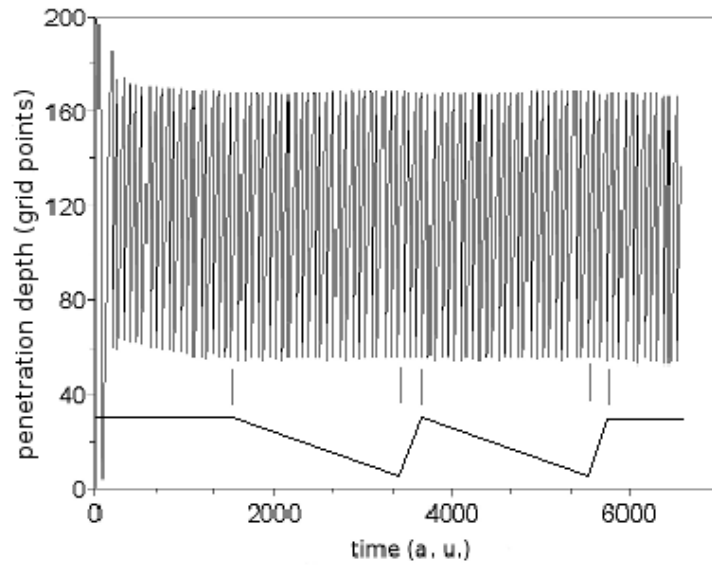
(a)

(b)

Figure 4.9: Position of an excitation pulse closest to the capillary tip as a function of time. ϕ_{out} was alternately decreased and increased over 300,000 and 40,000 time steps, varying between 0.1 and 0.11. The profiles of change in the parameter are given below the plots.

4.2   Discussion

The propagation of chemical waves of excitation in a capillary tube of triangular shape was first investigated in 2004 [80]. The capillary was prepared from a piece of glass and filled with the ferroin-catalysed BZ solution, and the waves were found to slow down and finally disappear as they approached the tip. The main factor influencing their disappearance was determined to be absorption of protons at the glass surface, which locally decreased acidity and therefore excitability. More complex patterns of pulse propagation inside such channels could be explored, with the aid of the photosensitive ruthenium catalyst, in a membrane soaked in the solution of all the BZ reagents and illuminated from below, with a dark mask creating the shape of a capillary similar to the one described in the present thesis [81]. The authors were able to discern two different regimes, one in which all pulses died out at the same distance from the tip, the other featuring every second pulse disappearing earlier. The particular regime the system was in at a given moment was apparently determined by the illumination intensity outside the capillary. It is of note, however, that the experiments supposedly confirming this finding differed in the frequency of the pulses entering the channel.

In fact, the frequency of incoming pulses was already proved to influence the behaviour of frequency-transforming systems [90], which finds its corroboration in my results, where a random rise in initial frequency leads to a switch from a simple 2:1 transformation regime to the one in which for each three pulses approaching the end of the capillary, each disappears at a different distance from the tip (Figure 4.3). One can envisage that for lower frequencies of arriving pulses the system should find itself in the 1:1 regime, although the fact that in none of the flow experiments was this behaviour actually observed forces us to treat the numerical results of the present work as corresponding to yet different case: systems with relatively low excitability. In such systems, when the illumination outside the capillary is high, none of the pulses are able to reach the tip and

the fronts of arriving pulses are spread over relatively wide area, which in connection with low initial frequency allows the next pulse to terminate at the same distance from the end as the preceding one. With the light intensity decreased, some pulses start to reach the tip and the pulses behind them are forced to enter the narrowest part of the capillary, whereby their fronts are too narrow to support propagation and they die out [91]. The direct reason for the disappearance of pulses is the high concentration of the inhibiting Br^- ions in the illuminated areas, resulting from the light-mediated reactions described in 1.3.4.

The system investigated in the present thesis presents a clear improvement over the membrane-based systems described above, in the sense that it involves constant replenishment of reagents and therefore allows for a much longer observation time. The presented results clearly point also to the existence of adaptive properties of the system, because slow changes in reaction conditions allow the 1:1 regime to survive in the region which would normally be reserved for the 2:1 regime. This is a demonstration of a general property of excitable systems [92].

Chapter 5

Belousov-Zhabotinsky reaction in droplets stabilized by lipid monolayers

5.1 Results

5.1.1 Chemical oscillations in droplets: general characteristics

Initial investigation

In the initial experiments, utilizing the commonly used ferroin catalyst described in 1.3.4, the droplets were created by agitation of a 1:3 mixture of the aqueous BZ solution and the oil phase. The agitation led to formation of group of droplets exhibiting oscillatory behaviour. The typical appearance of the system, when placed in a Petri dish, was as illustrated in Figure 5.1.

In order to verify whether the presence of lipids was in itself a necessary condition for the stability of this compartmentalized medium, a series of experiments was conducted in which the pure decane was used, in the same setting, instead of the lipid solution.

Figure 5.1: BZ droplets immersed in 5 mg/ml asolectin solution in a Petri dish. The thickness of the dish wall is 1 mm. The standard BZ solution composition: 0.3 M sulphuric acid, 0.45 M bromate, 0.35 M malonic acid, 0.06 M bromide, 1.7×10^{-3} M ferroin (video 1 on the accompanying CD).

As can be seen in Figure 5.2, the coherence of the system is significantly impaired when there are no lipids available. I performed a series of experiments in order to establish the lipid concentration needed for the optimal stability of the medium. As an approximate measure of the overall droplet stability, a time necessary for the majority of the droplets to merge into a big one was used. Figure 5.3 demonstrates the existence of a threshold lipid concentration value above which the stability-lipid concentration curve tends to flatten out. This value was close to the actual concentration of the stock asolectin solution, and increasing it above that value did not give significant benefits with respect to stability.
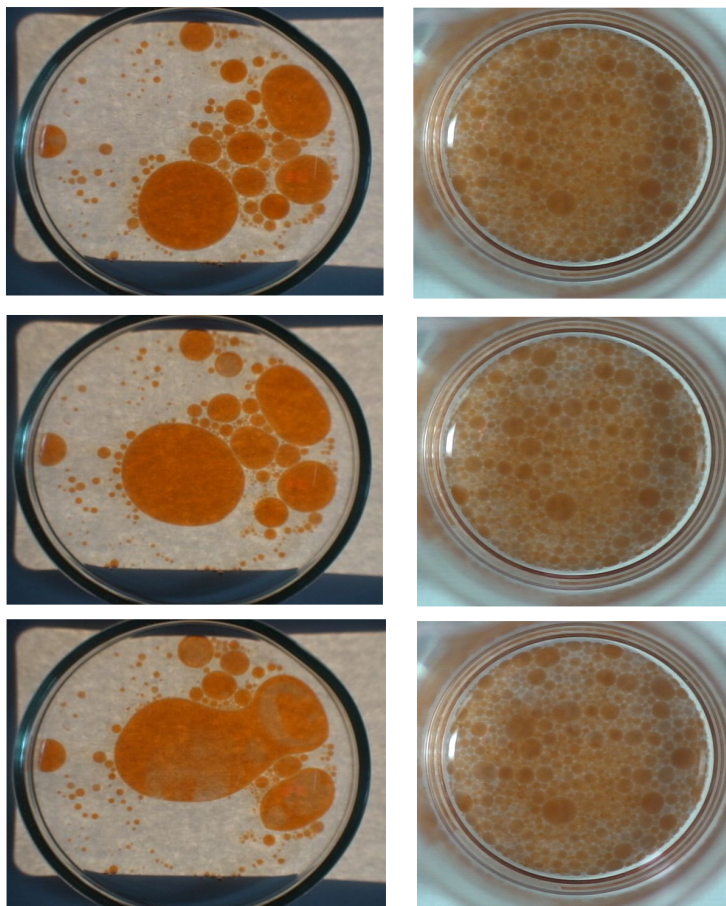
Figure 5.2: Comparison of stability of droplets in pure decane (left) and in the solution of lipids in decane (right). The subsequent figures show the system at times: t=0, t=16.5 s, t=31.5 s and at t=0, t=100 s, t=200 s for droplets in pure decane and in the solution of lipids in decane, respectively. The lighter blue areas correspond to a high concentration of oxidized catalyst. The diameter of Petri dish is 50 mm.
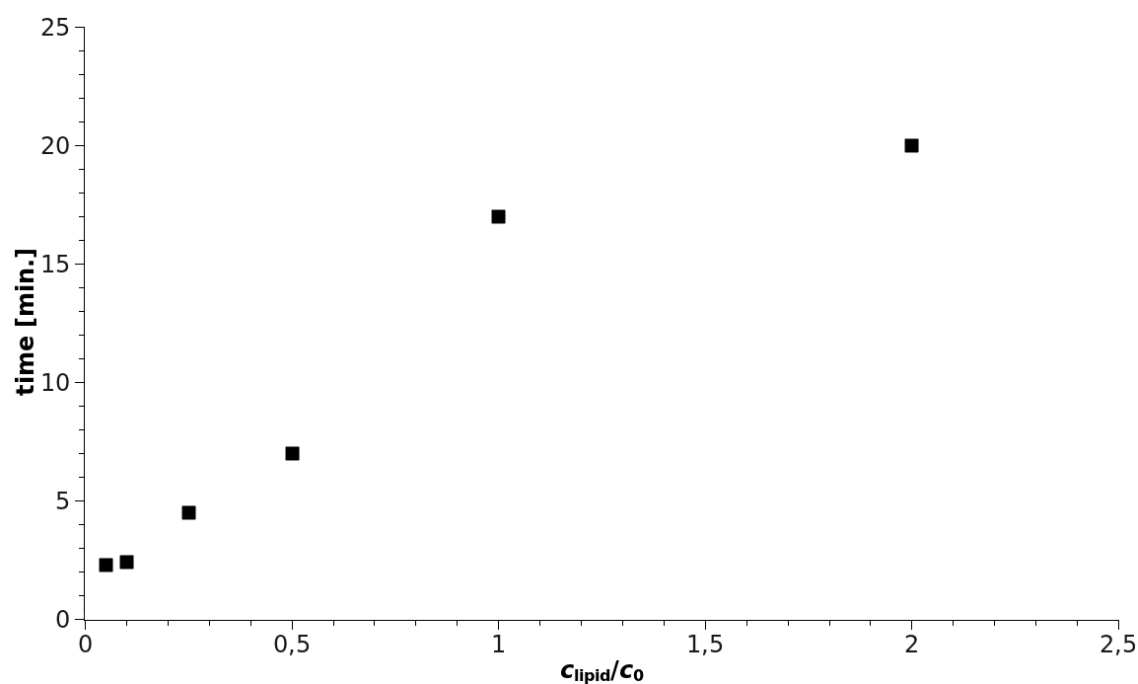
Figure 5.3: Stability of the droplets expressed as the time needed for them to merge as a function of lipid concentration c, where c_0 stands for the standard concentration, 5 mg/ml.

Period dependence on chemical composition

The second stage of the research on lipid-covered BZ droplets focused on determining the relation between oscillation period for individual droplets and the chemical composition of the BZ medium. A series of experiments was performed in which the droplets of volume 2.0 μl were pipetted each into a separate small glass tube containing the lipid solution (Figure 5.4(a)). The stable, clearly visible oscillations were observed in most cases, as demonstrated in a sample space-time plot of Figure 5.4(b). These plots, created by joining together 1-pixel wide fragments of the successive frames along the diameter of each droplet, prove the inhomogeneity of the oscillations, which is to be expected in droplets of the dimensions used.

The experiments were conducted for different combinations of reagent concentrations, giving a consistent pattern of oscillation period increasing with the concentration of the ferroin catalyst (Figure 5.5) and decreasing with the concentration of most of the other reagents: sodium bromate (Figure 5.6), malonic acid (Figure 5.7) and sulphuric acid (Figure 5.8). The Rovinsky-Zhabotinsky model of ferroin-catalyzed BZ reaction (1.3.5), after an optimization procedure taking the acidity dependence into account, showed qualitative agreement with the experimental data, as demonstrated in Figure 5.9.
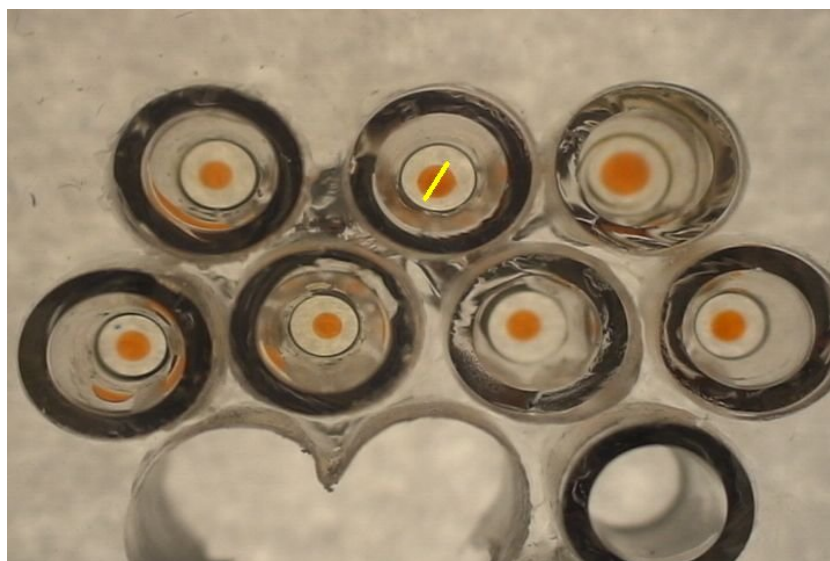
(a)

(b)
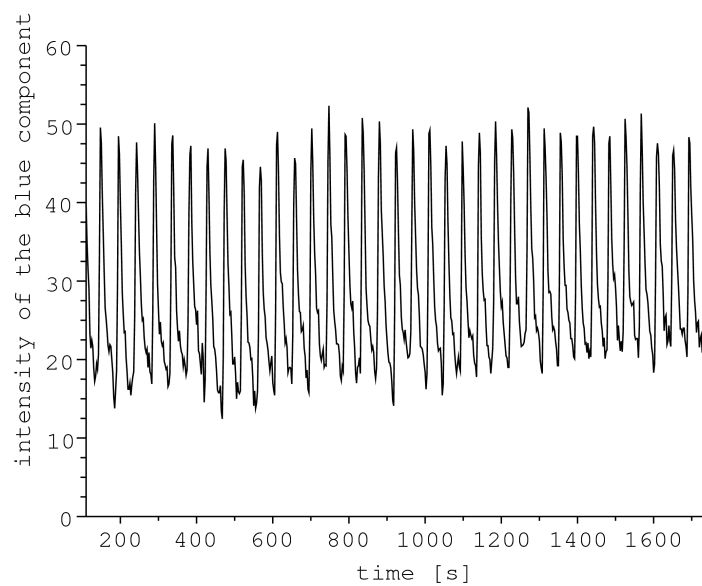
(c)

Figure 5.4: Oscillations in the droplets: in the upper panel, the setup used for the measurements of oscillation period in individual droplets; in the middle, the space-time plot; in the lower, the plot showing changes of blue color intensity (i.e. ferriin concentration) in time.
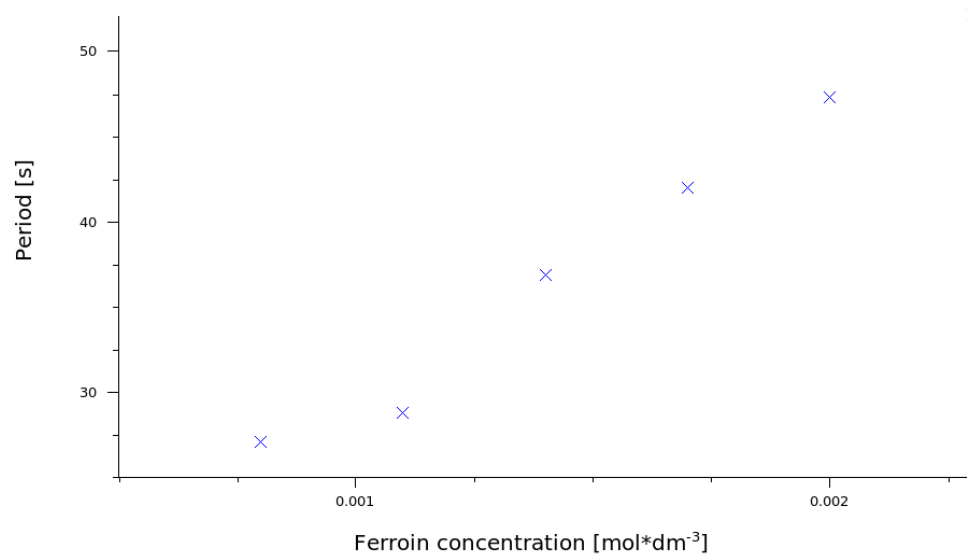
Figure 5.5: Oscillation period as a function of ferroin concentration. The remaining concentrations were: 0.3 M H_2SO_4, 0.35 M MA, 0.45 M $NaBrO_3$, 0.06 M KBr.
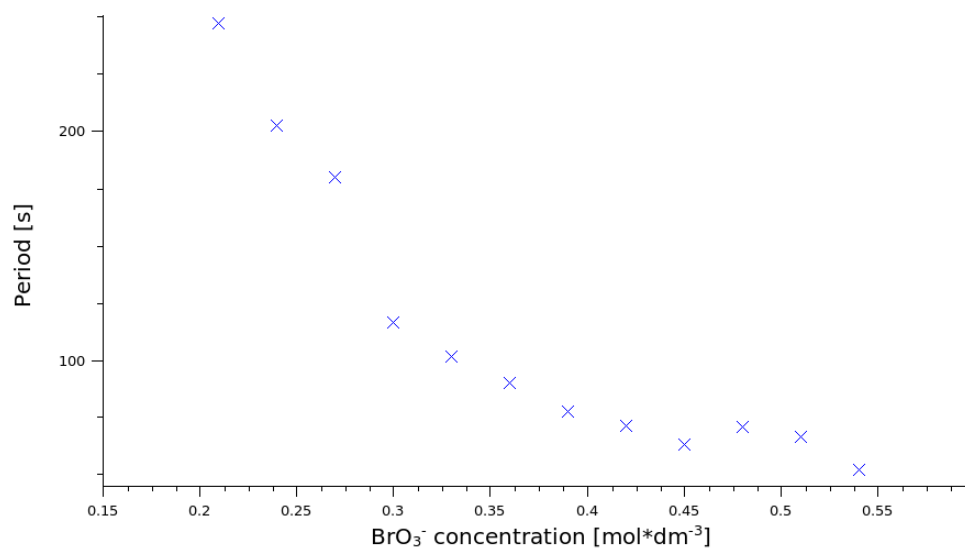

Figure 5.6: Oscillation period as a function of bromate concentration. The remaining concentrations were 0.3 M H_2SO_4, 0.35 M MA, 0.06 M KBr, $1{,}7 \times 10^{-3}$ M ferroin.
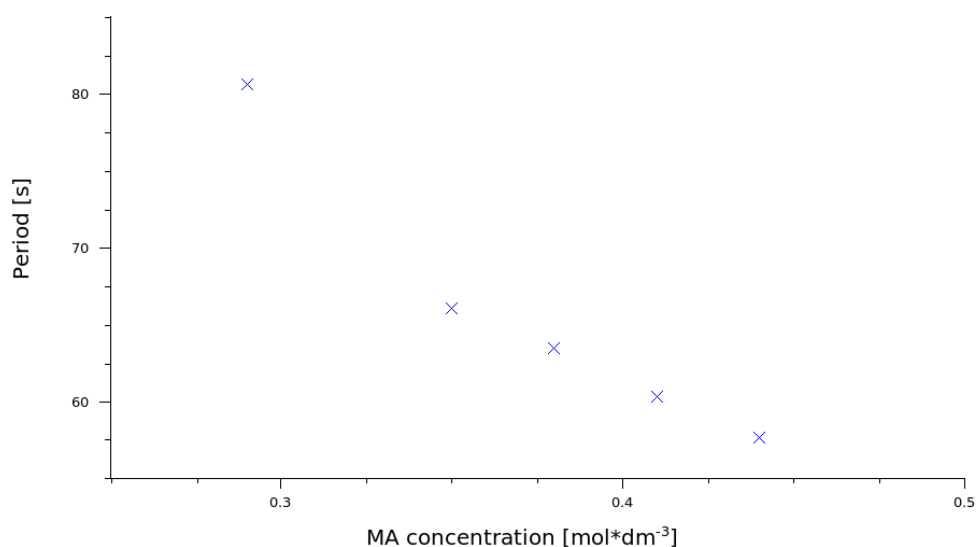
Figure 5.7: Oscillation period as a function of malonic acid concentration. The remaining concentrations were 0.3 M H_2SO_4, 0.45 M $NaBrO_3$, 0.06 M KBr, 1,7$\times$ 10^{-3} M ferroin.
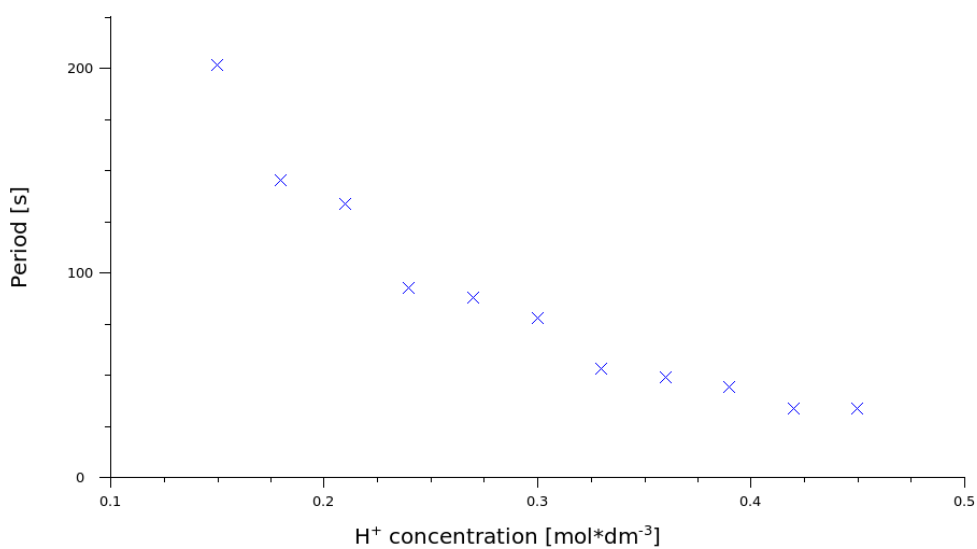
Figure 5.8: Oscillation period as a function of sulphuric acid concentration. The remaining concentrations were 0.35 M MA, 0.45 M $NaBrO_3$, 0.06 M KBr, 1,7$\times$ 10^{-3} M ferroin.

Figure 5.9: The experimental dependence of oscillation period on solution acidity described by the Hammett function (crosses). The solid line shows the period of oscillations calculated using the Rovinsky-Zhabotinsky model with the parameters $\epsilon = 0.3$, $\mu = 0.002$, $\alpha h_0^2 = 1.13 \times 10^{-3}$, $\beta h_0 = 5.9 \times 10^{-4}$.

Period dependence on droplet size

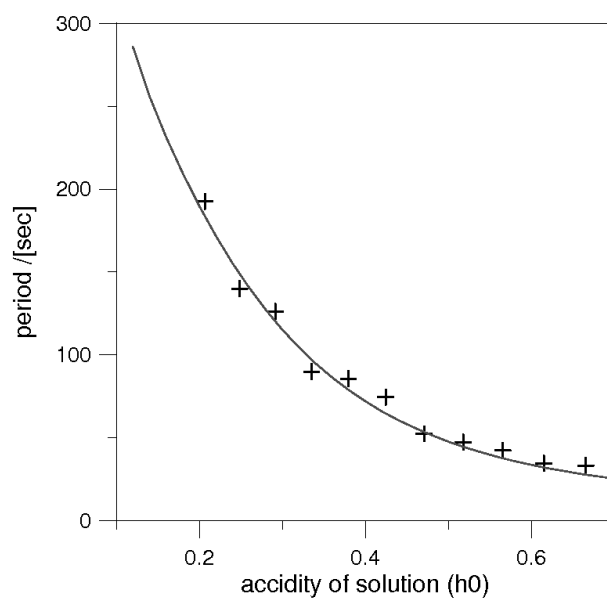The dependence of oscillation period on droplet size is a phenomenon which has already attracted some attention [93], although the investigation took place for a system with droplets surrounded by silicone oil. For the lipid–enclosed droplets, comparison of droplets with different diameters was made possible by manually stirring the mixture of the aqueous BZ medium and the lipid solution in a volume ratio 1:3. A typical plot illustrating the dependence of oscillation period on the diameter of the droplet is presented in Figure 5.10.
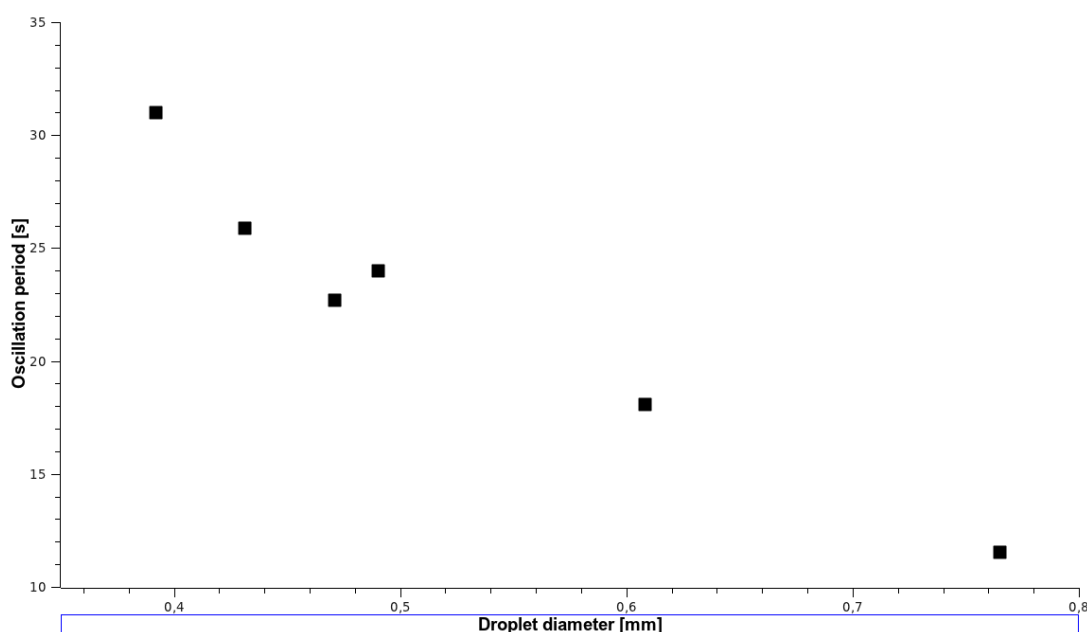

Figure 5.10: Oscillation period as a function of droplet diameter for the BZ solution composition: 0.45 M H_2SO_4, 0.45 M $NaBrO_3$, 0.35 M MA.

I also observed a strong dependence of the minimum droplet diameter that supported oscillations on the BZ solution composition. The findings are summarized in Table 5.1

[H$_2$SO$_4$]	[NaBrO$_3$]	[MA]	r_{min} [mm]
0.30 M	0.45 M	0.35 M	0.74
0.45 M	0.45 M	0.35 M	0.39
0.45 M	0.30 M	0.35 M	0.76
0.30 M	0.60 M	0.35 M	0.62
0.30 M	0.45 M	0.44 M	0.50
0.15 M	0.60 M	0.44 M	0.98
0.45 M	0.30 M	0.44 M	0.50
0.45 M	0.60 M	0.26 M	0.30
0.45 M	0.45 M	0.26 M	0.63
0.30 M	0.60 M	0.26 M	0.59

Table 5.1: Approximate minimum sizes (diameters) of a droplet in which chemical oscillations can arise for a given BZ medium composition.

5.1.2 Pulse propagation between droplets

Initial studies

Having established the basic conditions necessary for the occurrence of oscillations in a BZ droplet, I focused my attention on investigating the interactions between droplets. In the initial experiments two droplets were placed next to each other in a Petri dish. In some cases, a pulse arising in one of the droplets seemed to trigger excitation in the other droplet (Figure 5.11) but the behaviour was not consistent. As a next step, the droplets were pipetted into small hemispherical holes 1.5 mm in diameter, drilled in a PMMA (plexi) plate, in order to have better control over their exact locations; the whole system looked as in Figure 5.12. Because of this new arrangement, the droplets could be placed arbitrarily close to each other, and reproducible pulse transmission was achieved, as illustrated in Figure 5.13. There existed, however, a problem with stability, as the droplets forced into close contact tended to merge (this can be spotted in the space-time plot of Figure 5.13 where the droplet boundary disappears at some point).
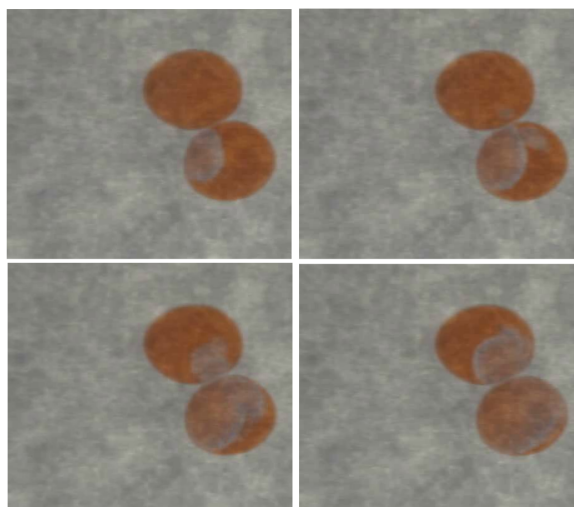
Figure 5.11: Two droplets (diameter: 2mm) placed next to each other in a Petri dish filled with the lipid solution. The frames are separated by 2-second time intervals. The BZ solution composition: 0.3 M sulphuric acid, 0.45 M NaBrO$_3$, 0.35 M malonic acid, 0.06 M KBr, 1.7×10^{-3} M ferroin.
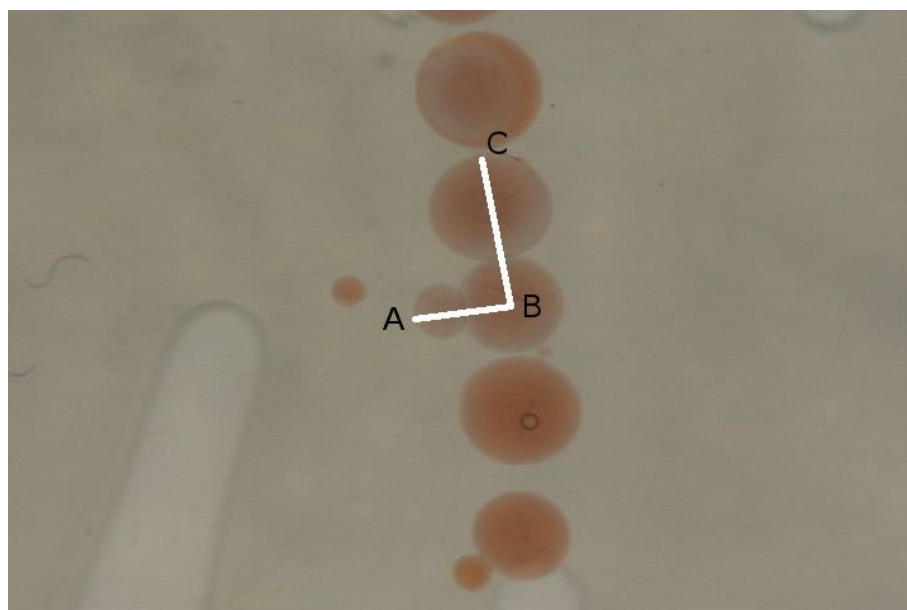
Figure 5.12: Top view of the droplets placed in holes in PMMA plate; the biggest ones are 1 mm in diameter. The space-time plot was created from pixels situated along the line ABC. The BZ solution composition: 0.3 M sulphuric acid, 0.45 M NaBrO$_3$, 0.35 M malonic acid, 0.06 M KBr, 1.7×10^{-3} M ferroin.

Figure 5.13: The space-time plot created from pixels situated along the white line in Figure 5.12. The horizontal axis covers approximately 25 minutes passing from left to right; the upper boundary of the plot corresponds to the leftmost point on the white line. The top arrow indicates the droplet boundary along which the signal transmission is observed; the bottom one shows the boundary which disappears when two droplets merge.

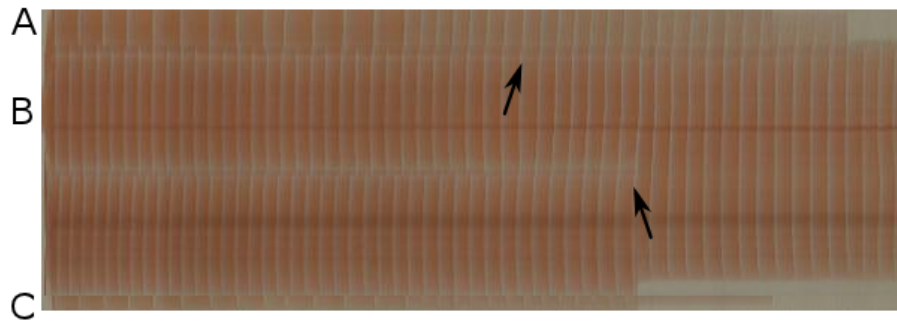**Catalyst replacement**

The low stability of contact bilayers between droplets was seen as a significant drawback with respect to further investigation of inter-droplet communication, and therefore I studied possible modifications of the system described in the preceding section. Assuming the production of carbon dioxide bubbles to be responsible for undesired droplet merging, we sought to substitute a cyclic ketone, 1,4-cyclohexanedione, for malonic acid, in order to eliminate gas formation [94]. I have also used a new catalyst, 1,10-bathophenanthroline disulphonate (BPDS) complex with iron (II), in place of ferroin in order to increase the colour contrast. BPDS, as a direct derivative of 1,10-phenanthroline (substituted with two (4'-sulpho)phenyl groups - Figure 5.14), readily forms complexes with iron ions, which are analogues of ferroin and ferriin [89]. Due to the presence of negatively charged sulphonic groups (six per one iron cation), the whole complex, contrary to ferroin, has a net negative charge, -4 when reduced and -3 when oxidized.
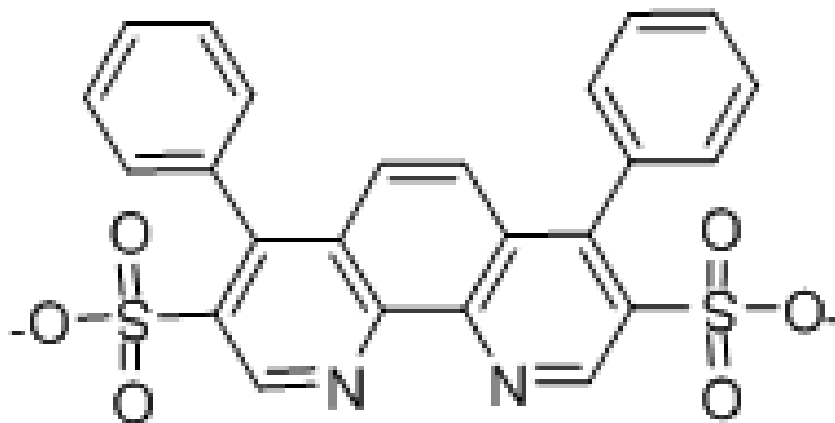

Figure 5.14: Structure of 1,10-bathophenanthrolinedisulphonate anion.

While 1,4-cyclohexanedione proved to be unsatisfactory (because of known drawbacks of this version of the BZ reaction, mainly long induction period preceding the onset of oscillations), the experiments with the new catalyst (BPDS) and ordinary malonic acid

have immediately demonstrated the following properties:

1. For a given reaction composition, the system is slightly less excitable, and therefore the oscillation period is greater, than in the ferroin-catalysed system with the same composition;

2. When placed on a flat surface, the droplets spread out considerably as the reaction progresses;

3. The droplets, when in close contact, are much more stable and the probability of merging is smaller.

The last fact, vividly demonstrated in Figure 5.15 proved to be a decisive factor influencing the permanent replacement of ferroin with the new catalyst.
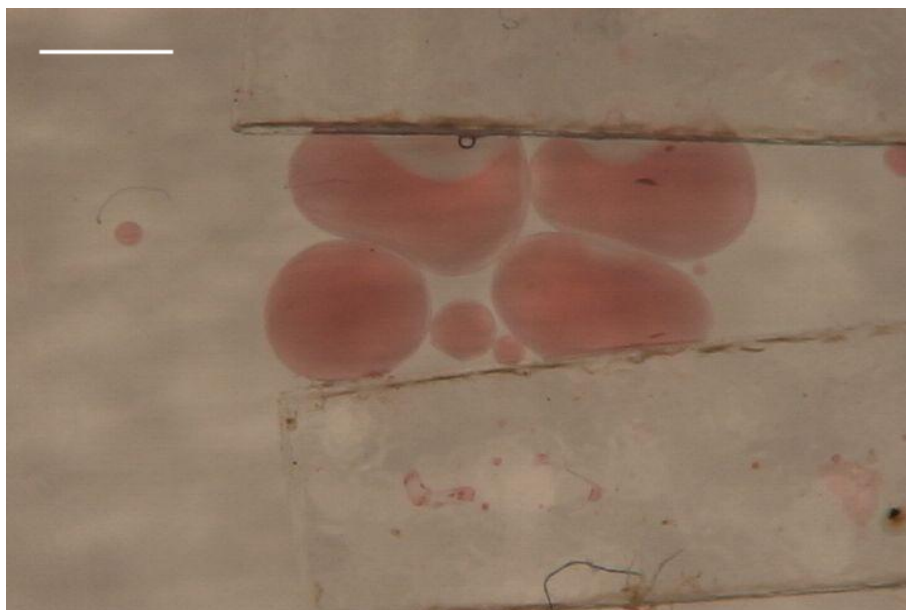

Figure 5.15: Droplets in which ferroin is replaced with BPDS complex can be squeezed without causing their merging. The scale bar is 1 mm.

Frequency transformation

Figure 5.16 shows the arrangement of droplets in a typical experiment during investigation of inter-droplet communication. The droplets are placed in a 1 mm-wide trench drilled in the bottom of a PMMA reaction vessel. As the BZ reaction progressed, they became more spread and the length of contact bilayers increased, which at some point led to appearance of a regular, repetitive pattern of pulse transmission (Figure 5.17). The pattern was fairly stable with respect to perturbations, which can be seen in the case where it successfully overcomes a locally formed spiral (Figure 5.18).
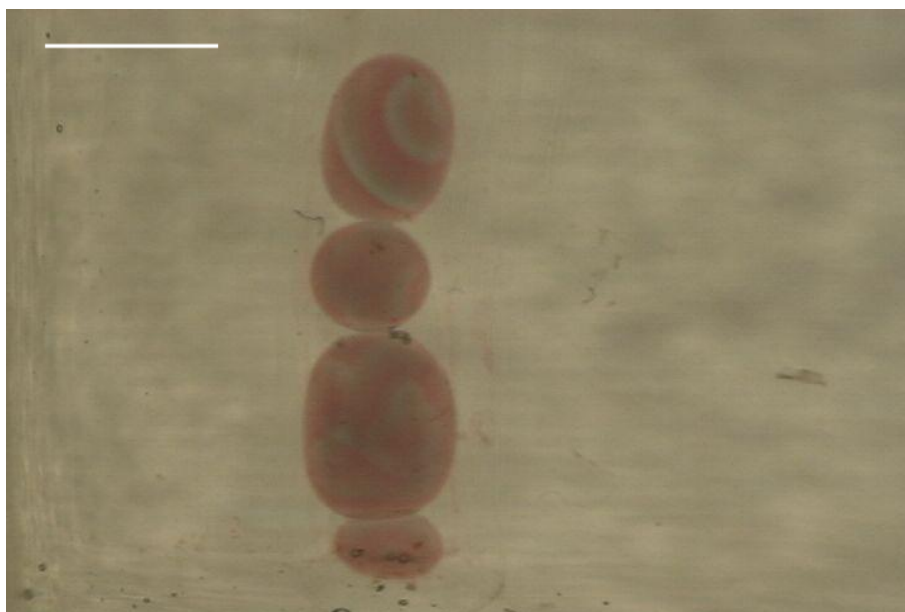
Figure 5.16: Initial droplet arrangement for a typical experiment in a trench. The BZ solution composition: 0.6 M sulphuric acid, 0.45 M NaBrO$_3$, 0.35 M malonic acid, 0.06 M KBr, 1.7×10^{-3} M BPDS complex. The scale bar is 1 mm.

Because implementation of most information processing operations typically requires the presence of several different excitability levels, a comparison of systems with varying concentrations of bromate and malonic acid in one of the droplets (the topmost one in the droplet chain) was then undertaken (concentration of sulphuric acid was kept constant because of its strong influence on the stability of contact bilayers). It was initially

(a)   (b)
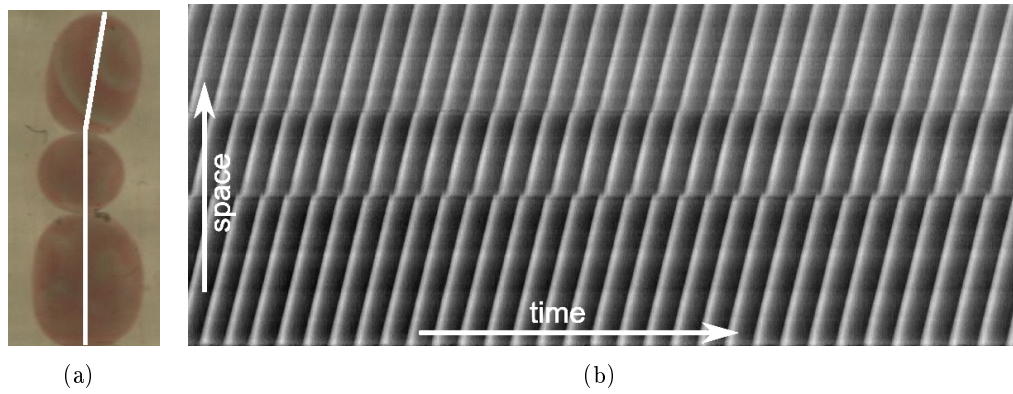
Figure 5.17: Space-time plot showing regular pulse propagation across droplet boundaries for the system pictured in Figure 5.16, created from pixels situated along the white line. The horizontal axis covers approximately 8.5 minutes.

expected, as bromate concentration is the second most important factor influencing excitability [95], that decreasing the amount of BrO_3^- ions with the MA concentration kept constant would lead for example to the gradual decrease in the frequency of pulses transmitted into the droplet in question. It turned out, however, that when MA concentration was kept at 0.29 M the decrease in bromate concentration led at some point to a sharp switch into a regime in which there was no pulse transmission whatsoever (Figure 5.19).
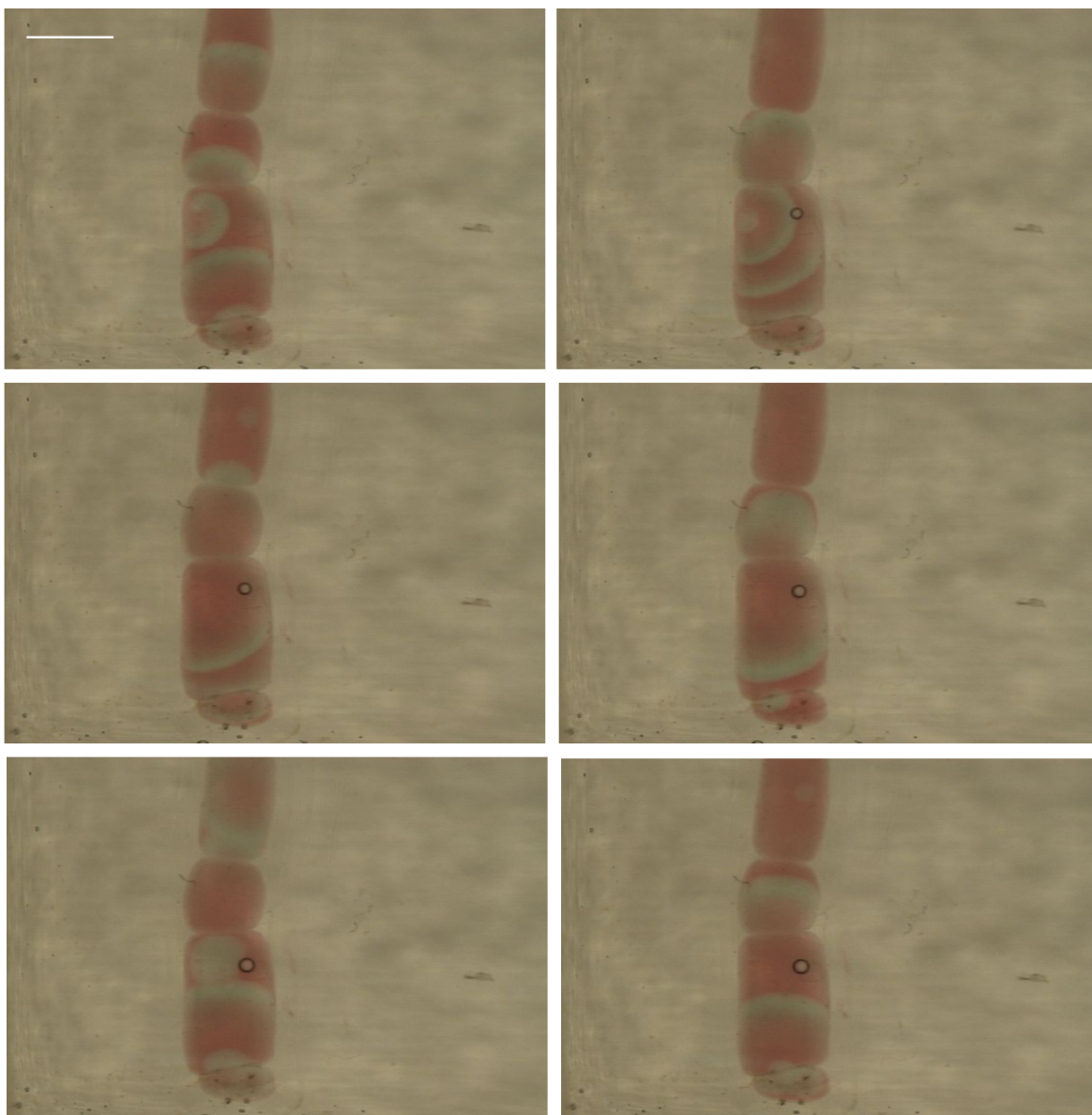
Figure 5.18: From left to right, top to bottom: a spiral formed in the system from Figure 5.16 transforms into a high-frequency target pattern, which is nevertheless effaced by the high-frequency excitation centre at the boundary of the two bottom droplets. Taking zero time at the first snapshot, the subsequent ones correspond to 159, 178.5, 208.5, 526 and 544 seconds respectively. The scale bar is 1 mm (video 2 on the accompanying CD).
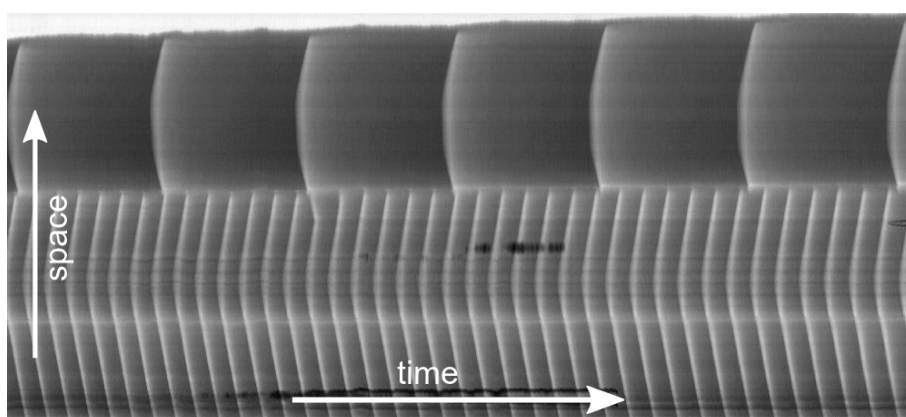
Figure 5.19: Space-time plot showing the system for which no pulses are able to enter the topmost droplet. The horizontal axis covers approximately 8.5 minutes, the concentrations are: $[H_2SO_4] = 0.6$ M, $[BrO_3^-] = 0.225$ M, $[MA] = 0.29$ M, $[KBr] = 0.06$ M, $[BPDS$ complex$] = 1.7 \times 10^{-3}$ M for the topmost droplet, for the other droplets $[H_2SO_4] = 0.6$ M, $[BrO_3^-] = 0.45$ M, $[MA] = 0.35$ M, $[KBr] = 0.06$ M, $[BPDS$ complex$] = 1.7 \times 10^{-3}$ M.

On the other hand, changing the malonic acid concentration while keeping that of bromate constant gave more promising results. Setting [NaBrO$_3$] at 0.225 M at decreasing [MA] from 0.35 M, no propagation was observed at first, but then the system started to exhibit frequency transformer properties. Figure 5.20 illustrates the system which for a short time allows only one in three signals to move from the row of the droplets of standard composition into the topmost, less excitable droplet. As the malonic acid concentration was further decreased, the aforementioned 3:1 transformation pattern disappeared altogether, replaced by the much more stable 2:1 pattern (Figure 5.21). For slightly lower malonic acid concentration the 2:1 pattern tended to lose
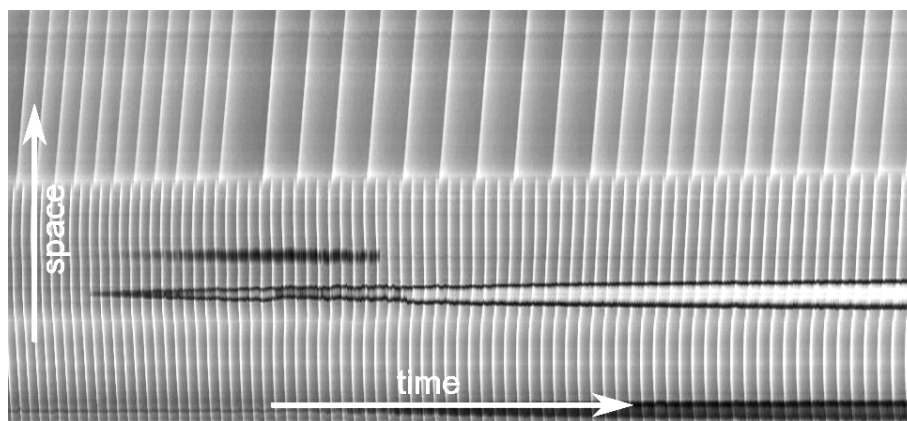
Figure 5.20: Space-time plot showing the transient 3:1 signal transformation pattern. The horizontal axis covers approximately 8.5 minutes, the concentrations are: [H$_2$SO$_4$] = 0.6 M, [BrO$_3^-$] = 0.225 M, [MA] = 0.26 M, [KBr] = 0.06 M, [BPDS complex] = 1.7×10^{-3} M for the topmost droplet, for the other droplets [H$_2$SO$_4$] = 0.6 M, [BrO$_3^-$] = 0.45 M, [MA] = 0.35 M, [KBr] = 0.06 M, [BPDS complex] = 1.7×10^{-3} M.

its stability and give way to transmission of all pulses (Figure 5.22). Table 5.2 gives an overview of different regimes occurring for various combinations of malonic acid and bromate concentrations.

It is important to note here that for the [BrO$_3^-$]/[MA] ratio greater than 1.5 dark precipitate appeared in the droplets (Figure 5.23). The most likely chemical species responsible for this phenomenon is the oxidized form of bathophenanthroline disulphonic
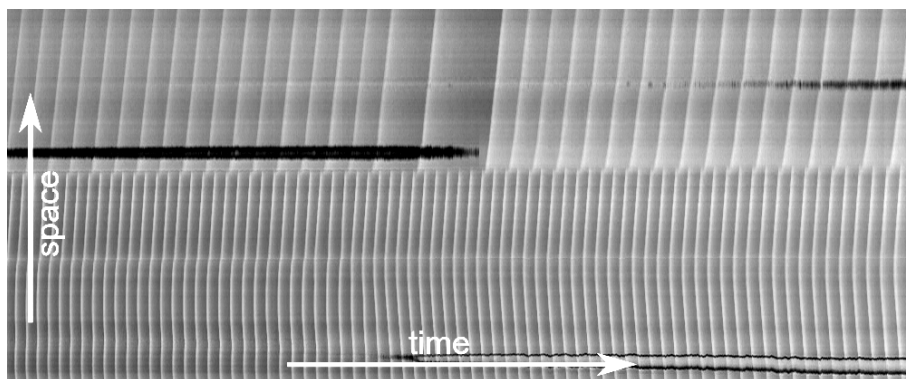
Figure 5.21: The 2:1 signal transformation pattern. The concentrations are: $[H_2SO_4]$ = 0.6 M, $[BrO_3^-]$ = 0.195 M, [MA] = 0.175 M, [KBr] = 0.06 M, [BPDS complex] = 1.7×10^{-3} M for the topmost droplet, for the other droplets $[H_2SO_4]$ = 0.6 M, $[BrO_3^-]$ = 0.45 M, [MA] = 0.35 M, [KBr] = 0.06 M, [BPDS complex] = 1.7×10^{-3} M.

acid $H_3[Fe(batho)_3(SO_3)_2]$, appearing when the bromate concentration relative to other species is too high. This hypothesis could be proved by adding some bromide ions to a solution containing 0.31 M sulphuric acid, 0.23 M bromate, 0.18 M malonic acid and 8.4×10^{-4} M catalyst, which led to the dissolution of the precipitate because the Br^- ions readily consume the BrO_3^- ions.
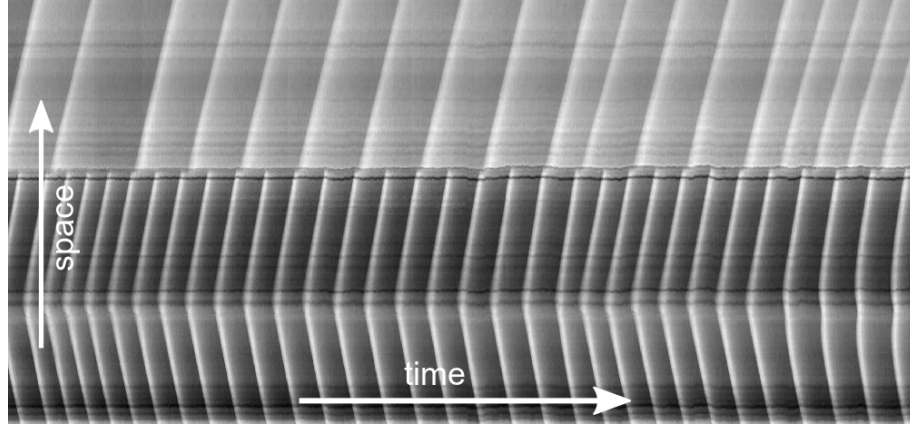
Figure 5.22: Space-time plot showing the unstable 2:1 pattern transforming to 1:1 regime, in which all the pulses are transmitted. The concentrations are: $[H_2SO_4]$ = 0.6 M, $[BrO_3^-]$ = 0.225 M, [MA] = 0.17 M, [KBr] = 0.06 M, [BPDS complex] = 1.7×10^{-3} M for the topmost droplet, for the other droplets $[H_2SO_4]$ = 0.6 M, $[BrO_3^-]$ = 0.45 M, [MA] = 0.35 M, [KBr] = 0.06 M, [BPDS complex] = 1.7×10^{-3} M.

$[NaBrO_3]$	[MA]	Behaviour
0.45 M	0.35 M	1:1
0.27 M	0.35 M	1:1
0.27 M	0.32 M	1:1
0.27 M	0.29 M	1:1
0.225 M	0.35 M	1:0
0.225 M	0.32 M	1:0
0.225 M	0.29 M	1:0
0.225 M	0.26 M	3:1 -> 2:1
0.225 M	0.23 M	2:1
0.225 M	0.175 M	2:1
0.225 M	0.170 M	2:1 -> 1:1

Table 5.2: Frequency transformation of signals propagating from a droplet with higher excitability to a droplet with lower excitability. 1:1 denotes transmission of all the pulses, while 1:0 indicates no transmission. The first row corresponds to the standard solution composition.
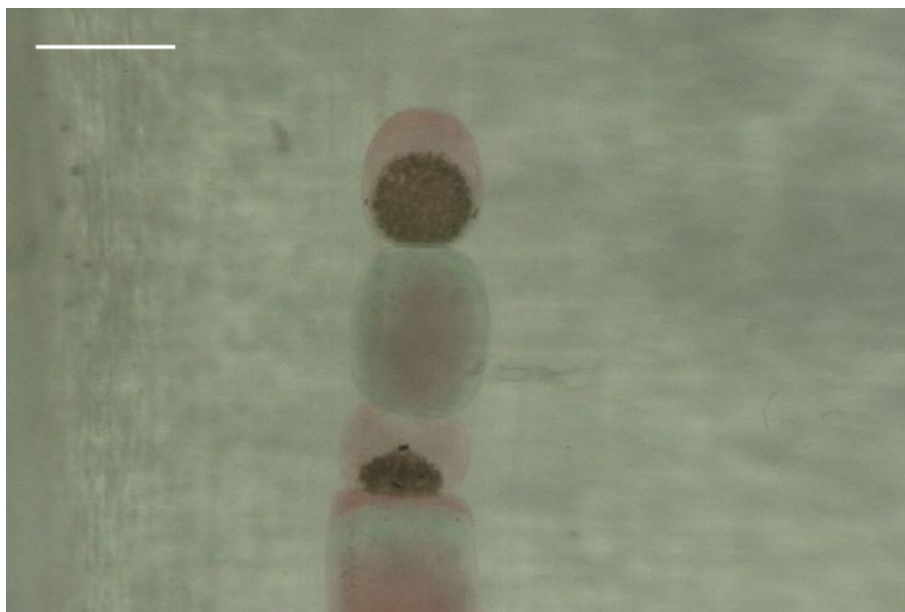
Figure 5.23: Dark precipitate appearing in two less excitable droplets (0.6 M sulphuric acid, 0.45 M NaBrO$_3$, 0.17 M malonic acid, 0.06 M KBr, 1.7×10^{-3} M BPDS complex) placed in between the standard concentration droplets (0.6 M sulphuric acid, 0.45 M NaBrO$_3$, 0.35 M malonic acid, 0.06 M KBr, 1.7×10^{-3} M BPDS complex). The scale bar is 1 mm.

5.1.3   Periodic pulsating of the droplets

Despite the fact that droplets possessing low excitability are of little use in the investigation of pulse transmission through bilayers, they exhibit another interesting effect, namely periodic shape changes. Because the oscillation period in such droplets is rather large, the correlation between chemical waves and those changes can be clearly made out (Figure 5.24)
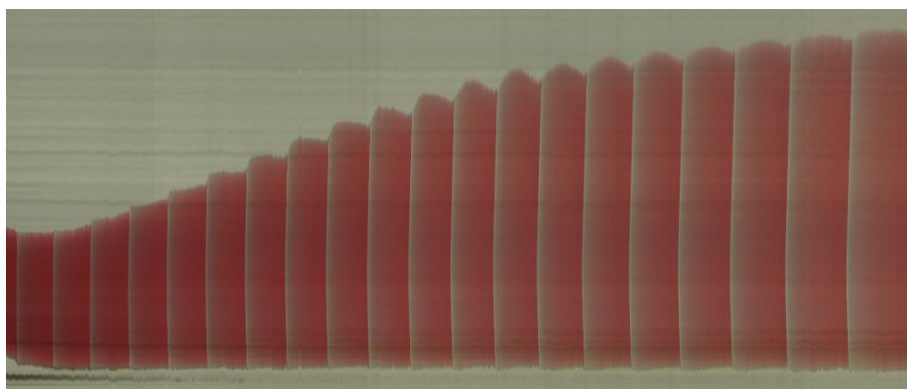

Figure 5.24: Space-time plot showing changes of shape for a single droplet placed in the trench reactor. The horizontal axis covers 50 minutes, the initial droplet diameter is 2 millimetres. The BZ solution composition: 0.6 M sulphuric acid, 0.1875 M NaBrO$_3$, 0.175 M malonic acid, 0.06 M KBr, 1.7×10^{-3} M BPDS complex (video 3 on the accompanying CD), the surroounding medium is 5 mg/ml solution of asolectin in decane.

In order to verify to what extent this behaviour was related to the presence of lipids, an experiment was performed in which a droplet of identical volume was placed in the same reactor, but the surrounding decane phase contained no lipids. The periodic swelling/shrinking was not observed in this case (Figure 5.25), which points to lipid molecules as the key factor. For comparison, the following series of figures illustrates the behaviour of a droplet surrounded by solutions with lipid concentrations changed from the standard value 5 mg/ml. While no striking difference exists between the concentrations in the spectrum from 2 (Figure 5.26) to 20 mg/ml (Figure 5.27), for still lower asolectin content the effect is clearly less noticeable (Figures 5.28 and 5.29).
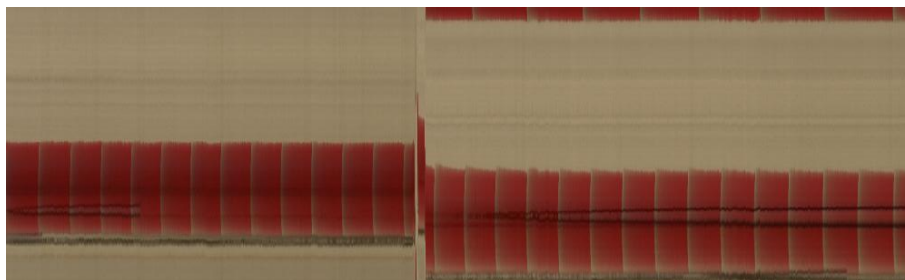
Figure 5.25: Space-time plot showing changes of shape for a droplet of composition identical as in the previous figure, but with pure decane as a surrounding medium.
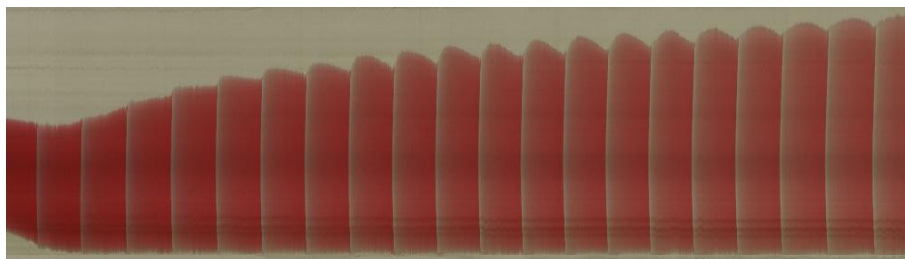
Figure 5.26: Space-time plot showing changes of shape for a droplet surrounded by solution with lipid concentration 2 mg/ml.
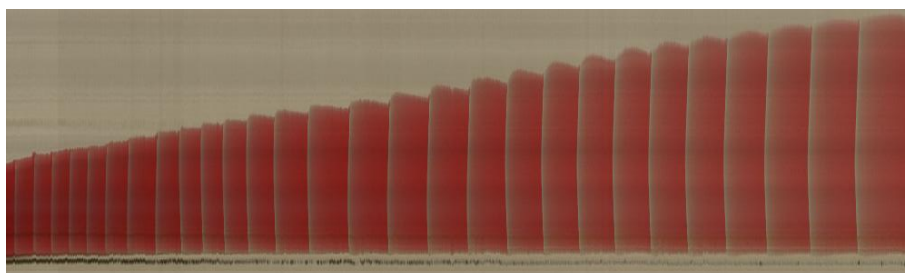
Figure 5.27: Space-time plot showing changes of shape for a droplet surrounded by solution with lipid concentration 20 mg/ml.
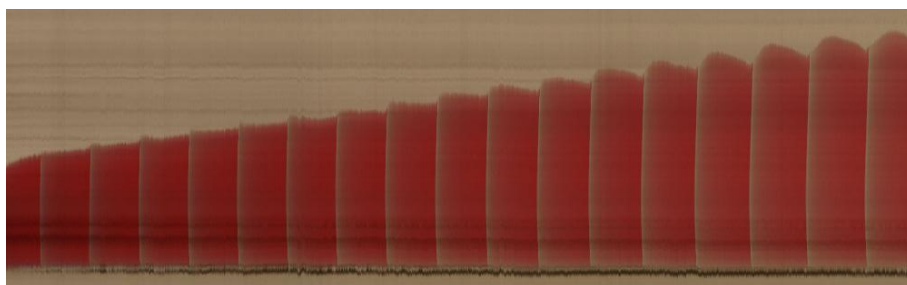
Figure 5.28: Space-time plot showing changes of shape for a droplet surrounded by solution with lipid concentration 1 mg/ml.
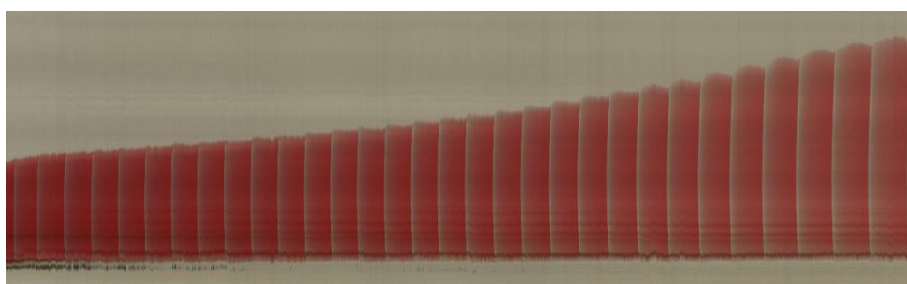
Figure 5.29: Space-time plot showing changes of shape for a droplet surrounded by solution with lipid concentration 0.5 mg/ml.

5.2   Discussion

The first results concerning the BZ reaction in a discrete system, that is proceeding in small volumes, date from the end of the 1990s and are due to Steinbock et al., whose paper was already mentioned [93]. The authors point to a remarkable influence of oxygen on the nature of oscillations, which is in itself a reflection of the known fact that oxygen molecules do indeed interfere with the BZ mechanism [96]; the chemical aspect of this interference was put forward by Krug and co-workers [36] as follows:

$$R\bullet + O_2 \rightarrow ROO\bullet \tag{5.1}$$

$$ROO\bullet + BrMA \rightarrow BrMA\bullet + ROOH \tag{5.2}$$

$$BrMA\bullet + H_2O \rightarrow \bullet COH(COOH)_2 + H^+ + Br^- \tag{5.3}$$
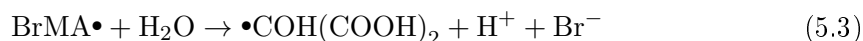
R may be assumed in this case to be some kind of organic radical. It is immediately noticeable that a BZ reaction inhibitor, bromide, is formed as a product in the above reaction sequence, thus making the oxygen molecules themselves inhibitors.

In Steinbock's paper, the droplets of diameter between 0.1 and 6.0 mm were immersed in inert silicone oil and the whole system was purged with nitrogen in some experiments. When the purging was not employed, the oscillations tended to be inhomogeneous and started in the droplet center, because the areas closer to the border were less excitable due to a higher concentration of oxygen molecules migrating from the oil phase through the phase boundary. The fact that the lipid-covered droplets investigated presently exhibit the same characteristics serves to prove that O_2 can migrate equally well through lipid monolayers.

The authors reported, for the medium in which oxygen is present, the increase of the oscillation period with the decreasing droplet diameter and the presence of a critical diameter value below which the oscillations disappeared altogether. For the solution

composition $[\text{NaBrO}]_3 = 0.2$ M, $[\text{MA}] = 0.4$ M, $[\text{ferroin}] = 4.0 \times 10^{-4}$ M and $[\text{H}_2\text{SO}_4] = 0.1$ M the critical value was approximately 1.3 mm, which can be compared with the highest value from the table 5.1, namely 0.98 mm for the concentrations equal to 0.60 M, 0.44 M, 1.7×10^{-3} M and 0.15 M, respectively.

The inspection of table 5.1 reveals two important facts. First of all, for the malonic acid concentration kept constant, the minimum droplet diameter (r_{min}) required for the oscillations depends only on the product of the concentrations of sulphuric acid and bromate, in accordance with the general influence of this quantity on the BZ excitability [95]. The second observation is that the malonic acid concentration has a pronounced effect as well; this could be explained if we consider the presence of oxygen. For relatively small droplets, around 0.5 mm in diameter, the surface-volume ratio is high when compared with larger ones, and therefore oxygen molecules migrating from the oil phase are able to quench the oscillations in such droplets relatively easy. However, if we increase the MA concentration, and therefore the concentration of various organic radicals, there is a greater chance that some O_2 will be consumed before it reaches the center of the droplet, allowing a pulse to arise there.

An empirical expression relating r_{min} and the three above-mentioned concentrations, for the data under consideration, has the form

$$r_{min}[\text{mm}] = 4.15 \times 10^{-3} \times [\text{H}_2\text{SO}_4]^{-1.7}[\text{NaBrO}_3]^{-1.8}[\text{MA}]^{-1.6}, \quad (5.4)$$

giving the values collected in table 5.3, with the experimental values presented for comparison. The equation expresses the fact that the minimum diameter for which the oscillations can arise depends most strongly on the bromate concentration, followed by sulphuric and malonic acid. The indirect influence of malonic acid, outlined above, manifests itself in slightly lower value of the exponent than that for the other two species, whereas the exponent for sulphuric acid does not equal that of bromide because of inter-

actions of the H^+ ions with charged groups on the catalyst ligands, as described in the following paragraphs.

[H$_2$SO$_4$]	[NaBrO$_3$]	[MA]	r_{min}^{exp} [mm]	r_{min}^{calc} [mm]
0.30 M	0.45 M	0.35 M	0.74	0.725
0.45 M	0.45 M	0.35 M	0.39	0.364
0.45 M	0.30 M	0.35 M	0.76	0.755
0.30 M	0.45 M	0.44 M	0.50	0.503
0.15 M	0.60 M	0.44 M	0.98	0.974
0.45 M	0.30 M	0.44 M	0.50	0.524
0.45 M	0.60 M	0.26 M	0.30	0.349
0.45 M	0.45 M	0.26 M	0.63	0.586
0.30 M	0.60 M	0.26 M	0.59	0.695

Table 5.3: Comparison of minimum droplet diameters for which the BZ oscillations are observable with values calculated according to the formula $r_{min}[\text{mm}] = 4.15 \times 10^{-3} \times [\text{H}_2\text{SO}_4]^{-1.7}[\text{NaBrO}_3]^{-1.8}[\text{MA}]^{-1.6}$.

The phenomenon of a chemical excitation pulse crossing a lipid bilayer membrane is one that has not been investigated previously. The important papers concerning BZ reaction limited to nanolitre volumes published by Epstein et al. [76, 77, 78] describe droplets which are much smaller, are not in a direct contact and there are no lipids present in the system. The authors nevertheless provide some hints as to what chemical species might be responsible for the observed oscillation synchronization phenomena: deeming ion and polar species not likely to cross the phase boundary into the oil, they consider Br$_2$ and •BrO$_2$ as candidates and manage to confirm this by constructing a model coupling the BZ mechanism with steps representing migration of those species into the hydrocarbon phase [76].

Taking those guidelines as a starting point, we first attempted to verify the degree to which molecular bromine is able to leave the droplets in our system. We prepared a solution containing 0.45 M sodium bromate, 0.3 M sulphuric acid and 0.06 M potassium bromide, which led to an immediate appearance of brown colour, due to the net process

$$\text{BrO}_3^- + 5\text{Br}^- + 6\text{H}^+ \rightarrow 3\text{Br}_2 + 3\text{H}_2\text{O} \tag{5.5}$$
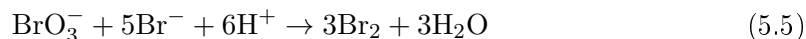
Droplets (1.5 μl in volume) of the resulting solution were pipetted into the standard trench reactor filled first with pure decane, and then with the standard 5 mg/ml asolectin solution. In the first case, brown colour disappeared relatively fast, which is expected considering the affinity of Br_2 to hydrocarbons as compared with water (Figure 5.30). In the second case, however, it took around 4 times longer for the Br_2 concentration inside the droplet to drop to a level at which no colour was visible (Figure 5.31).
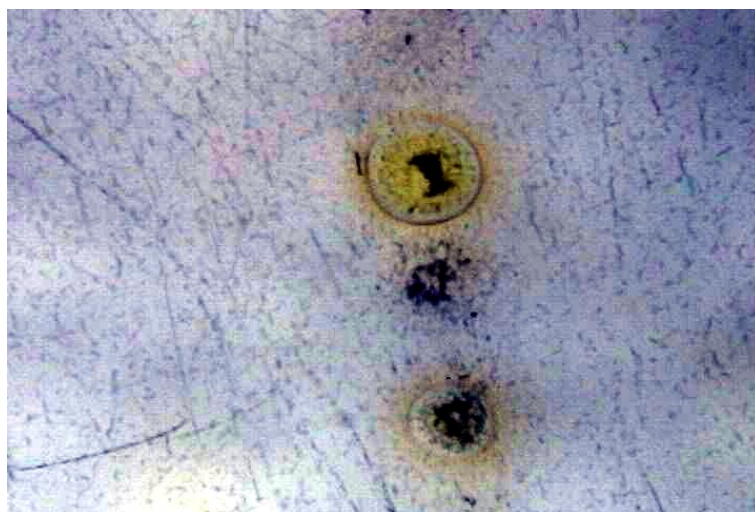
(a)
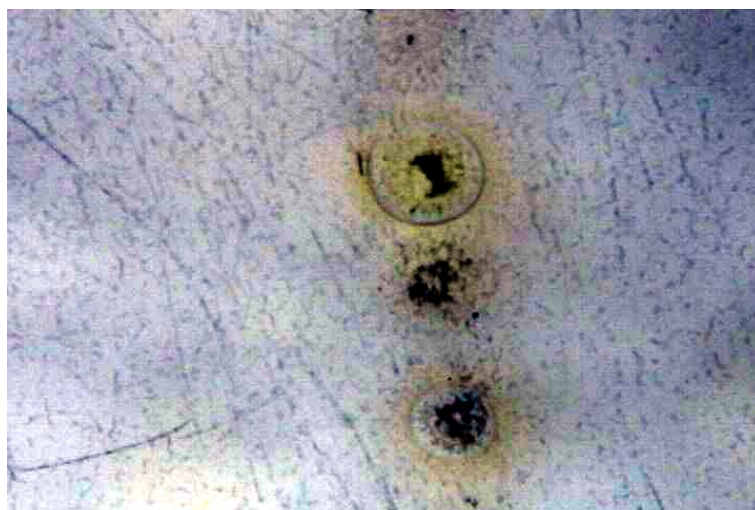
(b)

(c)

Figure 5.30: Changes in the amount of bromine present in a droplet surrounded by pure decane (colour enhanced). The snapshots were taken at 18, 48 and 78 seconds after immersing the droplet in the organic phase. Note the brown colour in the oil phase just outside the droplet boundary.
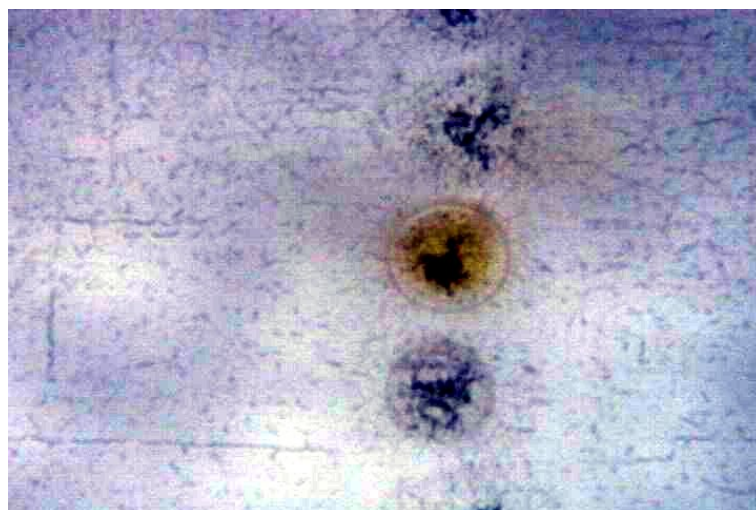
(a)
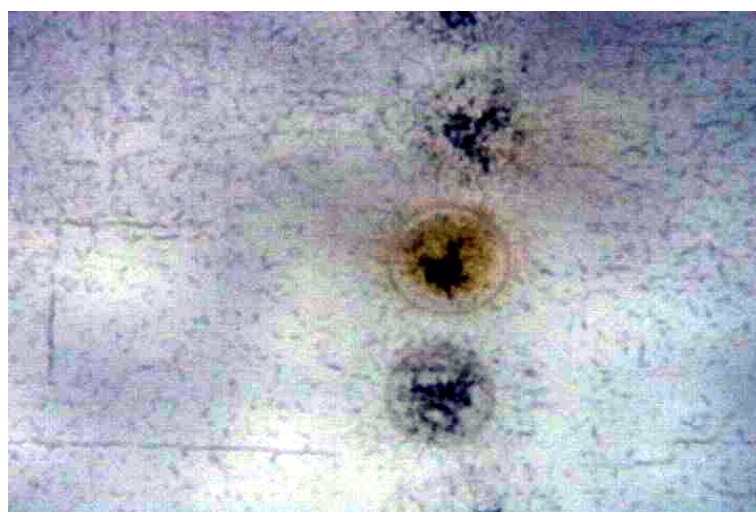
(b)
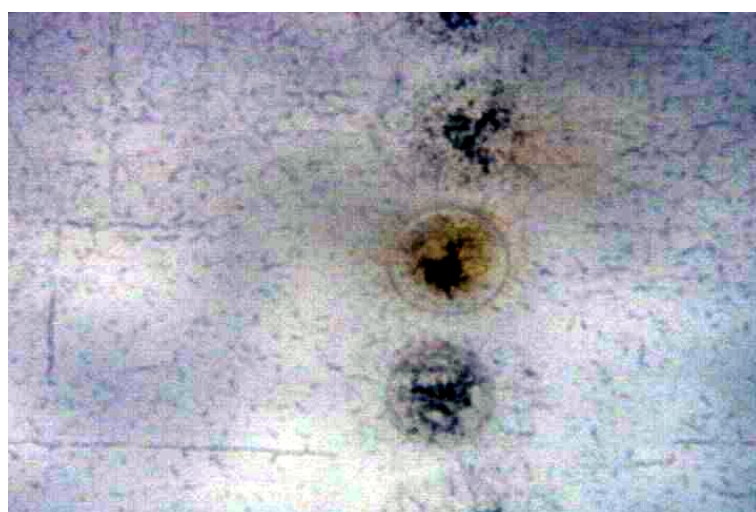
(c)

Figure 5.31: Changes in the amount of bromine present in a droplet surrounded by solution of asolectin in decane (colour enhanced). The snapshots were taken at 18, 48 and 78 seconds after immersing the droplet in the organic phase. Note the slow, but steady depletion of bromine starting at the droplet boundary.

Bromine, as a non-polar molecule, is potentially one of those species present in a reacting BZ system which are most prone to migration through a lipid layer; still, the passage into the oil phase is expected to be slower than in the case of simple phase boundary, where the lid layer does not separate the BZ solution from the decane phase. Another important fact that must be considered is that asolectin used in the experiments is a complex mixture of lipids of different sort, including saturated, mono-unsaturated and poly-unsaturated hydrocarbon chains (see Figure 5.33). It is now known that the
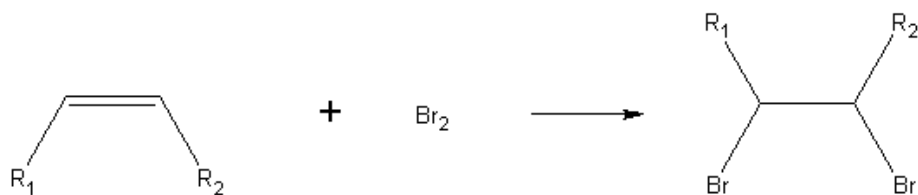
Figure 5.32: Schematic depiction of a bromination reaction on a double carbon-carbon bond.

BZ reaction proceeding in droplets surrounded by unsaturated lipid monolayers interacts with them by means of bromination of the double carbon-carbon bonds (Figure 5.32) [97, 98]. As a consequence, it has to be assumed that most of the Br_2 molecules end up becoming part of the lipid layer itself, which is corroborated by the fact that there is no noticeable formation of a brown "halo" around the droplet which is immersed in a lipid solution (Figure 5.31). Correspondingly, the presence of Br_2 in the oil phase can be readily spotted in the pure decane case.
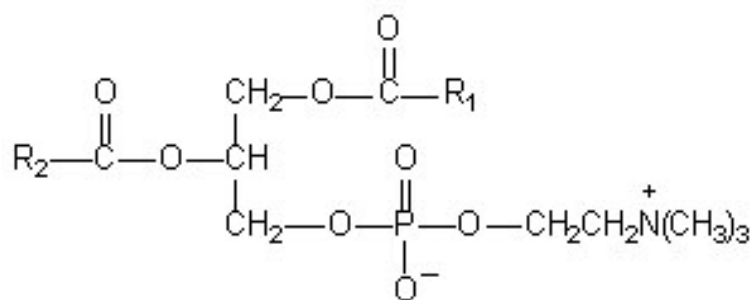
(a)
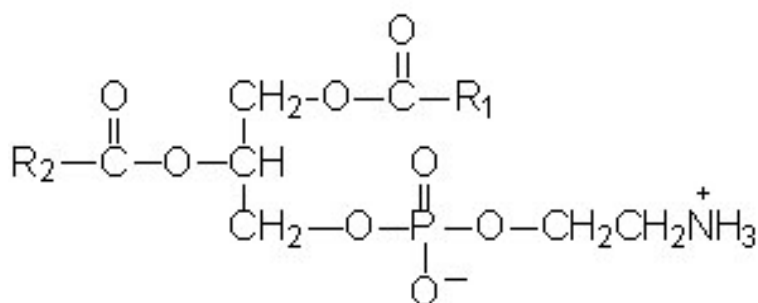
(b)
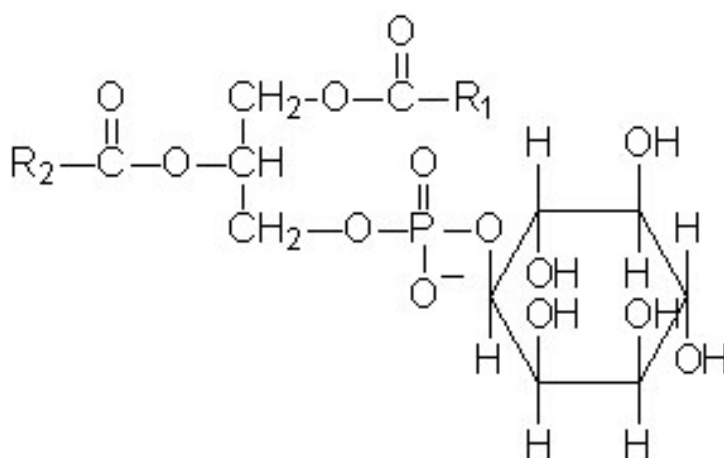
(c)

Figure 5.33: According to the specification, the lipid content of commercial asolectin is made up of roughly equivalent amounts of lipids with phosphatidylcholine (PC) 5.33(a), phosphatidylethanolamine (PE) 5.33(b) and phosphatidylinositol (PI) 5.33(c) hydrophilic heads. Note that the PI heads possess a net charge. 24 % of the hydrocarbon tails are saturated, 14 % - monounsaturated, 62 % - polyunsaturated.

Taking the above into account, it can be expected that when the BZ reaction is proceeding inside droplets, the presence of lipids around those droplets makes bromine removal slower than in the case of droplets surrounded by pure oil. Because Br_2 acts ultimately as an inhibitor of the oscillations (due to its hydrolysis giving Br^-), the excitability in the former case should be lower. This is indeed what is observed when droplets of composition used by Steinbock et al. are placed in a Petri dish filled with the lipid solution - in contrast to the article, which reports excitations appearing in droplets down to 1.3 mm in diameter (the surrounding medium is silicone oil), no oscillations are observed, even for much larger droplets. Note that our empirical equation for r_{min} required for the appearance of the oscillations in the lipid-containing system gives over 16 millimetres in this case.

Even though, in addition to Br_2, $\bullet BrO_2$ radicals were identified by Epstein et al. during simulations as contributing to the droplet synchronization, their influence was described as less crucial, the whole collective behaviour being conditioned chiefly by the inhibiting bromine molecules. On the other hand, the direct propagation of a large-scale chemical pulse from droplet to droplet must obviously be related to activatory coupling, as the arrival of a pulse at a bilayer separating two droplets leads to an immediate appearance of an excitation on the other side of the bilayer.

Let us consider two droplets surrounded by the lipid solution in decane and containing the substrates of the BZ reaction, assuming that a bilayer is formed in the area where the droplets are touching each other. There are two main inhibitors to be reckoned with, oxygen and molecular bromine, but their gradients are opposite: as discussed above, the concentration of oxygen is expected to decrease in the direction pointing towards the droplet center (because of its consumption by organic radicals), whereas that of bromine is lowest in the vicinity of the boundary, due to the ongoing bromination of unsaturated lipids, the constant rate of the latter process being ensured by dynamic equilibrium in the bilayer [98]. The areas directly bordering the contact bilayers are special in the sense

that they exhibit relatively low Br$_2$ concentration as well as being less exposed to the influence of O$_2$ when compared to the other outer zones of the droplets. The excitability conditions in those areas are therefore rather favourable; what remains to be unveiled is the exact cause of the direct association between pulses on both sides of a bilayer.

The literature sources devoted to the nature of interaction between the BZ reaction reagents and lipid phases focus exclusively on lamellar phases, consisting of long sheets of lipid bilayers separated by aqueous domains (Figure 5.34). The authors stress the lack of
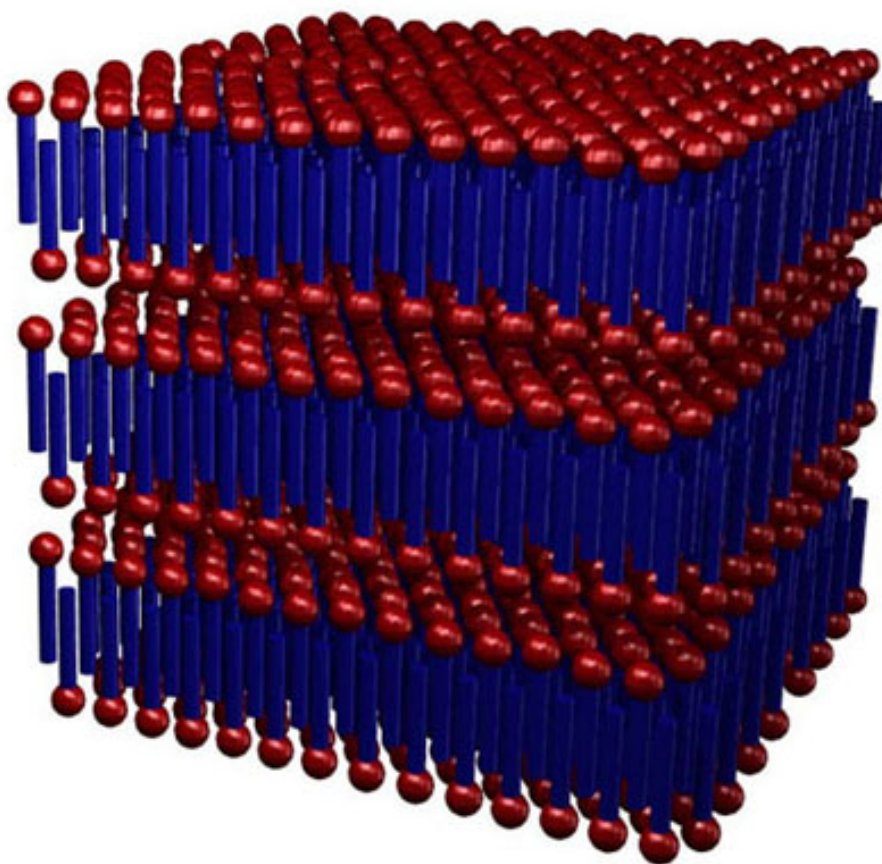

Figure 5.34: Morphology of a lamellar phase in lipid and general surfactant systems (source: barrett-group.mcgill.ca).

any marked chemical interference, whether due to the ionic strength or to the influence of acidity [99]. The interactions of physical nature, such as changes in the electron density

along the bilayers or increase in the length of regions in which the hydrophobic lipid tails are perpendicular to the bilayer plane, can however come into play [100]. In the light of this, it is perhaps safe to assume that when a pulse reaches a bilayer, it modifies its internal structure sufficiently enough for the activator molecules to pass through.

The frequency transformation on a bilayer gives further clues with respect to the nature of the whole process. According to earlier work [90, 101] an excitation pulse moving from one region of an excitable medium to another might undergo such transformations when the two regions are separated by an non-excitable barrier, and the role of the control parameter is played by the barrier width. For barriers of relatively small width, all pulses are able to pass, which is precisely what happens in the case of presently investigated droplets. This permits us to treat the separating bilayer as a comparatively narrow stripe of non-excitable medium. Frequency transformation may then arise when the separating barrier is wider; intuitively, when the excitability in the receiving droplet is slightly decreased, a similar effect is to be expected. However, the earlier results [65] fail to unveil any such behaviour. The passage of only one in two or one in three pulses is attained only when we add a "degradation" step describing additional decrease of the activator (presumably $\bullet\text{BrO}_2$) concentration in the lipid bilayer according to a first-order process which could simply represent escape of some of the molecules into the oil phase.

The experiments described in the thesis utilize mostly the modified BZ catalyst, iron (II) complex of bathophenanthrolinedisulphonate (BPDS). The prime difference between this species and ferroin lies in the negatively charged sulphonic groups at the ligands. These groups are able to accept protons in acidic medium, which explains the appearance of precipitate (composed mainly of the derivative of the complex in which the anionic sulpho groups SO_3^- become protonated, giving SO_3H) for some solution compositions and decreased excitability in comparison to the ferroin-catalyzed BZ reaction (due to lower effective proton concentration in the surrounding solution). Not only does their presence endow the whole complex with the negative charge, it also causes the bulk of

that charge to be placed at the sulphonic groups themselves, that is at the outer edges of the ligands (in contrast with ferroin, where the net charge resides on the iron ion surrounded by ligands). This makes the possibility of electrostatic interactions with the lipids much more likely, especially that roughly one-third of the asolectin lipid content possesses charged hydrophilic heads (cf. Figure 5.33). These interactions are most probably responsible for two of the most immediately noticeable differences between droplets containing ferroin and BPDS, namely the increased stability of the contact bilayers and the droplet spreading as well as pulsating synchronized with the BZ oscillation phase.

As regards this last property, it turns out to be exclusively related to changes in the oxidation state of the complex, which apparently causes the changes in the degree of electrostatic interactions with bilayers and lends itself to convenient observation when studied separately from the BZ oscillations. What is meant here is that we can follow the oxidation of the BPDS complex in detail by adding a small amount of bromate ions to its acidified solution. Figure 5.35 presents the dramatic change in the shape of a droplet brought about by oxidation, which is non-existent when ferroin plays the role of a reductant (Figure 5.36). The ferroin case also excludes the influence of bromination of double bonds on this behaviour. A third important fact is that the effect is also impossible to observe in pure decane, as exemplified in Figure 5.37 (in accordance with the results concerning the periodic shape changes).
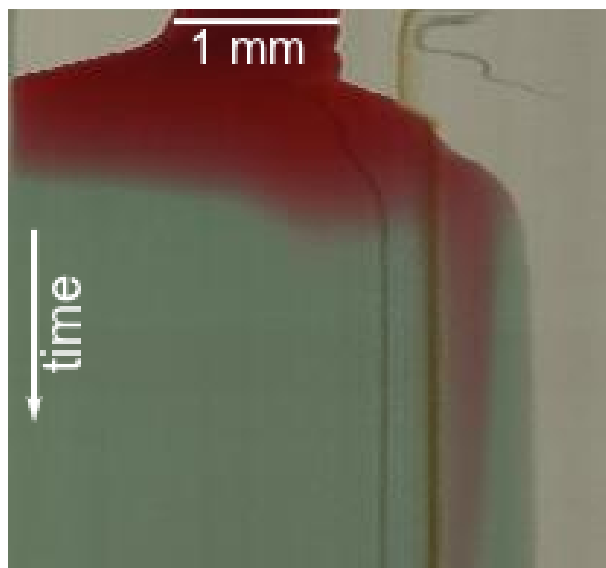
Figure 5.35: Space-time plot showing oxidation in a droplet containing 0.3 M H_2SO_4, 4.9 mM BPDS iron(II) complex and 0.0294 M $NaBrO_3$, immersed in asolectin solution in decane. The droplet of diameter 1 mm was placed in a trench and spread along its length. The time, flowing downwards, covers 97 seconds (video 4 on the accompanying CD).
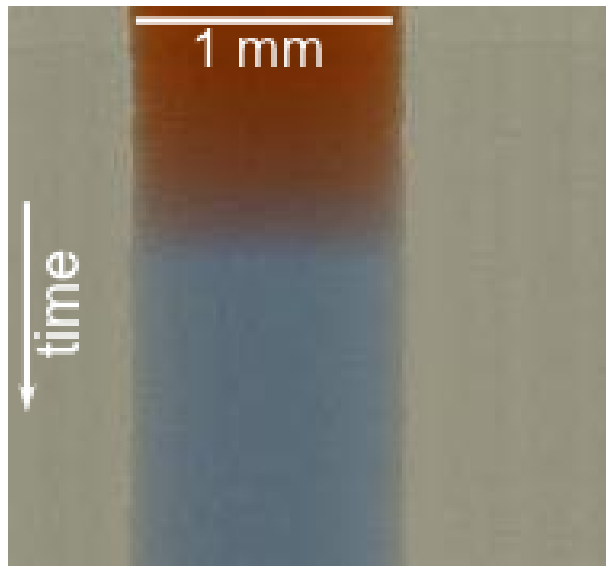
Figure 5.36: Space-time plot showing oxidation in a droplet containing 0.3 M H_2SO_4, 4.9 mM ferroin and 0.0149 M $NaBrO_3$, immersed in asolectin solution in decane. The droplet is 1 mm in diameter. The time, flowing downwards, covers 88 seconds.
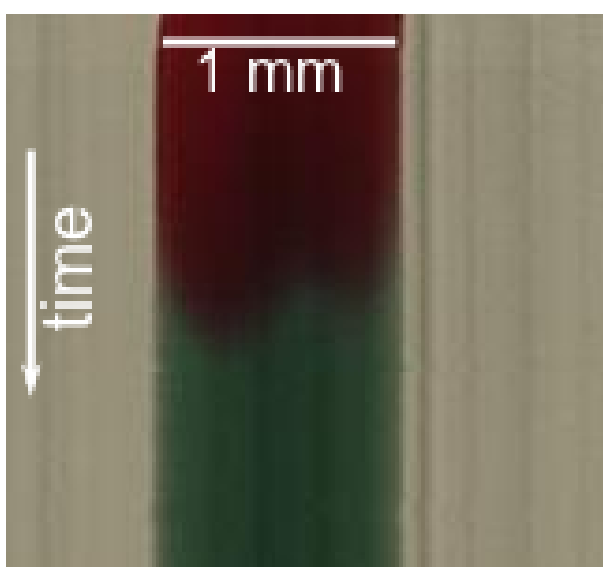
Figure 5.37: Space-time plot showing oxidation in a droplet containing 0.3 M H_2SO_4, 4.9 mM BPDS iron(II) complex and 0.0222 M $NaBrO_3$, immersed in pure decane. The droplet is 1 mm in diameter. The time, flowing downwards, covers 75 seconds.

The peculiar properties of the BPDS complex do not influence the very phenomenon of pulse transmission between droplets, however. Figure 5.38 presents a series of top views of a 9 mm × 10 mm × 27 mm spectrophotometric cuvette filled with 4.2 mg/ml solution of asolectin in the decane ($d = 0.73$ g/ml)/carbon tetrachloride ($d = 1.59$ g/ml) mixture, of proportions selected such as to make the density of the medium equal to the density of water (0.688 ml decane, 0.512 ml CCl$_4$). After pipetting them in, the droplets become suspended in the mixture and are ultimately forced together due to the convective motion of the surrounding organic phase. As the experimental snapshots show, there is no change in their shape, which allows us to conclude that the striking phenomena observed on a flat surface must be related to the fact that the changes in the electron density along the lipid layer result in changes in the nature of interaction between droplets and the PMMA surface, because, as the experiment with suspended droplets shows, there is no change in the interfacial tension between the two liquid phases. Nevertheless, the propagation of excitation pulses between droplets is clearly observable.
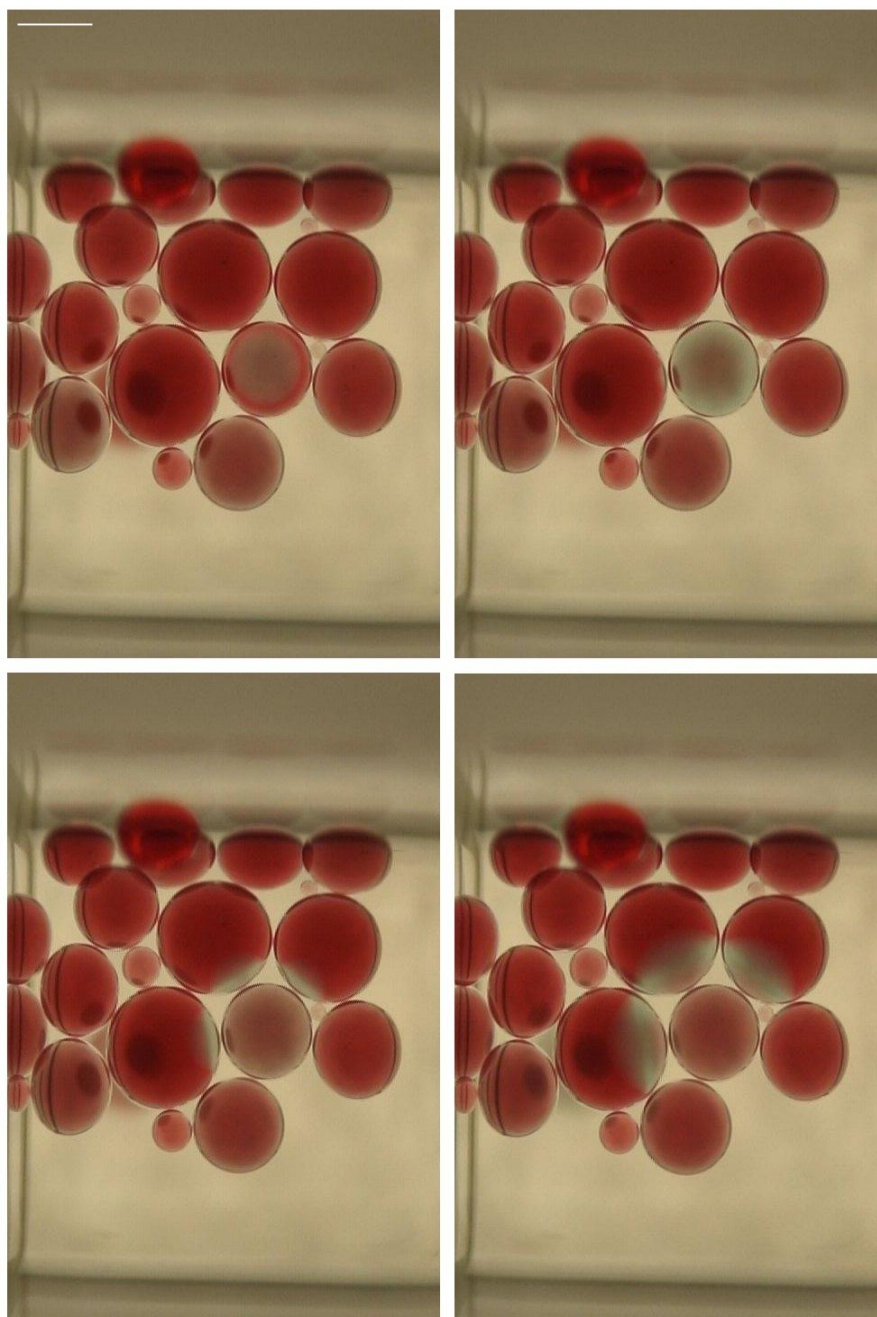
Figure 5.38: Propagation of an excitation pulse among droplets suspended in a solution of asolectin in decane/CCl$_4$ mixture of density roughly equal to that of water. The frames are separated by 3 seconds. The scale bar is 1 mm. The BZ solution composition: 0.6 M sulphuric acid, 0.315 M bromate, 0.26 M malonic acid, 0.06 M bromide, 1.7×10^{-3} M BPDS complex. The scale bar is 1 mm (video 5 on the accompanying CD).

Chapter 6

Conclusions and future work

The two systems investigated in the present thesis give us different insights regarding the feasibility of construction of chemical media exhibiting properties characteristic of the nervous system. While the first part, namely that regarding the optical capillary, may be thought of as an extension and generalization of earlier results, the second part describes a completely novel information processing system.

The utilization of a flow reactor in studies on the properties of trains of chemical pulses proved that whether the pulses entering a narrowing triangular channel disappear all at the same point or a more complex pattern emerges depends primarily on their initial frequency, which is in accordance with known properties of excitable systems and may in the future give us clues as to how exactly the neurons work. The adaptation property, in turn, may be used when constructing photosensitive information processing systems which respond to the rate and termination of changes in environment parameters. The long observation time provided by the flow system described in the thesis is crucial for both applications.

The system composed of droplets containing the reacting Belousov–Zhabotinsky medium turned out to be very robust and capable of information processing operations. Most importantly, while its functions are strictly determined by structure (as in similar chem-

ical computing systems), this structure arises spontaneously. This is especially evident when droplets are immersed in an organic phase whose density approaches that of water: although it can be argued that the trenches drilled in PMMA plates amount to some kind of structure imposition, the same cannot be said of the arrays of suspended droplets, which additionally exhibit a degree of self-organization. This also opens up new possibilities of constructing more effective, three-dimensional chemical computing systems.

Information processing taking place in systems based on a layer of excitable medium whose excitability levels are controlled by external illumination is possible when using flow reactors (as demonstrated in the first part of the thesis), but that makes the whole working setup unnecessarily bulky. In the case of the discrete droplet system, however, we can always imagine adding new small volumes to a system approaching exhaustion. This direction of research allows for radical extension of analogies to biological systems, such as nerve networks, which are a blueprint for parallel computing media.

The most important future direction to follow when investigating the droplet systems described involves devising methods of external control, for example of ensuring that the excitation arises in a precisely selected droplet. A promising means to this end could be adding some ruthenium catalyst to the droplets [76], another - perhaps more natural - method would be to make the BZ medium inside the droplets strictly excitable (responding only to stimuli exceeding some threshold) and to excite one of them, for example by placing a cation-exchange bead with Ag^+ cations immobilized on its surface (which would bind the inhibitory Br^- ions) inside. Then, basic logic gates could be constructed easily [102]; as we have seen at the beginning, the ability to build the gates would then pave the way for implementation of a whole array of computing operations.

Appendix A

List of publications by the author

1. J. Szymański, J. Górecki *Chemical Pulses Propagating Inside a Narrowing Channel and Their Possible Computational Applications*, International Journal of Unconventional Computing **6**, 461–471, (2010).

2. J. Szymański, J. N. Górecka, Y. Igarashi, K. Giżyński, J. Górecki, K.-P. Zauner, M. de Planque *Droplets with Information Processing Ability*, International Journal of Unconventional Computing **7**, 185–200, (2011).

3. J. Górecki, J. Szymański, J. N. Górecka *Realistic Parameters for Simple Models of the Belousov-Zhabotinsky Reaction*, Journal of Physical Chemistry A **115**, 8855–8859, (2011).

Appendix B

Contents of the CD-ROM

The CD-ROM contains supporting material for the thesis, namely the video clips from the droplet experiments:

1. BZ droplets immersed in 5 mg/ml asolectin solution in a Petri dish. The thickness of the dish wall is 1 mm. The standard BZ solution composition: 0.3 M sulphuric acid, 0.45 M bromate, 0.35 M malonic acid, 0.06 M bromide, 1.7×10^{-3} M ferroin. The video speed is $12 \times$ real time.

2. Pulse propagation through a train of identical droplets arranged in a 1 mm wide trench on the bottom of a PMMA vessel filled with 5 mg/ml asolectin solution in decane. The BZ solution composition: 0.6 M sulphuric acid, 0.45 M $NaBrO_3$, 0.35 M malonic acid, 0.06 M KBr, 1.7×10^{-3} M BPDS complex. The video speed is $24 \times$ real time.

3. Changes of shape for a single droplet placed in the trench reactor. The horizontal axis covers 50 minutes, the initial droplet diameter is 2 millimetres. The BZ solution composition: 0.6 M sulphuric acid, 0.1875 M $NaBrO_3$, 0.175 M malonic acid, 0.06 M KBr, 1.7×10^{-3} M BPDS complex, the surroounding medium is 5 mg/ml solution of asolectin in decane. The video speed is $24 \times$ real time.

4. Oxidation in a droplet containing 0.3 M H_2SO_4, 4.9 mM BPDS iron(II) complex and 0.0294 M $NaBrO_3$, immersed in 5 mg/ml asolectin solution in decane. The droplet of diameter 1 mm was placed in a trench and spread along its length. The video speed is real time.

5. Propagation of excitation pulses among droplets suspended in a 5 mg/ml solution of asolectin in decane/CCl_4 mixture of density roughly equal to that of water. The BZ solution composition: 0.6 M sulphuric acid, 0.315 M bromate, 0.26 M malonic acid, 0.06 M bromide, 1.7×10^{-3} M BPDS complex. The video speed is $24 \times$ real time.

Bibliography

[1] J. von Neumann, "First Draft of a Report on the EDVAC," *IEEE Annals of the History of Computing*, vol. 15, pp. 27–42, 1993.

[2] A. M. Turing, "On computable numbers, with an application to the Entscheidungsproblem," *Proceedings of the London Mathematical Society*, vol. s2-42, no. 1, pp. 230–265, 1937.

[3] R. P. Feynman, *Feynman Lectures on Computation.* Addison-Wesley, 1997.

[4] R. J. Baker, *CMOS: Circuit Design, Layout, and Simulation.* Wiley-IEEE, 2010.

[5] A. Adamatzky, B. De Lacy Costello, and T. Asai, *Reaction-Diffusion Computers.* Elsevier, 2005.

[6] J. W. Mills, "The new computer science and its unifying principle," in *The Grand Challenge in Non-Classical Computation: International Workshop*, 2005.

[7] M. Orlik, *Reakcje oscylacyjne. Porządek i chaos.* Wydawnictwa Naukowo-Techniczne, 1996.

[8] A. J. Lotka, "Contribution to the theory of periodic reactions," *The Journal of Physical Chemistry*, vol. 14, no. 3, pp. 271–274, 1910.

[9] A. J. Lotka, "Undamped oscillations derived from the law of mass action," *Journal of the American Chemical Society*, vol. 42, no. 8, pp. 1595–1599, 1920.

[10] A. J. Lotka, "Analytical note on certain rhythmic relations in organic systems," *Proceedings of the National Academy of Sciences of the United States of America*, vol. 6, no. 7, pp. 410–415, 1920.

[11] V. Volterra, "Fluctuations in the abundance of a species considered mathematically," *Nature*, vol. 118, pp. 558–560, 1926.

[12] S. S. Mader, *Biology*. McGraw-Hill, 1998.

[13] W. C. Bray, "A periodic reaction in homogeneous solution and its relation to catalysis.," *Journal of the American Chemical Society*, vol. 43, no. 6, pp. 1262–1267, 1921.

[14] W. C. Bray and H. A. Liebhafsky, "Reactions involving hydrogen peroxide, iodine and iodate ion. I. Introduction," *Journal of the American Chemical Society*, vol. 53, no. 1, pp. 38–44, 1931.

[15] F. O. Rice and O. M. Reiff, "The thermal decomposition of hydrogen peroxide," *The Journal of Physical Chemistry*, vol. 31, no. 9, pp. 1352–1356, 1927.

[16] M. G. Peard and C. F. Cullis, "A periodic chemical reaction. The reaction between hydrogen peroxide and iodic acid," *Trans. Faraday Soc.*, vol. 47, pp. 616–630, 1951.

[17] K. R. Sharma and R. M. Noyes, "Oscillations in chemical systems. 13. A detailed molecular mechanism for the Bray-Liebhafsky reaction of iodate and hydrogen peroxide," *Journal of the American Chemical Society*, vol. 98, no. 15, pp. 4345–4361, 1976.

[18] A. T. Winfree, "The prehistory of the Belousov-Zhabotinsky oscillator," *Journal of Chemical Education*, vol. 61, no. 8, p. 661, 1984.

[19] B. P. Belousov, "A periodic reaction and its mechanism," in *Sbornik Referatov po Radiatsionnoi Meditsine*, vol. 145, 1958.

[20] A. M. Zhabotinsky, "Periodic kinetics of oxidation of malonic acid in solution," *Biofizika*, vol. 9, pp. 306–311, 1964.

[21] H. Degn, "Effect of bromine derivatives of malonic acid on the oscillating reaction of malonic acid, cerium ions and bromate," *Nature*, vol. 213, no. 5076, pp. 589–590, 1967.

[22] R. J. Field, E. Koros, and R. M. Noyes, "Oscillations in chemical systems. II. Thorough analysis of temporal oscillation in the bromate-cerium-malonic acid system," *Journal of the American Chemical Society*, vol. 94, no. 25, pp. 8649–8664, 1972.

[23] H. D. Foersterling and Z. Noszticzius, "An additional negative feedback loop in the classical Belousov-Zhabotinskii reaction: malonyl radical as a second control intermediate," *The Journal of Physical Chemistry*, vol. 93, no. 7, pp. 2740–2748, 1989.

[24] L. Gyorgyi, T. Turanyi, and R. J. Field, "Mechanistic details of the oscillatory Belousov-Zhabotinskii reaction," *The Journal of Physical Chemistry*, vol. 94, no. 18, pp. 7162–7170, 1990.

[25] L. Hegedus, M. Wittmann, Z. Noszticzius, S. Yan, A. Sirimungkala, H. Forsterling, and R. J. Field, "HPLC analysis of complete BZ systems. Evolution of the chemical composition in cerium and ferroin catalysed batch oscillators: experiments and model calculations," *Faraday Discussions*, vol. 120, pp. 21–38, 2002.

[26] A. N. Zaikin and A. M. Zhabotinsky, "Concentration wave propagation in two-dimensional liquid-phase self-oscillating system," *Nature*, vol. 225, no. 5232, pp. 535–537, 1970.

[27] A. T. Winfree, "Spiral waves of chemical activity," *Science*, vol. 175, no. 4022, pp. 634–636, 1972.

[28] J. Tyson and J. Murray, "Cyclic amp waves during aggregation of dictyostelium amoebae," *Development*, vol. 106, no. 3, pp. 421–426, 1989.

[29] M. J. Berridge, "Calcium oscillations.," *Journal of Biological Chemistry*, vol. 265, no. 17, pp. 9583–9586, 1990.

[30] R. Toth and A. F. Taylor, "The tris(2,2-bipyridyl)ruthenium-catalysed Belousov–Zhabotinsky reaction," *Progress in Reaction Kinetics and Mechanism*, vol. 31, pp. 59–115(57), 2006.

[31] J. N. Demas and D. Diemente, "An oscillating chemical reaction with a luminescent indicator," *Journal of Chemical Education*, vol. 50, no. 5, p. 357, 1973.

[32] V. Gaspar, G. Bazsa, and T. Beck, "The influence of visible light on the Belousov-Zhabotinskii oscillating reactions applying different catalysts," *Zeitschrift für Physikalische Chemie-Leipzig*, vol. 264, pp. 43–48, 1983.

[33] S. Kádár, T. Amemiya, and K. Showalter, "Reaction mechanism for light sensitivity of the $Ru(bpy)_3^{2+}$-catalyzed Belousov–Zhabotinsky reaction," *The Journal of Physical Chemistry A*, vol. 101, no. 44, pp. 8200–8206, 1997.

[34] R. J. Field and R. M. Noyes, "Oscillations in chemical systems. IV. Limit cycle behavior in a model of a real chemical reaction," *The Journal of Chemical Physics*, vol. 60, no. 5, pp. 1877–1884, 1974.

[35] J. J. Tyson and P. C. Fife, "Target patterns in a realistic model of the Belousov–Zhabotinskii reaction," *The Journal of Chemical Physics*, vol. 73, no. 5, pp. 2224–2237, 1980.

[36] H. J. Krug, L. Pohlmann, and L. Kuhnert, "Analysis of the modified complete Oregonator accounting for oxygen sensitivity and photosensitivity of Belousov-

Zhabotinskii systems," *The Journal of Physical Chemistry*, vol. 94, no. 12, pp. 4862–4866, 1990.

[37] M.-L. Smoes, "Period of homogeneous oscillations in the ferroin-catalyzed Zhabotinskii system," *The Journal of Chemical Physics*, vol. 71, no. 11, pp. 4669–4679, 1979.

[38] W. M. Latimer, *Oxidation Potentials*. Prentice Hall, 1952.

[39] R. M. Noyes, "Chemical oscillations and instabilities. 39. A generalized mechanism for bromate-driven oscillators controlled by bromide," *Journal of the American Chemical Society*, vol. 102, no. 14, pp. 4644–4649, 1980.

[40] N. Ganapathisubramanian and R. M. Noyes, "Chemical oscillations and instabilities. Part 49. Additional complexities during oxidation of malonic acid in the Belousov-Zhabotinskii oscillating reaction," *The Journal of Physical Chemistry*, vol. 86, no. 26, pp. 5158–5162, 1982.

[41] A. B. Rovinskii and A. M. Zhabotinskii, "Mechanism and mathematical model of the oscillating bromate-ferroin-bromomalonic acid reaction," *The Journal of Physical Chemistry*, vol. 88, no. 25, pp. 6081–6084, 1984.

[42] L. P. Hammett and A. J. Deyrup, "A series of simple basic indicators. I. The acidity functions of mixtures of sulfuric and perchloric acids with water1," *Journal of the American Chemical Society*, vol. 54, no. 7, pp. 2721–2739, 1932.

[43] M. A. Paul and F. A. Long, "h_0 and related indicator acidity function," *Chemical Reviews*, vol. 57, no. 1, pp. 1–45, 1957.

[44] E. B. Robertson and H. B. Dunford, "The state of the proton in aqueous sulfuric acid," *Journal of the American Chemical Society*, vol. 86, no. 23, pp. 5080–5089, 1964.

[45] A. M. Zhabotinsky, F. Buchholtz, A. B. Kiyatkin, and I. R. Epstein, "Oscillations and waves in metal-ion-catalyzed bromate oscillating reactions in highly oxidized states," *The Journal of Physical Chemistry*, vol. 97, no. 29, pp. 7578–7584, 1993.

[46] D. C. Johanson, *From Lucy to language*. Simon and Schuster, 1996.

[47] M. W. Barnett and P. M. Larkman, "The action potential," *Practical Neurology*, vol. 7, no. 3, pp. 192–197, 2007.

[48] L. F. Abbott, "Lapicque's introduction of the integrate-and-fire model neuron (1907)," *Brain Research Bulletin*, vol. 50, no. 5-6, pp. 303 – 304, 1999.

[49] A. L. Hodgkin and A. F. Huxley, "A quantitative description of membrane current and its application to conduction and excitation in nerve," *The Journal of Physiology*, vol. 117, no. 4, pp. 500–544, 1952.

[50] W. Gerstner and W. M. Kistler, *Spiking Neuron Models. Single Neurons, Populations, Plasticity*. Cambridge University Press, 2002.

[51] R. FitzHugh, "Mathematical models of threshold phenomena in the nerve membrane," *Bulletin of Mathematical Biology*, vol. 17, pp. 257–278, 1955.

[52] R. FitzHugh, "Impulses and physiological states in theoretical models of nerve membrane," *Biophysical Journal*, vol. 1, no. 6, pp. 445 – 466, 1961.

[53] J. Nagumo, S. Arimoto, and S. Yoshizawa, "An active pulse transmission line simulating nerve axon," *Proceedings of the IRE*, vol. 50, no. 10, pp. 2061–2070, 1962.

[54] T. Kanamaru, "Van der Pol oscillator," *Scholarpedia*, vol. 2, no. 1, p. 2202, 2007.

[55] A. Toth, V. Gaspar, and K. Showalter, "Signal transmission in chemical systems: propagation of chemical waves through capillary tubes," *The Journal of Physical Chemistry*, vol. 98, no. 2, pp. 522–531, 1994.

[56] A. Toth and K. Showalter, "Logic gates in excitable media," *The Journal of Chemical Physics*, vol. 103, no. 6, pp. 2058–2066, 1995.

[57] O. Steinbock, P. Kettunen, and K. Showalter, "Chemical wave logic gates," *The Journal of Physical Chemistry*, vol. 100, no. 49, pp. 18970–18975, 1996.

[58] K. Agladze, R. R. Aliev, T. Yamaguchi, and K. Yoshikawa, "Chemical diode," *The Journal of Physical Chemistry*, vol. 100, no. 33, pp. 13895–13897, 1996.

[59] T. Kusumi, T. Yamaguchi, R. R. Aliev, T. Amemiya, T. Ohmori, H. Hashimoto, and K. Yoshikawa, "Numerical study on time delay for chemical wave transmission via an inactive gap," *Chemical Physics Letters*, vol. 271, no. 4-6, pp. 355 – 360, 1997.

[60] I. Motoike and K. Yoshikawa, "Information operations with an excitable field," *Phys. Rev. E*, vol. 59, pp. 5354–5360, May 1999.

[61] I. N. Motoike, K. Yoshikawa, Y. Iguchi, and S. Nakata, "Real-time memory on an excitable field," *Phys. Rev. E*, vol. 63, p. 036220, Feb 2001.

[62] J. Gorecki, K. Yoshikawa, and Y. Igarashi, "On chemical reactors that can count," *The Journal of Physical Chemistry A*, vol. 107, no. 10, pp. 1664–1669, 2003.

[63] T. Ichino, Y. Igarashi, I. N. Motoike, and K. Yoshikawa, "Different operations on a single circuit: field computation on an excitable chemical system," *The Journal of Chemical Physics*, vol. 118, no. 18, pp. 8185–8190, 2003.

[64] K. Suzuki, T. Yoshinobu, and H. Iwasaki, "Unidirectional propagation of chemical waves through microgaps between zones with different excitability," *The Journal of Physical Chemistry A*, vol. 104, no. 28, pp. 6602–6608, 2000.

[65] J. N. Gorecka, J. Gorecki, and Y. Igarashi, "One dimensional chemical signal diode constructed with two nonexcitable barriers," *The Journal of Physical Chemistry A*, vol. 111, no. 5, pp. 885–889, 2007.

[66] J. Gorecka and J. Gorecki, "Multiargument logical operations performed with excitable chemical medium," *The Journal of Chemical Physics*, vol. 124, no. 8, p. 084101, 2006.

[67] V. K. Vanag and D. V. Boulanov, "Behavior of the Belousov–Zhabotinskii oscillator in reverse micelles of AOT in octane," *The Journal of Physical Chemistry*, vol. 98, no. 5, pp. 1449–1453, 1994.

[68] A. M. Turing, "The chemical basis of morphogenesis," *Philosophical Transactions of the Royal Society of London. Series B, Biological Sciences*, vol. 237, no. 641, pp. 37–72, 1952.

[69] V. K. Vanag and I. R. Epstein, "Pattern formation in a tunable medium: the Belousov–Zhabotinsky reaction in an aerosol ot microemulsion," *Phys. Rev. Lett.*, vol. 87, p. 228301, Nov 2001.

[70] V. K. Vanag and I. R. Epstein, "Dash waves in a reaction-diffusion system," *Phys. Rev. Lett.*, vol. 90, p. 098301, Mar 2003.

[71] V. K. Vanag and I. R. Epstein, "Segmented spiral waves in a reaction-diffusion system," *Proceedings of the National Academy of Sciences*, vol. 100, no. 25, pp. 14635–14638, 2003.

[72] I. R. Epstein and V. K. Vanag, "Complex patterns in reactive microemulsions: self-organized nanostructures?," *Chaos*, vol. 15, no. 4, p. 047510, 2005.

[73] M. J. Fuerstman, P. Garstecki, and G. M. Whitesides, "Coding/decoding and re-versibility of droplet trains in microfluidic networks," *Science*, vol. 315, no. 5813, pp. 828–832, 2007.

[74] M. Prakash and N. Gershenfeld, "Microfluidic bubble logic," *Science*, vol. 315, no. 5813, pp. 832–835, 2007.

[75] I. R. Epstein, "Can droplets and bubbles think?," *Science*, vol. 315, no. 5813, pp. 775–776, 2007.

[76] M. Toiya, V. Vanag, and I. Epstein, "Diffusively coupled chemical oscillators in a microfluidic assembly," *Angewandte Chemie International Edition*, vol. 47, no. 40, pp. 7753–7755, 2008.

[77] M. Toiya, H. O. González-Ochoa, V. K. Vanag, S. Fraden, and I. R. Epstein, "Synchronization of chemical micro-oscillators," *The Journal of Physical Chemistry Letters*, vol. 1, no. 8, pp. 1241–1246, 2010.

[78] J. Delgado, N. Li, M. Leda, H. O. Gonzalez-Ochoa, S. Fraden, and I. R. Epstein, "Coupled oscillations in a 1D emulsion of Belousov-Zhabotinsky droplets," *Soft Matter*, vol. 7, pp. 3155–3167, 2011.

[79] M. Häusser, N. Spruston, and G. J. Stuart, "Diversity and dynamics of dendritic signaling," *Science*, vol. 290, no. 5492, pp. 739–744, 2000.

[80] H. Kitahata, R. Aihara, Y. Mori, and K. Yoshikawa, "Slowing and stopping of chemical waves in a narrowing canal," *The Journal of Physical Chemistry B*, vol. 108, no. 49, pp. 18956–18959, 2004.

[81] H. Kitahata, K. Fujio, J. Gorecki, S. Nakata, Y. Igarashi, A. Gorecka, and K. Yoshikawa, "Oscillation in penetration distance in a train of chemical pulses

propagating in an optically constrained narrowing channel," *The Journal of Physical Chemistry A*, vol. 113, no. 39, pp. 10405–10409, 2009.

[82] I. Sendiña Nadal, E. Mihaliuk, J. Wang, V. Pérez-Muñuzuri, and K. Showalter, "Wave propagation in subexcitable media with periodically modulated excitability," *Physical Review Letters*, vol. 86, no. 8, pp. 1646–1649, 2001.

[83] T. Sakurai, E. Mihaliuk, F. Chirila, and K. Showalter, "Design and control of wave propagation patterns in excitable media," *Science*, vol. 296, no. 5575, pp. 2009–2012, 2002.

[84] R. Toth, C. Stone, A. Adamatzky, B. de Lacy Costello, and L. Bull, "Dynamic control and information processing in the Belousov–Zhabotinsky reaction using a coevolutionary algorithm," *The Journal of Chemical Physics*, vol. 129, no. 18, p. 184708, 2008.

[85] K. Funakoshi, H. Suzuki, and S. Takeuchi, "Lipid bilayer formation by contacting monolayers in a microfluidic device for membrane protein analysis," *Analytical Chemistry*, vol. 78, no. 24, pp. 8169–8174, 2006.

[86] N. Malmstadt, M. A. Nash, R. F. Purnell, and J. J. Schmidt, "Automated formation of lipid-bilayer membranes in a microfluidic device," *Nano Letters*, vol. 6, no. 9, pp. 1961–1965, 2006.

[87] M. A. Holden, D. Needham, and H. Bayley, "Functional bionetworks from nanoliter water droplets," *Journal of the American Chemical Society*, vol. 129, no. 27, pp. 8650–8655, 2007.

[88] G. Maglia, A. J. Heron, W. L. Hwang, M. A. Holden, E. Mikhailova, Q. Li, S. Cheley, and H. Bayley, "Droplet networks with incorporated protein diodes show collective properties," *Nature Nanotechnology*, vol. 4, pp. 437–440, June 2009.

[89] T. Yamaguchi, L. Kuhnert, Z. Nagy-Ungvarai, S. C. Mueller, and B. Hess, "Gel systems for the Belousov–Zhabotinskii reaction," *The Journal of Physical Chemistry*, vol. 95, no. 15, pp. 5831–5837, 1991.

[90] J. Sielewiesiuk and J. Górecki, "Complex transformations of chemical signals passing through a passive barrier," *Phys. Rev. E*, vol. 66, p. 016212, Jul 2002.

[91] P. Kettunen, T. Yamaguchi, H. Hashimoto, T. Amemiya, B. Steinbock, and S. C. Müller, "Emergent reaction–diffusion phenomena in capillary tubes," vol. 16, no. 3, p. 037111, 2006.

[92] M. Tanaka, H. Nagahara, H. Kitahata, V. Krinsky, K. Agladze, and K. Yoshikawa, "Survival versus collapse: abrupt drop of excitability kills the traveling pulse, while gradual change results in adaptation," *Phys. Rev. E*, vol. 76, p. 016205, Jul 2007.

[93] O. Steinbock and S. C. Müller, "Radius-dependent inhibition and activation of chemical oscillations in small droplets," *The Journal of Physical Chemistry A*, vol. 102, no. 32, pp. 6485–6490, 1998.

[94] K. Kurin-Csörgei, A. M. Zhabotinsky, M. Orbán, and I. R. Epstein, "Bromate–1,4-cyclohexanedione–ferroin gas-free oscillating reaction. 1. Basic features and crossing wave patterns in a reaction–diffusion system without gel," *The Journal of Physical Chemistry*, vol. 100, no. 13, pp. 5393–5397, 1996.

[95] K. Showalter and R. M. Noyes, "Oscillations in chemical systems. 15. Deliberate generation of trigger waves of chemical reactivity," *Journal of the American Chemical Society*, vol. 98, no. 12, pp. 3730–3731, 1976.

[96] A. M. Zhabotinsky, S. C. Muller, and B. Hess, "Interaction of chemical waves in a thin layer of microheterogeneous gel with a transversal chemical gradient," *Chemical Physics Letters*, vol. 172, no. 6, pp. 445 – 448, 1990.

[97] S. Thutupalli, S. Herminghaus, and R. Seemann, "Bilayer membranes in micro-fluidics: from gel emulsions to soft functional devices," *Soft Matter*, vol. 7, pp. 1312–1320, 2011.

[98] S. Thutupalli, R. Seemann, and S. Herminghaus, "Swarming behavior of simple model squirmers," *New Journal of Physics*, vol. 13, no. 7, p. 073021, 2011.

[99] A. Magnani, N. Marchettini, S. Ristori, C. Rossi, F. Rossi, M. Rustici, O. Spalla, and E. Tiezzi, "Chemical waves and pattern formation in the 1,2-dipalmitoyl-sn-glycero-3-phosphocholine/water lamellar system," *Journal of the American Chemical Society*, vol. 126, no. 37, pp. 11406–11407, 2004.

[100] S. Ristori, F. Rossi, G. Biosa, N. Marchettini, M. Rustici, and E. Tiezzi, "Interplay between the Belousov–Zhabotinsky reaction–diffusion system and biomimetic matrices," *Chemical Physics Letters*, vol. 436, no. 1-3, pp. 175 – 178, 2007.

[101] J. Sielewiesiuk and J. Gorecki, "On the response of simple reactors to regular trains of pulses," *Phys. Chem. Chem. Phys.*, vol. 4, pp. 1326–1333, 2002.

[102] J. Holley, A. Adamatzky, L. Bull, B. D. L. Costello, and I. Jahan, "Computational modalities of Belousov–Zhabotinsky encapsulated vesicles," *Nano Communication Networks*, vol. 2, no. 1, pp. 50 – 61, 2011.